Faculty of Health Sciences
Department of Medical Biology

Biomarkers Discovery:

The Benefit of the Study Exosomes Originated from Merkel Cell Carcinoma Cell Lines

—

Aelita Gloria Virginia Konstantinell

A dissertation for the degree of Philosophiae Doctor - April 2019

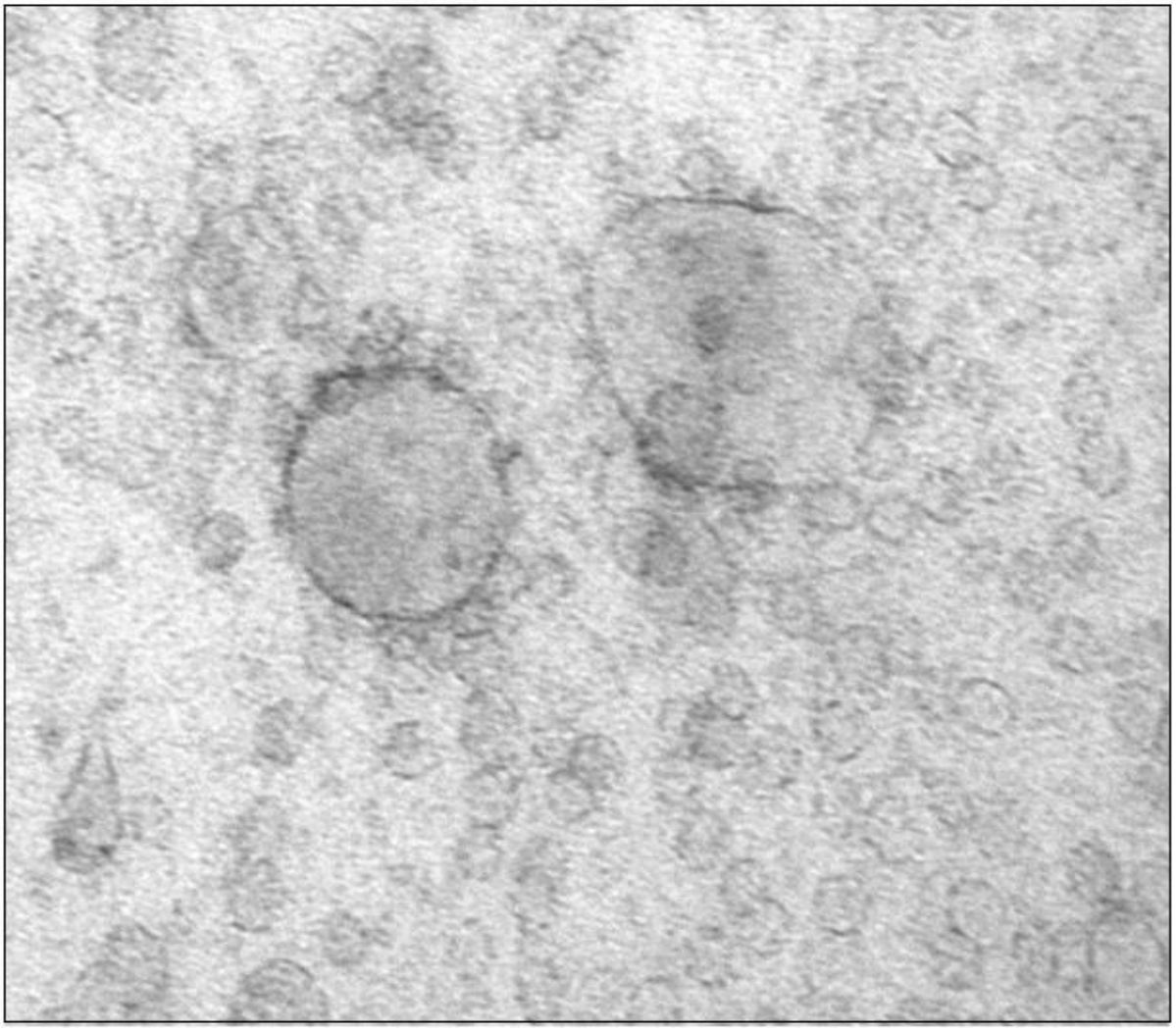

"Tender love and care toughen you up because they nurture and strengthen your capacity to learn and adapt, including learning how to fight and adapting to later hardship"

Noam Shpancer

Acknowledgments

This thesis done at the **Molecular Inflammation Research Group**, Department of Medical Biology, University of Tromsø, **The Arctic University of Norway**.

I want to single out my supervisor **Ugo Moens**, and I want to thank you for all of the opportunities you have given to me, from being able to conduct my research, to further my dissertation at the University of Tromsø. Your kindness gives me space and strength to work independently. Also, I want to thank my co-supervisor, **Baldur Sveinbjørnsson**, for your valuable guidance. You provided me with the tools that I needed to choose the right direction and complete my dissertation.

Thank the members of my dissertation committee **Virve Koljonen**, **Hanna Eriksson** and **Jan-Olaf Winberg** for generously offering your time, support, guidance, and goodwill throughout the preparation.

I am also grateful to the following university staff: **Gunbjørg Svineng**, **Karen Kristine Sørensen** and **Bård Smedsrød** for their unfailing support and assistance, and the **Faculty of Health Science**, **University of Tromsø** for funding the Ph.D. research. I want to thank at the **Odd Fellow Medisinsk-Vitenskapelig Forskningsfond**, **Helse Nord** and **Familien Blix' Fond** for helping and providing the funding for the work.

Thanks to all down my colleagues from MIRG group: **Dag Coucheron**, **Gianina Dumitriu**, **Maria Ludvigsen Conny Tümmler**, **Kashif Rasheed**, and **Diana Diaz Cánova** for being friendly.

Extraordinary gratitude goes out to my internship at Medical Biology Department: **Jack-Ansgar Bruun**, **Augusta Hlin Aspar**, **Randi Olsen**, **Tom Ivar Eilertsen** and **Kenneth Bowitz Larsen**; and at Pharmacy Department: **Nataša Škalko-Basnet** for the knowledge that I possess now. Thank my externship at Karolinska Institute, Department of Oncology-Pathology, Stockholm, Sweden: **Hao Shi**, **Satendra Kumar**, **Weng-Kuan Huang**, **Patrick Scicluna**, **Jiwei Gao** and **Weng-Onn Lui** for your collaboration and help.

I was born on the peak of the midnight sun, and I cannot stand the long dark polar night without observing The North Star, Polaris. Thank you, **Lars Ailo Bongo**, **Institute of**

Informatics, Tromsø, Norway, and **Mika Gustafsson**, **Department of Physics, Chemistry and Biology, Linköping, Sweden** for your belief in my ability to grow as a researcher.

Big thanks go to **Ingrid Tangevold** and **Arne-Wilhelm Theodorsen** for giving me "roof overhead" and I stay in their friendly, cozy and warm house for a while. Thanks for being kind and supportive whatever I need help.

I would like to thank my life-coaches: my lifelong cheerleader and daughter, **Apollinaria Arianné Gabriel**, who always achieves what she wants, and my dear **Edmund Østerberg**, whom is always ready to build and fight for a new project, where he is an entrepreneur, and I, a manager. What incredible partnership! As our house grows, we grow as builders, architects, carpenters, and designers. **Edmund** was always keen to know what I am doing and how I am proceeding, even though he had never grasped what it is all about, but he is still proud of me.

Thanks to our neighbors, **Jan Ragnar Thomas Dagsvold** and **Maria Mathisen**, who always find time to help us and serve a cup of coffee almost every day all year around. Therefore, I promise when I buy a pack of coffee I will buy one more for you. **Many Thanks!**

Thank **Arne Nikolai Pedersen**, who treats and support me as his daughter.

Thank you to my driving teacher, **Jon Terje Karlsen**! I always drive on my own alone on the road of life. However, what I could do without your lessons on the streets of the Tromsø?! I cannot imagine!

I am grateful to my other family members and friends who have supported me along the way. **Olga Filipova**, **Irina** and **Ludmila Grozina**, **Elena Andersson** and their family members, who provided me with moral and emotional support through my life.

Last but not least, thank you, everyone, who directly or indirectly helped and assisted me in my life long adventure.

Thank you very much!

Aelita Gloria Virginia Konstantinell

April 2019, Tromsø

Contents

List of Papers

Paper I

Aelita Konstantinell*, Jack-Ansgar Bruun, Randi Olsen, Augusta Hlin Aspar, Nataša Škalko-Basnet, Baldur Sveinbjørnsson, and Ugo Moens. **Secretomic analysis of extracellular vesicles originating from polyomavirus-negative and polyomavirus-positive Merkel cell carcinoma cell lines.** *Proteomics* **2016**, 16, 2587-2591.

Paper II

Aelita Konstantinell[#]*, Augusta Hlin Aspar Sundbø, Hao Shi, Nataša Škalko-Basnet, Weng-Onn Lui[#], Baldur Sveinbjørnsson, and Ugo Moens[#]. **Comparative analysis of microRNA expression profiles of exosomes derived from polyomavirus-negative and –positive Merkel cell lines by next-generation sequencing.** *Manuscript*.

Paper III

Aelita Konstantinell[#]*, Jack-Ansgar Bruun[#], Weng-Onn Lui, Baldur Sveinbjørnsson, and Ugo Moens[#]. **Comparative and integrated analyses of Merkel cell polyomavirus-negative and –positive cell lines and their exosomes proteomic profiles.** *Manuscript*.

# These authors contributed equally to this work;

* The corresponding author.

Abbreviations

ALTO	Alternative Large T Open reading frame
CK20	Cytokeratin 20
CTLA-4	Cytotoxic T-lymphocyte antigen 4
DAA	Direct acting antiviral drug
DCN	Decorin
FBXW7	F-box/WD repeat-containing protein 7
HCV	Hepatitis C-virus
KSHV	Kaposi's sarcoma-associated herpevirus
LCA	Leukocyte common antigen
LDHB	Lactate Dehydrogenase B enzyme
LT	Large T antigen
MBV	Multivesicular body
MCPyV	Merkel cell polyomavirus
NADH	NADH-dehydrogenase
NK	Natural killer
PARP1	Poly (ADP-ribose) polymerase 1
PTM	Post-translational modification
PD-1	Program Cell Death Protein 1
SOCS3	Suppressor of cytokine signaling 3
ST	Small T antigen
STMN1	Stathmin
TAM	Transcription-associated mutation
TAR	Transcription-associated recombination
TTF-1	Thyroid transcription factor 1
VCP	Valosin-containing protein
VP1/VP2/VP3	Capsid proteins
YWHAG	14-3-3 protein gamma

Summary

Merkel cell carcinoma (MCC) is a rare and aggressive neuroendocrine type of skin cancer associated with a poor prognosis. This carcinoma named after its presumed cell of origin, the Merkel cell, a mechanoreceptor cell located in the basal epidermal layer of the skin. However, this notion has challenged by suggesting epidermal stem cells, fibroblasts or pro/pre-B cells as possible cells of origin. Merkel cell polyomavirus (MCPyV) is the only known polyomavirus directly linked to human cancer. Approximately 80% of all MCCs are positive for viral DNA. UV exposure is the predominant etiological factor for virus-negative MCCs. Immune therapy is a promising treatment for MCC patients, but it has failed to arrest the cancer progression. Biomarkers discovery is an urgent, and high-throughput approaches were proposed. The high-dimensional data generation of genomic, transcriptomic, proteomic, and imaging data by high-throughput approaches are a new type of biomarkers discovery platform. These data analyses unveil the cell origin and phenotype. Characterization and phenotyping of cells and exosomes originating from polyomavirus-negative and polyomavirus-positive MCC cell lines and their content analyses uncovered differentially expressed proteins and exosomal miRNAs.

Paper I, the result showed that MCPyV-negative and –positive MCC cell lines' exosomes contain several proteins associated with tumor cell motility and metastasis. A list of vesicular proteins derived from the extracellular region identified for exosomes that could be recognition proteins by recipient cells.

Paper II, the result showed that the exosomal miR-222-3p presence in all type of samples derived from MCC cell lines, healthy donors and MCC patients. The miR-222-3p selectively sorted, and its expressed level dropped down dependent on cancer and viral status in MCC patients in the circulation system. The target genes' scanning indicates that the exosomal miR-222-3p play pleiotropic role dependent on recipient cells in health and disease.

Paper III, the result showed that MCPyV-positive cell lines and their exosomes contain polyomavirus proteins. The cell phenotyping investigation revealed the MCPyV-negative MCC cell lines indicate to loss DNA, RNA and protein synthesis and their regulation system activity, and have an unusual activity of protein expression at cell proliferation and post-translational

modification sites. These may lead to transcription-associated mutation (TAM) and transcription-associated recombination (TAR), which gave a rise a high mutational burden of MCPyV-negative MCCs. The MCPyV-positive MCC cell lines showed upregulated expression of proteins involved in DNA and its regulation that indicates harnesses of polyomaviruses for DNA integration. In addition, there are upregulation of proteins on RNA, protein synthesis and their initiation and control, modification machinery such as the protein acylation. As for following, this process culminates in the viral proteins and genome synthesis. However, a fixed exosome-ER accession ability and a low activity on endocytosis and exocytosis sites indicate to reduce the chance of MCPyV spreading.

The dissertation is the result of comparative and integrated analyses of polyomavirus-negative and -positive MCC cell lines' and their exosomes' protein and miRNA profiling; discussion of the potential application of exosomes, proteins and microRNAs as biomarkers for the diagnosis, progression, and prognosis for MCCs. During this project generated data and storied in publicly available repositories for further screening and validation studies. This project proved the benefit of exploring MCC cell lines as a model system for MCCs, and proteomic and sequencing approaches are potent tools for biomarkers discovery.

1 Chapter: Introduction

Cancer is a genetically and clinically diverse disease even within one type of cancer. The pathogenesis, aggressiveness, metastatic potential and response to treatment can be different among individual patients with the same kind of cancer that suggest the role of genetic factors in cancer pathogenesis [1]. Merkel cell carcinoma (MCC) is a rare, aggressive neuroendocrine form of skin cancer. The risk of developing Merkel cell carcinoma substantially increased among a large number of immunosuppressed patients, and precision medicine is needed [2]. Precision medicine is a core of biomarkers, which are highly specific in revealing information for diagnosis, prognosis, and therapy [3, 4]. Cancer biomarkers discovery approaches are molecular, cellular, and imaging methodologies focused on disease and drug mechanisms. Biomarkers play a role in cancer screening, early diagnosis, prognosis, prediction of treatment efficacy, and adverse reaction. Biomarkers have prognostic and predictive value [4].

1.1 Cancer Biomarker

Biomarkers are biological indicators of normal physiological and pathogenic processes, and pharmacological responses to a therapeutic intervention, which can be objectively measured and evaluated [5]. In cancer, biomarkers defined as biochemical substances elaborated by cancer cells due to the cause or effect of the malignant process [4, 6]. Ideally, cancer biomarkers should be detectable only in the presence of cancer. However, they can be endogenous products produced at a higher or less rate in cancer cells or products of newly switched on genes that remained inactive in normal cells [7]. Biomarkers include intracellular molecules or proteins in tissues or can be released into circulation and appear in body fluids such as blood, serum and plasma, urine, saliva, synovial, amniotic and vaginal fluids, semen and breast milk, and their presence in significant amount may indicate the presence of cancer [8]. Cancer biomarkers classified into prediction, detection, diagnostic, prognostic, and pharmacodynamic biomarkers [9]. Predictive biomarkers used in assessing the effect of administering specific agents, which will work best for an individual patient [10]. Diagnostic markers may be present in any stage of cancer development [11]. Prognostic biomarkers

based on the distinguishing features between benign and malignant tumors [10]. Pharmacodynamic biomarkers are cancer markers utilized in selecting doses of chemotherapeutic agents in a given set of tumor-patient conditions [12]. However, the biomarker utility lies in its ability to provide an early indication of a disease or its progression. The biomarker should be easy to detect and measure across populations.

1.2 Merkel Cell Carcinoma

MCC is a rare, aggressive neuroendocrine form of skin cancer with a rising incidence and a high mortality rate [13]. More than one-third of patients die of MCC, which making MCC twice as lethal as malignant melanoma [14]. Toker et al. initially described cancer in 1972, as a trabecular cancer of the dermis with a high risk of lymphoid metastasis [13]. The name was changed to MCC because tumor cells resemble Merkel cells, which are present in the basal layer of the epidermis around hair follicles, and share several neuroendocrine markers such as chromogranin A, synaptophysin and cytokeratin 20 [15]. However, this statement recently challenged by suggesting epidermal stem cells, fibroblasts or pro/pre-B cells as possible cells of origin with neuroendocrine differentiation because of the neoplastic transformation [15-17]. The MCC cells have a little cytoplasm and dense nuclear chromatin (**Figure 1**). The

pathologist classification, the MCCs are members of the group tumor, which includes small cell carcinoma of lung, lymphomas, and neuroblastomas [18].

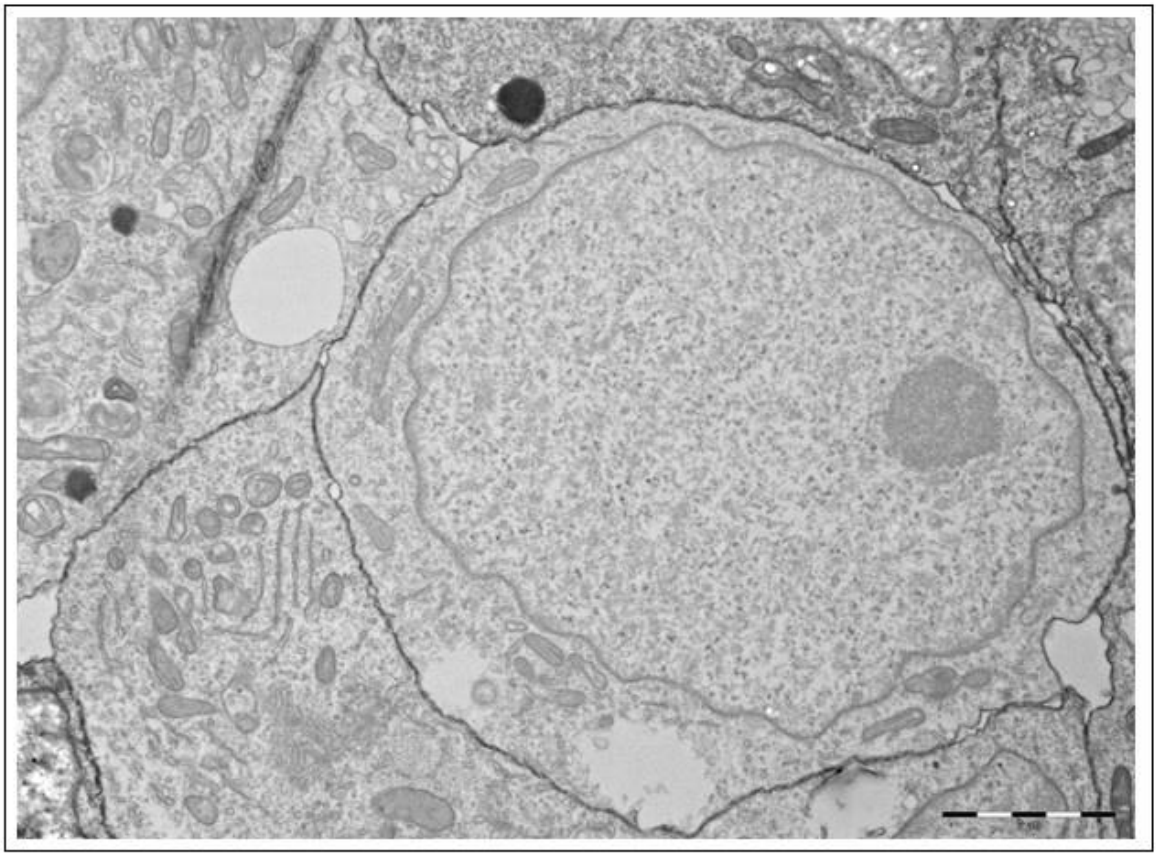

Figure 1. The MCC cells have a little cytoplasm and dense nuclear chromatin. The transmission electron microscopy (TEM) picture: Scale bar = 2 µm, x80 000 magnification.

1.2.1 Epidemiology

The incidence rate of MCC is variable across different regions of the world. The Surveillance of Rare Cancers in Europe (RARECARE) database reported an incidence rate of 0.13 per 100,000 between 1995 and 2002 [19]. In Norway, the incidence of MCC was stable over time, whereas the estimate continued to increase within the 2005-2008 period and achieved 0.3 per 100,000 people a year in Sweden, in 2012 [14, 15, 20].

The disease appears more often in men than in women, with men comprising 61 % of the cases. Though, in Finland and China have reported a slightly higher incidence in women [21, 22]. Older adults with fair skin, people exposed to excessive UV-radiation and immuno-

compromised patients are most susceptible to the MCC [2, 23]. The MCC is more frequent in patients with autoimmune disease, leukemia, lymphoma, HIV infected, and immunosuppressed due to organ transplantation or other causes [2, 23-27]. Chronic inflammatory disorders such as rheumatoid arthritis, Bowen's disease, and chronic arsenic exposure have also associated with a higher incidence of MCC [28, 29]. The most common primary site is in the head and neck region with 45 % of the cases, and the onset of the disease often occurs at more than 50 years of age [30, 31]. In immunosuppressed individuals, the age of onset of MCC is lower than 50 years, and the mortality is higher than in immunocompetent patients [2, 13]. These findings indicate the crucial role of efficient immune surveillance in the control of tumor growth and progression.

1.2.2 **Pathogenesis**

The pathogenesis of MCC not fully understood as the cell of origin, which mentioned in the previous section. Two causes can initiate MCC tumorigeneses, such as accumulation of UV-induced mutations in the MCPyV-negative MCCs and the UV-induced initiation of MCPyV-encoded primary transforming genes activity in Merkel cell polyomavirus (MCPyV)-positive tumors [32, 33].

The DNA sequencing revealed the crucial differences between MCPyV-negative and –positive MCCs, which are the abundance of UV-induced mutations as C-to-T pyrimidine dimers in MCPyV-negative MCCs, which are also typically evidence in other skin cancers associated with sun exposure, such as melanoma, basal cell carcinoma, and cutaneous squamous cell carcinoma [32]. Also, the comparative molecular genetics of MCPyV-negative and –positive MCCs identified significant differences in mutational burden, that was 0.4 mutations/mutational burden in MCPyV-positive tumors compared to 10 mutations/mutational burden in MCPyV-negative MCCs [15]. Moreover, exome sequencing of 49 MCCs showed 1121 somatic single nucleotide variants per exome in MCPyV-negative

tumors compared to 12.5 variants in MCPyV-positive MCCs, with no mutations in the retinoblastoma tumor suppressor (RB1) and p53 [34].

MCPyV is the only known polyomavirus that directly linked to human cancer [35]. MCPyV DNA clonally integrated into 80 % of the MCC tumors, and constant expression of MCPyV oncogenes required for MCC tumors cell survival, suggesting that the virus could be a causative agent in MCC tumors initiation and progression [35]. The polyomavirus genome consists of early and late coding regions that play a role in infectivity. The polyomavirus infection characterized by the expression of early antigens the large T antigen (LT), small T antigen (ST), and the 57 kD T antigen followed by late capsid proteins, such as VP1, VP2, and VP3 [36]. In MCC, the virus integrates into the genome at a nonspecific binding site and expresses the LT and ST antigens of viral oncogenesis [37]. The truncated domain of LT may play a role in shifting from the virus replication and virion release to clonal integration and tumorigenesis [38]. LT targets the RB1 and alter cell cycle progression and contributing to unregulated cell proliferation [39]. The ST bind the tumor suppressor protein phosphatase 2A regulates the function of F-box/WD repeat-containing protein 7 (FBXW7) in MCCs [40]. Murine models suggest that ST may be responsible for initiation of tumorigenesis, while LT maintains it, but the interplay of LT and ST in this oncogenic cascade has not been fully explored [41]. As mentioned above, the integration into the host genome is not part of the polyomavirus' normal life cycle gives rise the tendency that UV radiation may induce mutations in the viral genome that drive oncogenesis, while evasion of the immune response facilitates cellular proliferation [42].

1.2.3 **Diagnosis**

The clinical features of MCCs are a rapidly growing, cutaneous or subcutaneous tumor that is located mostly on the sun-exposed area, particularly the head and neck, less frequently, the genital part of body and buttocks [43, 44]. Lesions are red-to-violet nodules, which are

asymptomatic and multiple lesions arising at different body sites have been observed [15]. Ulceration is uncommon.

In addition to clinical examination, a biopsy's histopathological features and the immunological markers expression profile is sufficient for a definitive diagnosis. MCC cells express several of types I and II cytoskeletal keratins, such as cytokeratin 20 (CK20), CK8, CK18, and CK19 [45]. Also, MCC cells express neuroendocrine markers such as synaptophysin, chromogranin A, neural cell adhesion molecule 1 (CD56), neuron-specific enolase (NSE), calcitonin, neurofilament (NF), high molecular weight cytokeratin (CK-HMW), protein gene product 9.5/ubiquitin C-terminal hydrolase 1 (PGP9.5/UCHL-1), somatostatin, paired box protein Pax-5 (PAX5), DNA nucleotidylexotransferase (TdT) [45-47]. Positivity for oncoprotein huntingtin-interacting protein 1 (HIP1), cluster of differentiation 99 (CD99), mast/stem cell growth factor receptor Kit (CD117), epithelial cell adhesion molecule (EpCAM), neurogenic locus notch homologue protein 1 (NOTCH1) and tumor protein 63 (p63) has been observed [15, 48]. MCC is negative for thyroid transcription factor 1 (TTF1), transcriptional regulatory protein ASH1 (ASH1), vimentin, S100 calcium-binding protein B (S100B), and CK7 [15, 49].

The p63 linked associated with a worse prognosis, and variable numbers of tumor-infiltrating cytotoxic T lymphocytes in a subset of MCC cases related to a better prognosis for MCC patients [50, 51].

1.2.4 Treatment Options

To treat Merkel cell carcinoma using the following surgical procedures as the wide local excision and lymph node dissection [52]. The cancer specimen and a sentinel lymph node biopsy can be done during the surgery. After the cancer removal, some patients receive adjuvant therapy that is chemotherapy or radiation to kill any cancer cells that are left [52]. External radiation therapy is a machine outside the body to send radiation toward cancer [52]. External radiation therapy is used to treat Merkel cell carcinoma, and to relieve symptoms and improve quality of life as palliative therapy. Nowadays included in the course of Merkel cell carcinoma immunotherapy [53]. The immunotherapy treatment uses the patient's immune system to fight cancer. There are two types of immune checkpoint inhibitor

therapy: PD-1 inhibitor and CTLA-4 inhibitor [53, 54]. The PD-1 inhibitor is a protein on the surface of T cells that help keep the body's immune responses active. When PD-1 attaches to another protein called PDL-1 on a cancer cell, it stops the T cell from killing the cancer cell. PD-1 inhibitors attach to PDL-1 and allow the T cells to kill cancer cells [55]. Avelumab and pembrolizumab use to treat advanced Merkel cell carcinoma [55, 56]. Nivolumab studied to treat advanced Merkel cell carcinoma [56]. The CTLA-4 inhibitor is a protein on the surface of T cells that help keep the body's immune responses in check [54]. When CTLA-4 attaches to another protein called B7 on a cancer cell that stops the T cell kill the cancer cell. CTLA-4 inhibitors attach to CTLA-4 and allow the T cells to kill cancer cells [54]. Ipilimumab is a type of CTLA-4 inhibitor studied to treat advanced Merkel cell carcinoma [54].

1.3 Exosomes as a Source of Biomarkers

Exosomes are small (30-300 nm), circulating, membrane-bound vesicles, taken in via endocytosis from the outer cell membranes and released via exocytosis following membrane fusion of multivesicular bodies (MVBs) [57, 58]. Exosomes as a source of biomarkers have not entirely validated and explored yet.

1.3.1 Exosomes Sources

Exosomes can be isolated from nearly every fluid in the body, but for optimal diagnostic or prognostic value, blood is a reasonable first choice [59]. Blood contacts every organ system. Other biological fluids such as amniotic fluid, breast milk, saliva, tears, and urine content exosomes as well as *in vitro* in cell culture media [59].

1.3.2 Exosomes Characteristics

Exosomes created when intraluminal vesicles (ILVs) formed by inward budding of the endosomal membrane. These ILVs then cluster together to generate multivesicular bodies

that fuse with the plasma membrane and release their content as exosomes in the extracellular compartment [60, 61].

Initially, exosomes were considered to be involved in garbage disposal [62]. However, more experiments have revealed that exosomes are essential mediators for intracellular communication and subject to specific sorting mechanisms under both physiological and pathophysiological conditions, like cancer [63]. Increasing evidence suggests that exosomes are important in tumor growth and progression, cancer metastasis, avoiding apoptosis, mediate virus transmission and providing drug resistance [64-67].

1.3.3 Exosomes Composition

Exosomes formed to encapsulate a small sampling of the plasma membrane, which carries different types of molecules such as proteins, lipids, DNAs, RNAs, including mRNAs and microRNAs [68]. One of the more common exosomal cargos used in the diagnosis and prognosis of the disease is microRNAs (miRNAs) [68]. microRNAs are small non-coding RNAs, about 17-25 nucleotides in length. Their presence or absence used as a biomarker to directly predict disease risk, progression or remission [69]. Isolating miRNAs from exosomal fractions has been standardized and now its a commonly used method for enriching for disease-specific miRNAs from across the body or within a specific organ system [69]. Moreover, it has shown that exosomes derived from virus-infected cells, including the human tumor viruses Hepatitis C-virus (HCV), Epstein- Barr virus (EBV) and Kaposi's sarcoma-associated herpesvirus (KSHV), can contain both functional viral proteins and nucleic acids that can aid oncogenesis [70, 71]. It has also suggested that non-enveloped viruses deploy exosomes for infecting cells and immune system avoidance [71].

Decode disease states with exosome biomarkers, whether in a cell line or across a human population, still much to be gleaned the significant predictive value of these circulating messengers.

2 Chapter: Objective

The overall aim of this Ph.D. project was to investigate exosomes originated from MCPyV-negative and -positive MCC cell lines as a potential prognostic and diagnostic biomarker.

The specific objectives of **Paper I** are

1) To explore the protein content of MCC cell lines'-derived exosomes;

2) To perform the comparative analysis of exosomal protein expression originated from Merkel cell polyomavirus (MCPyV)-negative and MCPyV-positive MCC cell lines.

The specific objectives of **Paper II** are

1) To investigate the exosomal miRNAs from MCPyV-negative and –positive MCC cell lines' cells by next-generation sequencing (NGS);

2) To screen the significant exosomal miRNA findings in serum/plasma samples from healthy donors and patients.

The specific objectives of **Paper III** are

1) To investigate the MCC cell lines' cells' phenotype;

2) To perform comparative and integrative analyses to evaluate the role of exosomes on MCC cell lines.

3 Chapter: Choice of Methods

In this thesis were used experimental research methods, which described in detail in the individual studies. This part provides a broad overview of three methodologies such as proteomics, transcriptomics and high-dimensional data analyses for cancer-biomarkers discovery and methods' benefit and disadvantage.

3.1 Proteomics in Cancer Biomarkers Discovery

The technical approaches at the system level give great potential to aid in the identification of the novel therapeutic target and disease biomarkers. The proteome displays plasticity is owing to alternative splicing events, protein modifications, and the ability to merge into complexes and signaling networks [72]. Proteomics is the deciphering of how molecules interact as a system for our understanding of the functions of cellular systems in healthy and disease states. Post-translational modifications (PTMs) modulate protein activity, stability, localization, and capacity, which play essential roles in many critical cells signaling events both healthy and disease states [72-74]. Dysregulation of number of PTMs such as protein acetylation, glycosylation, hydroxylation, and phosphorylation implicated in a spectrum of human diseases including cancer [72-74]. Furthermore, genetic mutations give the rise different protein sequence variations, and alternative splicing are common causes of human diseases including cancer [75]. Discovery of potential biomarkers for MCC using Mass tandem spectrometry (MS) have chosen for the project. Protein identification by MS carried out in the form of whole-protein analysis, which is the top-down strategy (**Figure 2**). The top-down

strategy allows the complete characterization of protein isoforms and post-translational modifications [76, 77].

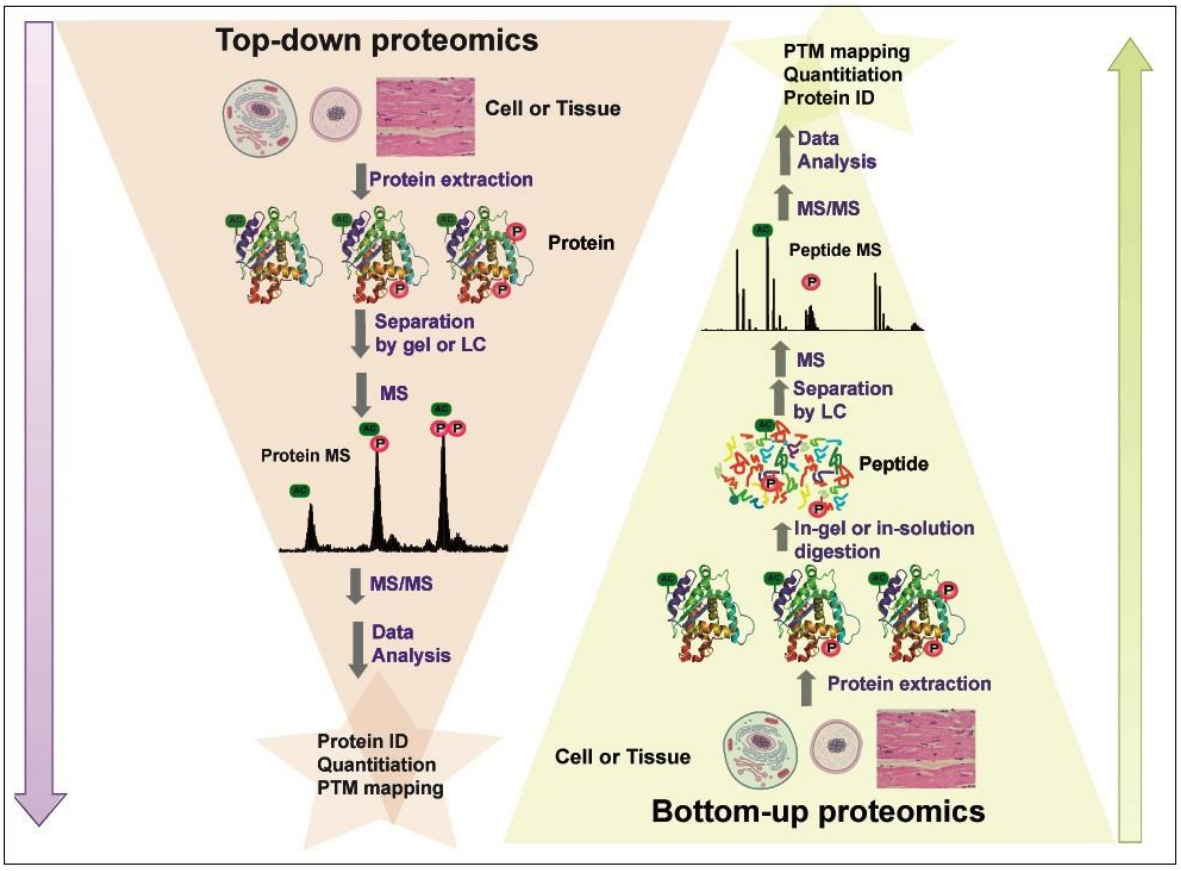

Figure 2. Procedures for MS-based protein identification and characterization. Proteins extracted from biological samples analyzed by bottom-up or top-down methods. The top-down approach fit for whole-protein analysis. The bottom-up strategy befits for analysis of enzymatically or chemically produced peptides.

We used Q Exactive HF-X hybrid Quadrupole-Orbitrap Mass Spectrometer. This MS involves a gas-phase ionization of intact proteins and subsequent high-resolution mass measurement of intact protein ions followed by their direct fragmentation inside the MS, particularly high-energy collision dissociation (HCD), without prior digestion [77, 78]. The proteins sequenced with higher activation energy and shorter activation time. HCD generates b- and y-type fragment ions, while the higher energy leads to a predominance of y-ions, b-ions can be fragmented to a-ions or smaller species [79]. This HCD ability provides more informative ion series that applied for de nonapeptide sequencing [79, 80]. For PTMs studies, certain

diagnostic ions specific to HCD could be recognized for PTMs identification. MS-based proteomics analysis detects PTMs that occurs on the amino acid side chains or the amine and carboxyl terminal of the protein [80, 81]. HCD works well for most stable modifications such as acetylation and methylation. HCD provides rich fragments ion spectra for phosphopeptides, and the optimized alternating acquisition method improves the identification coverage and accurate site localization for phosphoproteomics analysis [81]. HCD enables the identification of glycan structure and peptide backbone, allowing glycopeptide identification. HCD detects glycan oxonium ions from Orbitrap (MS2) [82]. Ubiquitination detection used alternative fragmentation or intelligent acquisition, which provides complementary information for peptide identification and modification site localization [83]. The protein S-nitrosylation is an extremely labile modification due to the nature of NO attachment to the specific protein cysteine suppressive peptide backbone fragmentation due to the neutral loss of NO group under the fragmentation mode [84]. SS-containing peptides efficiently can be fragmented with HCD in a Q Exactive Orbitrap MS, preserving SS for subsequent identification [85]. However, the top-down approach is facing challenges associated with protein solubility, separation, the detection of large intact proteins, as well as the complexity of the human proteome.

3.2 Transcriptomics: Comparative Evaluation of Exosomal microRNA Profiling by Next-Generation Sequencing and qPCR-based Method in Biofluids

MicroRNAs are a class of small RNAs that function as regulators involving in many biological processes [86]. The evaluation of miRNAs and their targets has aided by miRNA expression profiling studies including multiplex PCR, microarrays, and next-generation sequencing (NGS) tools [86-88]. In this project, the exosomal miRNA originated from MCPyV-negative and –positive MCC cell lines analyzed by NGS, and the main findings investigated in the

serum/plasma exosomal miRNAs from healthy donors and patients with MCC by the qPCR-based method.

There are pros with NGS [89, 90]:

- NGS provides thousands of genes profile in a single experiment;
- There are no background signal and cross-hybridization issues of microarrays;
- By NGS enables the identification of isomiRs, microRNA variants that differ in sequence or length from the annotated species in miRBase;
- NGS allows for the simultaneous confirmation of known miRNAs and discovery of new miRNAs;
- Costs reduced while providing billions of nucleotide information within a single experiment.

The procedure of generation of miRNA library for NGS is a prime part of the experiment (**Figure 3**) [90, 91]. The small RNA sequencing library generates by adapters ligated the miRNA in both ends, followed by reverse transcription (RT), template amplification by PCR and size selection of small RNA species. Several of these steps have shown to introduce biases and artifacts (**Figure 3**). Specific adapter-miRNA pairs or sequence compositions can be favored over others during ligation and PCR amplification, which resulting over- or underrepresentation of these miRNAs in the sequencing library [91]. The formation of adapter dimers or inefficient size-selection may lead to enrichment for miRNAs over other RNA species that are resulting in the reduced number of disposable reads [90, 91]. The major

challenge for the discovery of biofluids-based miRNA biomarkers is a low amount of RNA input [90, 91].

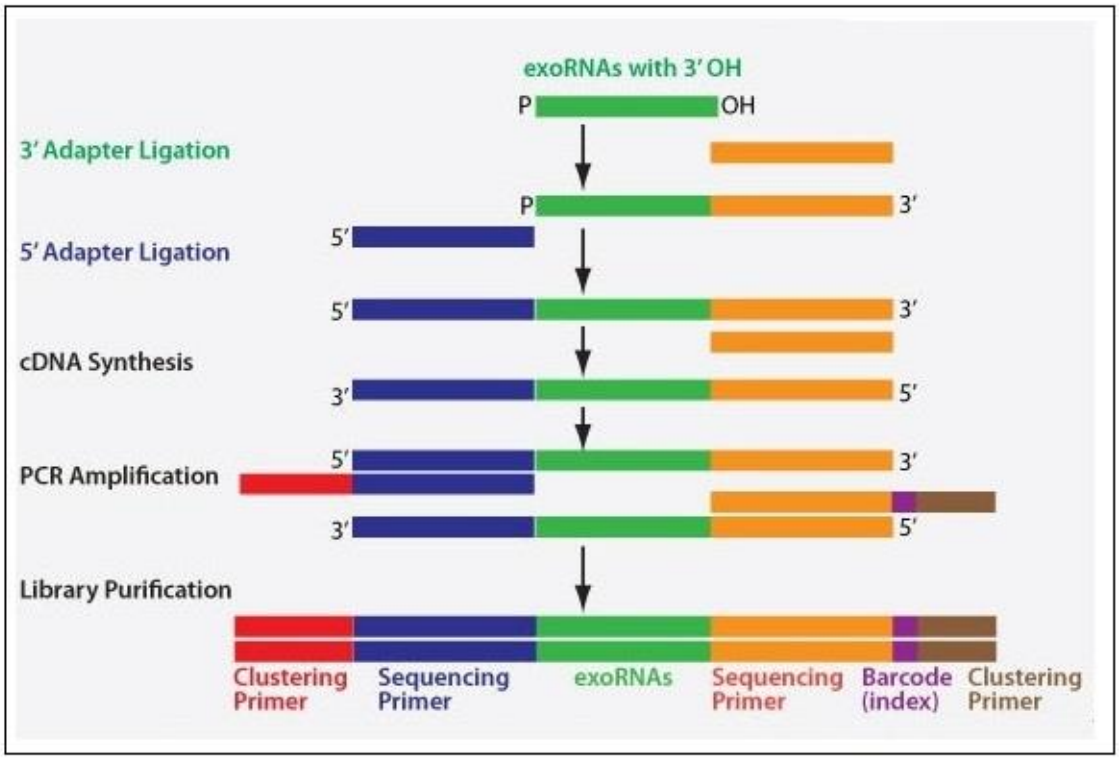

Figure 3. Overview of the small RNA sequencing library preparation workflow. Many kits adapted a ligation-based approach to attach 3' and 5' adapter to the miRNA. A unique barcode, unique molecular indices (UMI) connected at the RT stage. Illumina adapter and sequencing index for multiplexing added during the PCR amplification (https://www.biocat.com/ngs/exosomal-rna-sequencing).

There is an overall good agreement between NGS and qPCR, but some differences between the platforms, highlighting the importance of validation exist (**Table 1**) [92]. NGS and qPCR-based method differ in scalability and throughput. qPCR can detect only known sequences

and useful for low target numbers. The critical difference between NGS and qPCR-method is discovery power (89, 92).

Table 1. The benefits and challenges between the NGS and qPCR methods.

	NGS	qPCR
Benefits	• Higher discovery power • Higher sample throughput	• Familiar workflow • Equipment placed in most labs
Challenges	• Less cost-effective for low sequencing numbers of targets • Time-consuming for low sequencing numbers of targets	• A limited set of variants • No discovery power • Low scalability

3.3 **Biodata Platform and Analysis Tools**

Advances in high-throughput techniques including next-generation sequencing, RNA sequencing, and proteomics have generated an enormous volume of data [93–96]. The technological development reduces the amount of sample material, to collect raw data takes a short time and substantially decreased the costs. Hence, large-scale approaches are now available by many research laboratories. The complex high-throughput data interpretation needs software/bioinformatics tools, which are essential resources for the analysis [97-100].

Specific laboratories or groups and companies develop most of the software tools designed to perform the required examination for the group of data and professional [101].

In this project, for the comparative and integrated proteomic and sequencing data analyses performing used following different biodata platform and analysis tools:

The ExoCarta is a database for molecular data, such as proteins, RNA, and lipids, identified in exosomes [102]. The ExoCarta cataloged only exosomal studies reported by the authors, and the challenge is no segregation of extracellular vesicles (EVs) classes [102].

The Vesiclepedia is a repository with data from all types of EVs to understand molecular repertoire of a different kind of EVs and their biological functions [103]. Users can query or browse through proteins, lipids, and RNA molecules identified in EVs. The selected protein/miRNA of interest instructs to a gene page with information of external references to other primary databases, the experiment description of the study that identified the molecule, gene ontology-based annotations, protein-protein interactions, and a graphical display of network with relevance to molecules identified in EVs [103]. Gene ontology annotations of molecular functions, biological process, and subcellular localization retrieved from Entrez Gene [98]. The protein-protein interaction data obtained from HPRD, BioGRID, and Human Proteinpedia [104-107].

The FunRich is an open-access functional enrichment analysis tool for the omics data [108]. Using FunRich, users can perform functional enrichment analysis with minimal or no support from computational and database experts for more than 13,320 species. The database integrated from heterogeneous genomic and proteomic resources (>6.8 million annotations) [108]. The FunRich uniquely allows the users to update the background database for 13,320 species from UniProt, Gene Ontology and Reactome in real time [98, 108-110]. In miRNA enrichment analysis, users can submit a list of miRNA and identify biological pathways. Also, users can upload quantitative data and perform enrichment analysis for gene/protein

expression values [108]. The quantitative data can also be utilized to generate customizable heat maps. The FunRich allows users to download data from Vesiclepedia [108].

For the analysis and identification of miRNA-target interactions (MTIs), many web-based miRNA-related databases have established:

The miRBase is one of many primary miRNA sequence repositories that facilitate searches for comprehensive miRNA nomenclature, sequence, and annotation data [111].

The miRTarBase database aim is to provide a more comprehensive collection of experimentally supported MTIs in data content and the web-based function, to accelerate miRNA research [112].

The TargetScan is a web server for miRNAs target prediction by searching the presence of sites that match the seed region of miRNA [98, 111, 113-119].

Many databases integrated, such as:

- miRBase and HMDD for miRNA and disease information;
- The NCBI Entrez Gene and RefSeq for target gene information and 3' untranslated region of target sequences;
- The Gene Expression Omnibus (GEO) and The Cancer Genome Atlas (TCGA) for gene and miRNA expression profiling;
- KEGG and DAVID for functional annotations of miRNA target genes.

The PubMed integrated to provide article information [120].

The MaxQuant with the integrated **Andromeda** search engine is a quantitative proteomics software package, which designed for analyzing sizeable mass-spectrometric data sets, specifically a high-resolution MS data [121, 122]. Several labeling techniques and label-free quantification support the MaxQuant. MaxQuant is freely available. The download includes the search engine Andromeda integrated into MaxQuant and the viewer application for inspection of raw data, identification and quantification results [122]. For statistical analysis of MaxQuant output offers **the Perseus framework** [123].

The Perseus is a software platform for interpreting protein quantification, interaction and post-translational modification data [123]. The Perseus contains a broad scope of statistical tools for omics data analysis including normalization, pattern recognition, time-series

analysis, cross-omics comparisons, and multiple-hypothesis testing. A machine learning system supports the classification and validation of a group of samples for diagnosis and prognosis and detects predictive protein signatures [123, 124].

The Universal Protein Resource (**UniProt**) provides protein information [98]. The UniProt website provides ten main datasets and three main tools. The key UniProt datasets are the UniProt Knowledgebase (UniProtKB), the UniProt Reference Clusters (UniRef), the UniProt Archive (UniParc) and protein sets for completely sequenced genomes (Proteomes) [98, 125]. Supporting datasets include information about proteins that are present in UniProtKB protein entries like literature citations, taxonomy, subcellular locations, keywords, cross-referenced databases, and diseases [126]. The three tools that UniProt provides are the 'Blast' sequence search tool, the 'align' multiple sequence alignment tool and the 'Retrieve/ ID Mapping' tool, where users can upload lists of identifiers to download corresponding UniProt entries or map them to/ from external databases [125, 126].

The Proteome Discoverer is a software to process and report mass spectrometry data [127]. The raw data from mass spectrometry or spectral libraries compare the information from a selected **FASTA** database and identifies proteins from the mass spectra of digested fragments [127, 128]. The application does the following:

- The peak-finding search engines, such as Sequest™ HT and Mascot to process all MS data types and generate a peak list and relative abundances. The peaks represent the fragments of peptides with a given mass and charge [127];
- Results from several database searching engines and multiple analysis combine, filter and annotate [127].

The FASTA database utilities to add, delete, and find protein references and sequences [128].

The Gene Ontology (**GO**, www.geneontology.org) describes the function of gene products from all organism, specifically designed for supporting the computational representation of biological systems [98, 109, 129].

High-throughput techniques and big biological data analysis tools enable us to translate a massive amount of information for a better understanding of the basic biomedical

mechanisms and biomarkers discovery that further applicable to translational or personalized medicine.

4 Chapter: Summary of Main Results

4.1 Paper I. Secretomic Analysis of Extracellular Vesicles Originating from Polyomavirus-Negative and Polyomavirus-Positive Merkel Cell Carcinoma Cell Lines

In Paper I, we studied the protein content of MCC cell line-derived exosomes by mass tandem mass spectrometry. Since approximately 80% of all MCC cases contain Merkel cell polyomavirus (MCPyV), the exosome of two MCPyV-negative and two MCPyV-positive MCC cell lines compared. We identified with high confidence 164 exosome-derived proteins common for all four cell lines that annotated in ExoCarta and Vesiclepedia databases. These include proteins implicated in motility, metastasis and tumor progression, such as integrins and tetraspanins, intracellular signaling molecules, chaperones, proteasomal proteins, and translation factors.

4.2 Paper II. Comparative Analysis of microRNA Expression Profiles of Exosomes Derived from Polyomavirus-Negative and –Positive Merkel Cell Lines by Next-Generation Sequencing

In Paper II, we sequenced exosomal miRNAs of MCC cell lines MCPyV-negative and –positive, and main findings validated on exosomes from serum/plasma healthy donors and MCC patients by the qPCR-based method. Our results showed that the exosomal miR-222-3p presence in all type of samples derived from MCC cell lines, healthy donors and MCC patients. There is a statistically significant difference between the miR-222-3p levels in the exosome samples from MCPyV-negative and -positive MCC cell lines. The level of miR-222-3p in exosomes from MCPyV-negative MCC cell lines than MCPyV-positive, which we assume as a tumor environment. Because of previously in miRNA studies in MCCs were not the miR-222-3p mentioned, it indicates that the miR-222-3p sorted selectively in exosomes. Its expressed level dropped down dependent on cancer and viral status in MCC patients in the circulation system. The scanning of miR-222-3p target genes indicates that the exosomal miR-222-3p play pleiotropic role dependent on recipient cells in health and disease. Exosomes derived from MCCs may imply cell-to-cell communication within the tumor environment and the

circulation system. They appear to transport especially sorted functional proper such as miRNAs as messengers to target and recipient cells.

4.3 Paper III. Comparative and Integrated Analyses of Polyomavirus-Negative and –Positive Merkel Cell Carcinoma Cell Lines and their Exosomes Proteomic Profiles

In Paper III, using experimental and computational approaches, we identified MCPyV proteins in MCPyV-positive MCC cell lines and their extracellular vesicles. The viral oncoproteins large and small T-antigens detected in the MCPyV-positive cells, and exosomes derived from these cells. Our results suggest that exosomal transmission of MCPyV oncoproteins to recipient cells in the tumor microenvironment contributes to tumorigenesis. Moreover, our proteomic data may identify unique biomarkers for MCPyV-negative and –positive MCCs, reveal their origin and may allow the design of specific therapeutic strategies against two types of MCC with different phenotypes.

5 Chapter: General Discussion

In the present thesis, proteomics and transcriptomics provide an invaluable source of biological structures and function at proteins and global exosomal miRNAs levels in MCPyV-negative and –positive MCC cell lines and their exosomes.

This thesis aimed to research of MCC cell lines and their exosomes potential prognostic and diagnostic biomarkers by high-throughput techniques and big data analyses tools.

In this project done the first comparative proteomic study of exosomes originated from MCPyV-negative and –positive MCC cell lines (**Paper I**) and MCPyV-negative and –positive MCC cell lines to explore the phenotype of cells (**Paper III**). Proteomic profile revealed MCCs' cellular and molecular mechanisms of carcinogenesis and metastasis (**Paper III**). Moreover, we did the first study that identified MCPyV proteins in MCPyV-positive MCC cell lines and their extracellular vesicles by mass tandem spectrometry (**Paper III**). Integrative analyses of MCPyV cell lines and their extracellular vesicles from the previous study (PXD004198, **Paper I**) revealed that exosomes carried MCPyV oncoproteins, which may transmit to target and recipient cells in the tumor microenvironment and circulation system (**Paper III**). Furthermore, this is the first study that investigated the exosomal global miRNAs expression from MCPyV-negative and –positive MCC cell lines (**Paper II**). In addition, the screening done in exosomal serum/plasma samples from healthy donors and MCC patients (**Paper II**). Also, the current project provides proteomic and transcriptomic studies, and sharing data through publicly available data repositories with all research community for the understanding of MCCs pathophysiology (**Paper I, II,** and **III**). Proteomic and transcriptomic data are a core of biomarkers, which are highly specific in revealing information for diagnosis, prognosis, and therapy. Further analyses of high-dimensional data from this study may allow the design of specific therapeutic strategies against two types of MCC with different phenotypes (**Paper III**).

Update information

Exosomes are small bilayer proteolipid vesicles secreted by a variety of cell types, including MCC cell lines. Their sizes vary from 30-250 nm in diameter (**Paper I** and **II**). **In Paper I**, secretome profiling of two MCPyV-negative cell lines such as MCC13 and MCC26 and two

MCPyV-positive cell lines such as MKL1 and MKL2 resulted in the identification of 172 common microvesicular proteins of 500, 325, 258, and 228 proteins from MCC13, MCC26, MKL1, and MKL2, respectively. Variables of identified proteins' number explain the proteins expression variation between the cell lines and heterogeneity of human cancer [130]. The overlap with the Top 100 protein markers was about 69% (MCC13), 49% (MCC26), 47% (MKL1), and 39% (MKL2), and includes 37 exosomal markers (**Paper I**).

Five hundred thirteen biological pathways were composed of 114 proteins of 164 were mapped in the total network (**Paper I**). Cellular components comprise exosomes (71.2%), lysosome (43.6%), proteasome complexes (6.7%), and proteasome core complex (1.8%) with significance level $P<0.001$. Proteins from the extracellular region (33.7%, $P<0.001$) of Merkel carcinoma cell lines presuppose to located on the surface of EVs (**Paper I**). They might be potential biomarkers of MCC surface and proteins that recipient cells recognize, which allow the design of targeted treatment. Many of the exosomal proteins associated with metastasis and tumorigenesis/tumor progression: fibronectin [131, 132], thrombospondin [133], and laminin β1 [134]. Several of EVs proteins exploited as a therapeutic target: α-2-macroglobulin [135] and SERPINF1 [136], and others such as mannan-binding lectin serine peptidase 1 had an impact on the severity of disease in for example HCV infection [137] (**Paper I**). We identified the lactate dehydrogenase B at subnetwork mTOR pathway [130], and several 14-3-3 proteins at p75(NTR)-mediated signaling, p38 MAPK signaling and Wnt-pathway [138] (**Paper I**). The majority of proteins showed a positive association with autosomal dominant ($P<0.001$, **Paper I**). Chromosomal instability and loss of heterozygosity (LOH) are crucial steps in tumorigenesis [139]. The ranking of the EV proteins included in the network according to the enrichment analysis expressed in urine (89.0%), cerebrospinal fluid (73.0%), amniotic fluid (57.1%), saliva (49.1%), and tears (44.8%) with significance level $P<0.001$ (**Paper I**). The body fluids provide condition-specific biomarkers, which a potential source for diagnostic and development of targeted therapy [140, 141].

The computational analyses platform development gives us the opportunity to re-analyzed the raw data from the first study of exosomal proteomic profiling. In total, 311 proteins showed differential expression between two groups (***Supporting Information, Table S1***). We

performed hierarchical clustering to identify groups of samples with similar global protein expression profiles (**Figure 4**).

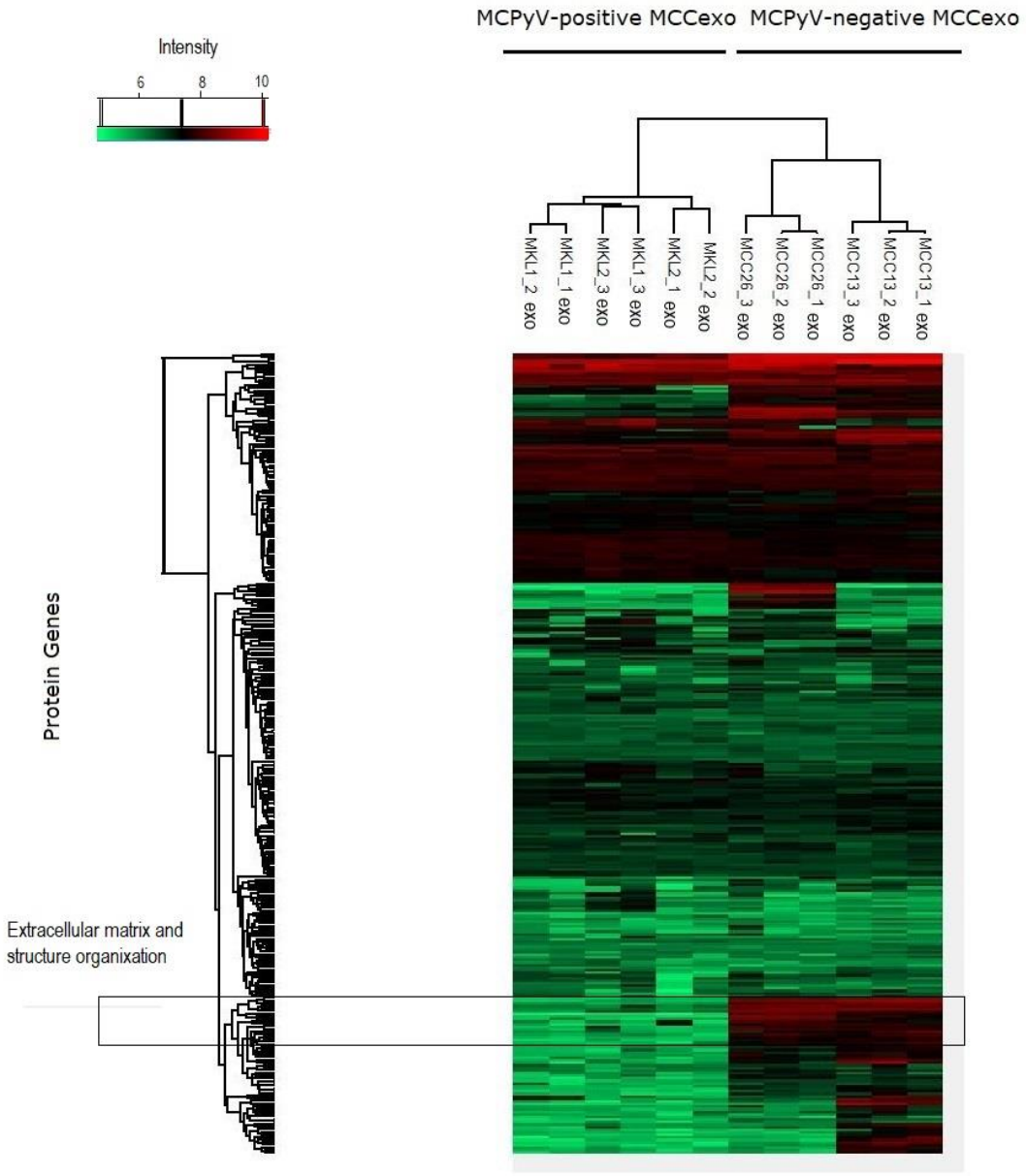

Figure 4. The dendrogram shows the hierarchical relationship between the samples with similar global protein expression profiles. The MCPyV-negative cell lines' exosomes are MCC13exo, MCC26exo, and the MCPyV-positive MCC cell lines' exosome are MKL1exo, MKL2exo. All sample run in triplicate. Each horizontal line

represents one protein/protein gene. In the box depicted differentially expressed proteins/protein genes involved in extracellular matrix and structure organization.

The differences in protein expression visualized in a principal components analysis (PCA) projection (**Figure 5**). The exosome from MCC cell lines formed different groups indicating that origin cells are distinct from each other.

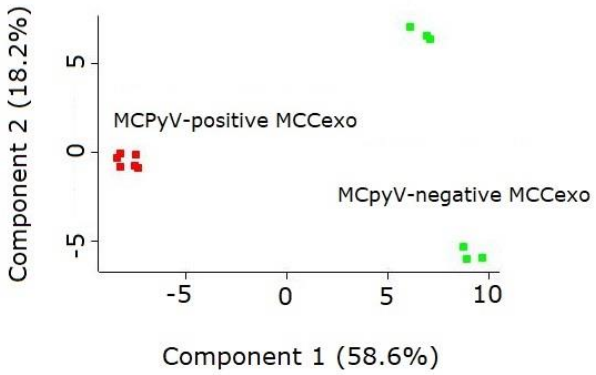

Figure 5. Two groups of different samples are exosomes originated from the MCPyV-negative and -positive cell lines, which depicted in a principal components analysis (PCA) projection.

In the PCA depicted differences due to origin cells are morphological, genetically and cultured discrepant [32, 45] (**Paper III)**. In line, a small number of proteins was uniquely differentially expressed between the exosome from MCPyV-negative and –positive MCC cell lines, depicted in **Figure 4**. Exosomes from MCPyV-negative MCC cell lines have upregulated proteins involved in biological pathways the extracellular structure (*P* = 9.39E-08) and extracellular matrix (*P* = 9.39E-08) organization, included 22 proteins (***Supporting Information, Table S2***). Nine exosomal proteins identified as biomarkers in different types of cancer, mesenchymal stem cells transition, and post-transcriptional regulation of gene expression, including the laminin subunit alpha-4 (LAMA4), fibulin-1 (FBLN1), transforming growth factor beta-1 (TGFB1), transforming growth factor beta-2 (TGFB2), annexin A2 (ANXA2), decorin (DCN), metalloproteinase inhibitor 1 (TIMP1), tenascin (TNC) and versican core protein (VCAN) [142-154]. Five of nine proteins the fibulin-1, transforming growth factor beta-1, transforming

growth factor beta-2, annexin A2, and decorin expressed in MCC cell lines and their exosomes (***Supporting Information, Table S3;*** **Paper I** and **III**). The increased expression of annexin A2, transforming growth factor beta-1 and -2 found in polyomavirus-negative MCC cell lines and their exosomes compared to virus-positive MCC cell lines and their exosomes. Also, the increased expression of fibulin 1 and decorin in exosomes from MCPyV-negative MCC cell lines observed. All proteins imply on the cell motility, signal transduction, endocytosis, exocytosis, activation for degradation of extracellular matrix (ECM) and basement proteins (BM) for cancer cell invasion and metastasis [143, 145, 146, 149, 150, 154, 155] (**Paper I** and **III**). These results agree with our finding in **Paper III,** and the MCPyV-negative MCC is aggressive cancer with resistance to anticancer drugs, shorter disease-free survival and worse overall survival [156, 157]. In addition, the result indicates a crucial role of exosomes as a messenger vehicle between cancer and healthy cells in the intercellular signaling in MCCs.

Exosomes contain cytosolic components, such as proteins, lipids, DNAs, RNAs, including mRNAs and microRNAs. **In Paper II**, the presented research proved that exosomes are stable in body fluids, including serum/plasma, and they can be isolated and preserved in PBS for long-term at -80 degrees [158]. In total, 519 miRNAs showed differential expression between two groups (**Paper II**). The finding showed that the miRNA existent patterns were not homogenous among the same cancer cell types, and exosomes of MCC cell lines contain a unique expression profile of miRNAs (**Paper II**).

Eight miRNAs such as miR-31-5p, miR-125b-1-3p, miR-143-3p, miR-222-3p, miR-584-5p, miR-141-3p, miR-375 and miR-532-5p selected based on their involvement in MCCs and other tumor types for further validation on serum/plasma samples from healthy donors and MCC patients by the qRT-PCR-based method. The qRT-PCR result confirmed the result from NGS that exosomal miR-222-3p upregulated in MCPyV-negative MCC cell lines. Moreover, the difference was statistically significant between the miR-222-3p expression levels in the exosomes from MCPyV-negative and -positive MCC cell lines (**Paper II**). There is evidence that the miRNA-222-3p promotes tumor cell migration and invasion and inhibits apoptosis, and it correlates with an unfavorable prognosis of patients with renal cell carcinoma, which support

results mentioned above of the exosomal proteomic study and the selectivity of miR-222-3p in exosomes [159] (**Paper I** and **II**).

Also, the exosomal miR-222-3p presented at a higher level in healthy condition than in pathophysiological state (**Paper II**). In the early studies, the plasma miR-222-3p identified as a robust intrinsic reference miRNA useful for the research of estrogen-responsive miRNAs in pregnancy [160]. The other study concluded that there was no significant difference in the designation of miRNAs between plasma and plasma-derived exosomal miRNAs, but the frequency was higher in plasma in healthy people [161].

Further, the investigation of exosomal miR-222-3p expression changes in progress upon viral and cancer status showed the statistically significant difference between the fold change in miR-222-3p expression in exosome samples from healthy donors and patients in relation to the MCC MCPyV-negative cell line (**Paper II**). This result indicates that the level of miR-222-3p in exosomes dropped down dependent on cancer and viral status of MCC in the circulation system, which may lead that target genes can become overexpressed distantly in recipient cells on higher proportion vid MCPyV-negative MCC and less vid MCPyV-positive MCC. There is evidence that the downregulation of miR-222-3p and upregulation of its target gene poly [ADP-ribose] polymerase 1 (PARP1) in the triple negative breast cancer patients associated with poor prognosis [162].

MiR-222-3p predicted target genes from three different databases (ExoCarta, TargetScan, and miRTarBase) showed 20 common targets (**Paper II**). The enrichment analysis showed that they expressed in leukocytes. The cancer cells and their exosomes likely interfere with the induction of an efficient immune response via several mechanisms inducing triggering T cell suppression mechanisms, attenuating NK cell cytotoxicity, and engaging pro-metastatic inflammatory processes and generating an immunosuppressive environment to escape from the immune system and eventually, treatment failure [163, 164]. Initially revealed that the exosomal miR-222-3p derived from epithelial ovarian cancer induces polarization of tumor-associated macrophages [165].

Further, transferred exosomal miR-222-3p into subcellular sites in recipient cells induced repression of expression target genes [166]. One of the miR-222-3p target gene is the SOCS

family, which is a major negative regulator of cytokine signaling that regulates development, subsets profiling and function of immune cells in carcinogenesis [167].

Moreover, the exosomal miR-222-3p demonstrated malignant characteristics and function such a regulator of gemcitabine resistance by targeting suppressor of cytokine signaling 3 (SOCS3) [166]. Further study, the hepatitis C virus (HCV) related immuno-pathogenesis found to be miR-222-3p enriched in exosomes from patients, which markedly reduced by direct-acting antiviral (DAA) therapy that consistent with our finding (**Paper II**). Exosomes from HCV patients inhibited natural killer cells (NK) degranulation activity and this effect correlated with the exosomal miR-222-3p level [168].

MiR-222-3p has described neither in tissues nor in cells from MCCs that support selectivity of exosomal miRNAs, particularly miR-222-3p [169-171]. Also, the enrichment analysis showed the predicted 6 of 20 common miR-222-3p targets expressed in MCC cell lines (**Paper II and III**). There are sorting nexin 4 (SNX4), Sad1 and UNC84 domain containing 2 (SUN2), stathmin 1 (STMN1), 14-3-3 protein gamma (YWHAG), RNA binding protein S1 (RNPS1), and karyopherin alpha 2 (KPNA2) identified as differentially expressed proteins in MCC cell lines (***Supporting Information, Table S4;*** **Paper I, II,** and **III**). Also, MCPyV-negative MCC cell line showed have upregulated protein expression on immune system process pathway (*P* = 2.64E-06), including 162 proteins (***Supporting Information, Table S5***; and **Paper III**).

There is a clear implication of exosomal miR-222-3p in the immunopathogenesis of MCCs. The sorting nexin 4, inner nuclear membrane protein SUN2, and RNA binding protein with serine-rich domain 1 were never mentioned to be associated with MCCs, but a stathmin 1 associated with MCPyV ST antigen, which mediates microtubule destabilization to promote cell motility and migration in MCCs [172, 173] (**Paper II** and **III**). The karyopherin alpha 2 induced expression found in MCCs and it is essential for ribosomal RNA (rRNA) transcription and protein synthesis in proliferating keratinocytes [174] (**Paper II** and **III**). Interestingly, MCC cell lines' exosomes content 14-3-3 protein gamma [175] (**Paper I, II** and **III**). The 14-3-3

protein gamma is one of the oncogenic Wnt pathway's activation factor, and an additional factor of PI3/Akt/beta-catenin signaling on cell proliferation [176, 177].

Recently, Chu and colleagues showed that level of miR-222 in the patient's group was significantly lower than in the healthy group, and their over-expression decreased cell proliferation and invasion in osteosarcoma [178]. This result agrees with our investigation result (**Paper II**). Moreover, reduced miR-222 promoted YWHAG expression and up-regulation of YWHAG restored the inhibiting effect of miR-222 mimics [178]. Wei and colleagues study of exosomal miR-222-3p concluded that a higher level of this exosomal miRNAs in serum usually predicted worse prognosis in non-small cell lung cancer (NSCLC) patients [166]. It can applyed to the cancer environment since MCPyV-negative MCC cell lines' exosomal miR-222-3p level higher compared the level in MCPyV-positive cell lines, and MCPyV-negative MCC patients have worse outcomes [19, 179] (**Paper II**). Thus, the result indicates the exosomal miR-222-3p and its targets play a pleiotropic role in MCC tumorigenesis and drug resistance.

Several MCC cell lines are available, but little has been done to characterize MCC cell lines phenotype. **In Paper III** (PXD012909), we analyzed global proteomics in seven MCC cell lines: the MCPyV-negative cell lines such as MCC13, MCC26, and UISO and the MCPyV-positive MCC cell lines such as MKL1, MKL2, MS1, and WaGa. In all samples, we identified 4898 proteins in total (**Paper III**). We performed statistical validation between each sample and each group of cell lines: MCC13, MCC26, UISO, and MKL1, MKL2, MS1, and WaGa, and as MCPyV-negative and –positive cell lines, respectively. In total, 3312 proteins of 4898 identified showed differential expression between two groups (**Paper III**). Guastafierro and colleagues identified differences in various diagnostic markers for MCCs between MCPyV-negative and –positive cell lines by immunohistochemistry analysis (IHC) [45] (**Paper III**). According to another study, the IHC diagnostic panel includes the neurofilament as a positive marker also [46]. In comparison to data published previously, this study is the proteomic profile, and sample expanded to include WaGa (***Supporting Information, Table S6.A,*** and ***S6.B;*** and **Paper III**). We found in all samples expressed cytokeratin 20, pan-keratin, cytokeratin 1, cytokeratin 8, cytokeratin 18, neuron-specific enolase, chromogranin A. MCC13 expressed a high number

of unique peptides for cytokeratin 7 (CK7) compare to other cell lines, except MKL1, which is negative for CK7. Synaptophysin expressed only in MCPyV-positive cell lines, and all cell lines are negative for leukocyte common antigen and thyroid transcription factor 1.

Also, we looked for all neurofilament subunit proteins and corresponded to the previous study result [46]. Our study showed the MCPyV-positive MCC cell lines have a high number of unique proteins for the low molecular weight neurofilament protein (FN-L) compared to MCPyV-negative MCC cell lines. This result agrees with the previous study result ***(Supporting Information, Table S6.C)***. Further, MCPyV-positive MCC cell lines expressed a high number of unique peptides for the medium molecular weight neurofilament protein (NF-M) and neuronal intermediate filament proteins, alpha-internexin compared to MCPyV-negative cell lines. MCPyV-negative MCC cell lines are negative for the high molecular weight neurofilament protein (FN-H). The peripherin is negative in MCC13, MCC26 and WaGa, and a high number of unique peptides found in MKL2. A high amount of neuronal intermediate filament protein, nestin, found in MCC13 and UISO.

Finally, we investigated expression of neural cell adhesion molecule 1 (NCAM1), ubiquitin C-terminal hydrolase 1 (PGP9.5/UCHL1), oncoprotein hunting-interacting protein 1 (HIP1), epithelial cell adhesion molecule (EpCAM), and vimentin (VIM) mentioned in other studies [15, 45-49] ***(Supporting Information, Table S6.D)***. The neural cell adhesion molecule 1, ubiquitin C-terminal hydrolase 1, and oncoprotein hunting-interacting protein 1 upregulated in MCPyV-positive cell lines compared to MCPyV-negative MCC cell lines. The vimentin over-expressed in MCPyV-negative MCC cell lines compared to MCPyV-positive MCC cell lines. The only epithelial cell adhesion molecule is uniquely expressed in MCPyV-positive cell lines (**Paper III**).

Results consistent with the IHC diagnostic panel and other MCC markers' studies, but with the proteomic approach was detected even a small amount of proteins in samples, and proteins expression differentiates cell types. The result confirmed that the proteomic method is the more sensitive approach for cells phenotyping and exploring biomarkers.

We performed hierarchical clustering to identify groups of samples with similar global protein expression profiles (**Paper III**). The MCPyV-negative cell line samples formed a group

divergent from the MCPyV-positive cell line, indicating that these cell lines are distinct from each other. These differences in protein expression can also be visualized in a principal components analysis (PCA) projection (**Paper III**). The result supports previous comparative studies between MCC cell lines [45, 180]. In line, many proteins uniquely differentially expressed between the MCPyV-negative and –positive MCC cell lines. The Spearman's rank correlation coefficients between individual expression profiles of MCC cell lines calculated to find the relationship in protein expression between MCPyV-negative and –positive MCC cell lines. The result showed a strong, positive correlation, r = 0.70, n = 9, *P* = 0.0433 (**Paper III**). Two major clusters with a size of 1510 and 1170 proteins differentially expressed between MCPyV-negative and –positive MCC cell lines include 61 (***Supporting Information, Table S7***) and 46 (***Supporting Information, Table S8***) biological pathways upregulated with MCPyV-negative and -positive MCC cell lines, respectively (**Paper III**). Proteomic profile revealed MCC cellular and molecular mechanisms of carcinogenesis and metastasis. MCPyV-positive MCC cell line cells had up-regulated proteins involved in cellular pathways among epigenetic regulation of gene expression (*P* = 5.83E-07), histone modification (*P* = 2.82E-04), gene silencing (*P* = 6.46E-04), and transcription from RNA polymerase II promoter (*P* = 5.15E-06) (***Supporting Information, Table S9***). In addition, data indicates that they have active control over DNA replication (*P* = 1.89E-12), DNA recombination (*P* = 8.15E-09), DNA modification (*P* = 1.11E-03), DNA-dependent transcription termination (*P* = 1.73E-04), DNA repair (*P* = 3.52E-07), and DNA ligation (*P* = 8.93E-03) (***Supporting Information, Table S10***). These actions are essential at single and double breaks in duplex DNA molecules and proliferating cells. MCPyV-positive MCCs have a low mutational burden, which explained by high activity and regulation of transcriptional, translational and repair system [181]. The increased demand for DNA synthesis required on one-carbon (*P* = 3.01E-03), nucleobase-containing (*P* = 7.94E-22), cellular nitrogen compound (*P* = 7.08E-22), and nitrogen compound (*P* = 1.43E-20) metabolic processes for the proliferative cancer phenotype [182-184] (***Supporting Information, Table S11***). Upregulated nitrogen metabolic processes indicate that glutamine and asparagine (*P* = 2.64E-03) use for supporting high proliferative polyomavirus-transformed cells [183] (***Supporting Information, Table S11***). Cancer cells enhance "aerobic" glycolysis for the

support the rapid cell proliferation [185, 186]. This so-called Warburg effect seems to apply for MCPyV-positive MCC cell lines because they have upregulated expression of proteins involved in oxidative phosphorylation (*P* = 4.06E-03), particularly the NADH dehydrogenase complex (*P* = 1.87E-05) associated with mitochondrion (*P* = 1.05E-02) (***Supporting Information, Table S12***). An active transforming cell phenotype requires high energy. Lactate dehydrogenase B (LDHB) catalyzes the reversible conversion of lactate to pyruvate, and NAD to NADH, in the glycolytic pathway. With NADH accumulation decreased mitochondrial oxidative phosphorylation [187]. Cells that have a greater impairment of oxidative phosphorylation and high NADH production become more aggressive and metastatic phenotypes like the MCPyV-positive MCC [187]. In contrast, the MCPyV-negative MCC cell lines profile indicates that cells' metabolism switched to amine (*P* = 1.57E-03), polysaccharide (*P* = 8.61E-03) and carbohydrate (*P* = 4.20E-03) metabolic processes for cell growth (*P* = 1.05E-02), proliferation (*P* = 4.99E-03) and differentiation (*P* = 1.64E-03) (***Supporting Information, Table S13***). Polyamines play a pleiotropic role, from modulating nucleic acid conformation to promoting cellular proliferation and signaling (signal transduction, *P* = 4.55E-06; ***Supporting Information, Table S14***). [188]. Lipid particles (*P* = 7.49E-03) indicate ongoing energy store and a repository of fatty acids for potentially phospholipid biosynthesis [189] (***Supporting Information, Table S15***). Moreover, proteins involved in cell motility (*P* = 4.40E-04), maintenance of cell polarity (*P* = 5.47E-03), cell surface (*P* = 4.05E-09), locomotion (*P* = 9.57E-05), and cellular membrane organization (*P* = 7.49E-04) were upregulated indicating high invasiveness and metastasis of the MCPyV-negative MCC cells [190] (***Supporting Information, Table S16,*** **Paper I, II** and **III**). Post-translational modification such as protein glycosylation (*P* = 1.04E-05), peptidyl-amino acid modification (*P* = 2.05E-04), protein folding (*P* = 4.86E-03), and protein modification process regulation (*P* = 5.24E-03) were observed (***Supporting Information, Table S17***). Upregulation of protein glycosylation of surface molecules showed a key feature of cancer cells, which use the endoplasmic reticulum (ER, *P* =1.35E-08)/Golgi apparatus (*P* = 1.28E-03) to add carbohydrates to their cumulative glycoproteins [191] (***Supporting Information, Table S18***). Thus, data indicates that the MCPyV-negative MCC cell lines have a low expression of proteins in DNA, RNA and protein synthesis and regulation, but

have upregulated proteins engaged in post-translational modification. In these circumstances, cancer progression and high cell proliferation may lead to transcription-associated mutation (TAM) and transcription-associated recombination (TAR) that gave a rise a high mutational burden of MCPyV-negative MCC [181, 192-194].

We reused the previous study of proteomic data for integrated analysis and researched Merkel cell polyomavirus proteins in exosome samples from MCPyV-positive MCC cell lines (PXD004198, **Paper I**). Computational approach developments and ongoing proteomic studies of oncogenic viruses, particularly MCPyV, give us the opportunity to detect MCPyV proteins in MCPyV-positive MCC cell lines and their extracellular vesicles (**Paper III**).

Exosomes derived from virus-positive MCC cells are not only packed with cellular compounds, but they also contain viral protein fragments of large T antigen, LT chain E, small T antigen, major capsid protein VP1, and minor capsid protein VP2 (MKL2 exosomes). Also, integrated data of cellular and extracellular vesicles proteomic profiles showed that the cellular endosome transport and extracellular vesicles contain proteins involved in viral reproduction (P = 1.39E-03) similarly abundant in both MCC cell lines and their exosomes, but upregulated in MCPyV-positive cell lines *(**Supporting Information, Table S19**)*. However, upregulated proteins involved in endocytosis (P = 3.27E-06), exocytosis (P = 9.04E-03), vesicle-mediated transport (P = 8.24E-10), Golgi vesicle transport (P = 2.31E-05) and protein transport (P = 4.69E-03) were associated with MCPyV-negative MCC cell lines (***Supporting Information, Table S20****)*.

Except that, exosomes from MCPyV-negative cell lines were most abundant with extracellular vesicles-ER accession proteins. In contrast, the valosin-containing protein (VCP), aconitase 1 (ACO1) and argininosuccinate synthase 1 (ASS1) were only proteins detected in extracellular vesicles from MCPyV-positive cell lines. The valosin-containing protein required for the fusion of ER and Golgi membranes. The valosin-containing protein is a membrane ATPase involved in ER homeostasis and ubiquitination [195, 196]. The aconitase 1 is the moonlighting protein based on its ability to perform mechanistically distinct functions. One of the aconitase 1 ability is to bind glucose-regulated protein 94 kDa (Grp94), which is the ER-localized isoform of heat shock protein 90 (Hsp90). The Hsp90 is responsible for trafficking and maturation of

Toll-like receptors, immunoglobulins, and integrins [197]. The argininosuccinate synthase 1 is a key enzyme in the citrulline-nitric oxide (NO) cycle, which can be upregulated by nitrogen efflux at Kaposi's sarcoma-associated herpesvirus (KSHV) infection and an acid-induced downregulation contributes to the maintenance of intracellular pH in cancer [198, 199]. Evolutionary, exosomes maintain cellular homeostasis by carrying cellular remains from the misfolded proteins loaded on the ER through the Golgi and subsequently remove these waste products by exocytosis to prevent genotoxic conditions [63]. Data analysis suggests that MCPyV use the functional exosome secretion for their promotion through to ability packed exosomes in a certain condition with virus proteins, which end up in ER as misfolded proteins. The preserved virus protein in an exosome can proceed on the way to out of cells. Thus, extracellular vesicles as a cellular communication's mediators help facilitate the transfer of viral compounds to new cells in a cancer environment or/and distantly to recipient cells and promote pathogenic processes [200].

Limitations

These project findings require further evaluation studies. Development of methods with higher discovery power gives the rise the requirement to choose experimental methods to evaluate the result. Experimental validation of identified biomarkers in a completely independent data set representing an appropriate experimental system provides reliable, high-quality evaluation, but it costs and requires time.

Privacy and Ethics

In Paper II, the clinical samples from MCC patients used. The Ethics Committee of Karolinska Institutet approved the study, and all patients provided informed consent in written form.

This thesis content TEM pictures generated in collaboration with the Institute of Medical Biology, Core Facility of Advanced Microscopy, University of Tromsø, The Arctic University of Norway, Tromsø, Norway.

6 Chapter: Conclusions

The **Paper I** conclusion is our results showed that MCPyV-negative and –positive Merkel cell lines' exosomes contain several proteins associated with tumor cell motility and metastasis. Importantly, we identified a list of vesicular proteins derived from the extracellular region, which upregulated in exosome from MCPyV-negative MCC cell lines compare to MCPyV-positive MCC cell lines. They could reveal biomarkers specific for MCCs identification and exosomes recognition proteins by target and recipient cells.

The **Paper II** conclusion is our results showed that the exosomal miR-222-3p presence in all type of samples derived from MCC cell lines, healthy donors and MCC patients. There was a statistically significant difference between the miR-222-3p levels in the exosome samples from MCPyV-negative and -positive MCC cell lines. MCPyV-negative MCC cell lines' exosomal miR-222-3p was a higher level than MCPyV-positive MCC cell lines. The miR-222-3p selectively sorted, and its expressed level dropped down dependent on cancer and viral status in MCC patients in the circulation system. The target genes' scanning indicates that the exosomal miR-222-3p play pleiotropic role dependent on recipient cells in health and disease. Exosomes derived from MCC may imply cell-to-cell communication within the tumor environment and the circulation system. They appear to transport specifically sorted functional proper such as miRNAs as messengers to target and recipient cells.

Finally, the **Paper III** conclusion is a proteomic approach is a powerful tool for cell phenotyping and biomarkers discovery. To understand the underlying mechanisms of virus-independent and virus-dependent MCCs, we compared the proteome of MCPyV-negative (MCC13, MCC26, and UISO) and MCPyV-positive (MKL-1, MKL-2, MS-1, and WaGa) MCC cell lines. In total 4898 proteins were identified, of which 3312 differentially expressed between the virus-negative and virus-positive cell lines. Then, the MCPyV-negative MCC cell lines indicates to loss DNA, RNA and protein synthesis and their regulation system activity, and have an unusual event of protein expression at cell proliferation and post-translational modification sites that may lead to transcription-associated mutation (TAM) and

transcription-associated recombination (TAR), which gave a rise a high mutational burden. The MCPyV-positive MCC cell lines showed upregulated expression of proteins involved in DNA transcription initiation, termination, and repair, may harnesses of polyomaviruses for DNA integration. Following upregulated proteins of RNA, protein synthesis and modification machinery such as the protein acylation culminates in the viral proteins and genome synthesis. However, a fixed exosome-ER accession ability and a low activity on endocytosis and exocytosis sites indicate to reduce the chance of MCPyV spreading.

7 Chapter: References

1. A. W. Lambert, et al. Emerging biological principles of metastasis. *Cell*. **2017**, 168, 670-691.

2. J. E. Ma, and J. D. Brewer, et al. Merkel cell carcinoma in immunosuppressed patients. *Cancers (Basel).* **2014**, 6, 1328-1350.

3. I. Agache, and C. A. Akdis. Precision medicine and phenotypes, endotypes, genotypes, regiotypes, and theratypes of allergic diseases. *J. Clin. Invest*. **2019,** 130, 124611.

4. N. Goossens, et al. Cancer biomarker discovery and validation. *Transl. Cancer Res*. **2015**, 4, 256-269.

5. V. O. Puntmann. How-to guide on biomarkers: biomarker definitions, validation and applications with examples from cardiovascular disease. *Postgrad. Med. J.* **2009**, 85, 538-545.

6. K. Strimbu, and J. A. Tavel. What are biomarkers? *Curr. Opin. HIV AIDS.* 2010, 5, 463-466.

7. A. A. AlSalloom. An update of biochemical markers of hepatocellular carcinoma. *Int. J. Health. Sci (Qassim).* **2016**, 10, 121-136.

8. R. E. Lane, et al. Extracellular vesicles as circulating cancer biomarkers: opportunities and challenges. *Clin. Transl. Med.* **2018**, 7, 14.

9. S. Mehta, et al. Predictive and prognostic molecular markers for cancer medicine. *Ther. Adv. Med. Oncol*. **2010**, 2, 125-148.

10. E. Nalejska, et al. Prognostic and predictive biomarkers: Tools in Personalized Oncology. *Mol. Diagn. Ther.* **2014**, 18, 273-284.

11. M. Nagpal, et al. Tumor markers: A diagnostic tool. *Natl. J. Maxillofac. Surg.* **2016**, 7, 17-20.

12. J. F. Gainor, et al. Pharmacodynamic biomarkers: falling short of the mark? *Clin. Cancer Res.* **2014**, 20, 2587-2594.

13. H. Uchi. Merkel cell carcinoma: An update and immunotherapy. *Front. Oncol.* **2018**, 8, 48.

14. A. Stang, et al. The association between geographic location and incidence of Merkel cell carcinoma in comparison to melanoma: An international assessment. *Eur. J. Cancer.* **2018**, 94, 47-60.

15. J. C. Becker, et al. Merkel cell carcinoma. *Nat. Rev. Dis. Primers.* **2017**, 3, 17077.

16. A. Zur Hausen, et al. Early B-cell differentiation in Merkel cell carcinomas: clues to cellular ancestry. *Cancer res.* **2013**, 73, 4982-4987.

17. T. Tilling, et al. Immunohistochemical analyses point to epidermal origin of human Merkel cells. *Histochem. Cell Biol.* **2014**, 141, 407-421.

18. T. S. Wang, et al. Merkel cell carcinoma: Update and review. *Semin. Cutan. Med. Surg.* **2011**, 30, 48-56.

19. D. Schadendorf, et al. Merkel cell carcinoma: Epidemiology, prognosis, therapy and unmet medical needs. *Eur. J. Cancer.* **2017**, 71, 53-69.

20. O. Zaar, et al. Merkel cell carcinoma incidence is increasing in Sweden. *J. Eur. Acad. Dermatol. Venereol.* **2016**, 30, 1708-1713.

21. H. Kukko, et al. Merkel cell carcinoma – a population-based epidemiological study in Finland with a clinical series of 181 cases. *Eur. J. Cancer.* **2012**, 48, 737-742.

22. P. I. Song, et al. The clinical profile of Merkel cell carcinoma in Mainland China. *Int. J. Dermatol.* **2012**, 51, 1054-1059.

23. K. Hemminki, et al. Kaposi sarcoma and Merkel cell carcinoma after autoimmune disease. *Int. J. Cancer.* **2012**, 131, E326-E328.

24. C. M. Vajdic, et al. Cancer incidence and risk factors after solid organ transplantation. *Int. J. Cancer.* **2009**, 125, 1747-1754.

25. E. Lanoy, et al. Skin cancers associated with HIV infection and solid-organ transplantation among elderly adults. *Int. J. Cancer.* **2010**, 126, 1724-1731.

26. L. Popovic, et al. Concurrent chronic lymphocytic leukemia and Merkel cell carcinoma in primary skin tumor and metastatic lymph node. Indian. *J. Hematol. Blood Transfus.* **2014**, 30, 422-424.

27. V. Koljonen, et al. Joint occurrence of Merkel cell carcinoma and non-Hodgkin lymphomas in four Nordic countries. *Leuk. Lymphoma.* **2015**, 56, 3315-3319.

28. N. Li, et al. Merkel cell carcinoma metastatic to cervical lymph node in a patient with rheumatoid arthritis: a case report. *OncoTargets Ther.* **2019**, 12, 1395-1400.

29. D. Tsuruta, et al. Merkel cell carcinoma, Bowen's disease and chronic occupational arsenic poisoning. *Br. J. Dermatol.* **1998**, 139, 291-294.

30. M. Heath, et al. Clinical characteristics of Merkel cell carcinoma at diagnosis in 195 patients: the AEIOU features. *J. Am. Acad. Dermatol.* **2008**, 58, 375-381.

31. A. T. Saini, and B. A. Miles. Merkel cell carcinoma of the head and neck: pathogenesis, current and emerging treatment options. *OncoTarget Ther.* **2015**, 8, 2157-2167.

32. D. J. Erstad, and J. C. Cusack, Jr. Mutational analysis of Merkel cell carcinoma. *Cancers (Basel).* **2014**, 6, 2116-2136.

33. W. Liu, et al. Merkel cell polyomavirus infection and Merkel cell Carcinoma. *Curr. Opin. Virol.* **2016**, 20, 20-27.

34. G. Goa, et al. Mutational landscape of MCPyV-positive and MCPyV-negative Merkel cell carcinomas with implications for immunotherapy. *Oncotarget.* **2016**, 7, 3403-3415.

35. Y. Chang, and P. S. Moore. Merkel cell carcinoma: A virus-induce human cancer. *Annu. Rev. Pathol.* **2012**, 7, 123-144.

36. K. Coggshall, et al. Merkel cell carcinoma: An update and review: Pathogenesis, diagnosis, and staging. *J. Amer. Acad. Dermatol.* **2018**, 78, 433-442.

37. G. Stakaitytè, et al. Merkel cell polyomavirus: Molecular insights into the most recently discovered human tumor virus. *Cancer.* **2014**, 6, 1267-1297.

38. C. F. Baez, et al. Human polyomavirus: The battle of large and small tumor antigens. *Virology (Auck).* **2017**, 8, 1178122X17744785.

39. S. Borchert, et al. High-affinity Rb binding, p53 inhibition, subcellular localization, and transformation by wide-type or tumor-derived shortened Merkel cell polyomavirus large T antigens. *J. Virol*. **2014**, 88, 3144-3160.

40. S. Bhattacharjee, and S. Chattaraj. Entry, infection, replication, and egress of human polyomaviruses: an update. *Can. J. Microbiol*. **2017**, 63, 193-211.

41. M. E. Spurgeon, et al. Tumorigenic activity of Merkel cell polyomavirus T antigens expressed in the stratified epithelium of mice. *Cancer Res.* **2016**, 75, 1068-1079.

42. M. K. White, et al. Viruses and human cancers: a long road of discovery of molecular paradigms. *Clin. Microbiol. Rev.* **2014**, 27, 463-481.

43. D. P. Sarma, et al. An unusual clinical presentation of Merkel cell carcinoma: A case report. *Case Rep. Med*. **2010**, 2010, 905414.

44. M. J. Perman, et al. Giant Merkel cell carcinoma masquerading as a benign cyst on the buttock of an african american man. *Case Rep. oncol. Med.* **2011**, 2011, 849767.

45. A. Guastafierro, et al. Characterization of an early passage Merkel cell polyomavirus-positive Merkel cell carcinoma cell line, MS-1, and its growth in NOD scid gamma mice. *J. Virol. Methods.* **2013**, 187, 6-14.

46. S. Pasternak, et al. Immunohistochemical profiles of different subsets of Merkel cell carcinoma. *Hum. Pathol.* **2018**, 82, 232-238.

47. M. Sur, et al. TdT expression in Merkel cell carcinoma: potential diagnostic pitfall with blastic hematological malignancies and expanded immunohistochemical analysis. *Mod. Pathol.* **2007**, 20, 1113-1120.

48. M. A. Heather, et al. Huntingtin Interacting Protein 1: a Merkel cell carcinoma marker that interact with c-Kit. *J. Invest. Dermatol.* **2011**, 131, 2113-2120.

49. M. Bobos, et al. Immunohistochemical distinction between merkel cell carcinoma and cell carcinoma of the lung. *Am. J. Dermatopathol.* **2006**, 28, 99-104.

50. G. Y. Stetsenko, et al. p63 expression in Merkel cell carcinoma predicts poorer survival yet may have limited clinical utility. *Am. J. Clin. Pathol.* **2013**, 140, 838-844.

51. H. Sihto, et al. Tumor infiltrating immune cells and outcome of Merkel cell carcinoma: a popular-based study. *Clin. Cancer Res*. **2012**, 18, 2872-2881.

52. P. Tai. A practical update of surgical management of Merkel cell carcinoma of the skin. *ISRN Surg.* **2013**, 2013, 850797.

53. K. Nagase, and Y. Narisawa. Immunotherapy for Merkel cell carcinoma. *Curr. Treat. Options Oncol.* **2018**, 19, 57.

54. B. A. Williams, et al. A case of Merkel cell carcinoma treated with anti-CTLA-4 antibody (Ipilimumab). *J. Clin. Case Rep.* **2015**, 5, 659.

55. M. Baker, et al. Avelumab: a new standard for treating metastatic Merkel cell carcinoma. *Expert. Rev. Anticancer Ther.* **2018**, 18, 319-326.

56. I. S. Chan, et al. Immunotherapy for Merkel cell carcinoma: a turning point in patient care. *J. Immunother. Cancer*. **2018**, 6, 23.

57. C. Ciardiello, et al. Focus on extracellular vesicles: new frontier of cell-to-cell communication in cancer. *Int. J. Mol. Sci*. **2016**, 17, 175.

58. V. S. Chernyshev, et al. Size and shape characterization of hydrated and desiccated exosomes. *Anal. Bioana.l Chem.* **2015**, 407, 3285-3301.

59. S. Boukouris, and S. Mathivanan. Exosomes in bodily fluids are a highly stable resource of disease biomarkers. *Proteomics Clin. Appl.* **2015**, 9, 358-367.

60. S. Mathivanan, et al. Exosomes: extracellular organelles important in intercellular communication. *J. Proteomics.* **2010**, 73, 1907-1920.

61. Y. H. Soung, et al. Emerging roles of exosomes in cancer invasion and metastasis. *BMB Rep***. 2016**, 49, 18-25.

62. R. M. Johnstone, et al. Reticulocyte maturation and exosome release: transferrin receptor containing exosomes shows multiple plasma membrane functions. *Blood.* **1989**, 74, 1844-1851.

63. A. Takahashi, et al. Exosomes maintain cellular homeostasis by excreting harmful DNA from cells. *Nat. Commun*. **2017**, 8, 15287.

64. K. Al-Nedawi, et al. Intercellular transfer of the oncogenic receptor EGFRvIII by microvesicles derived from tumour cells. *Nat. Cell Biol*. **2008**, 10, 619-624.

65. W. Zhou, et al. Exosomes mediate Zika virus transmission through SMPD3 neutral Sphingomyelinase in cortical neurons. *Emerg. Microbes Infect*. **2019**, 8, 307-326.

66. J. Wang, et al. Exosomes released from Rabies virus-infected cells may be involved in the infection process. Virol. Sin. 2019, 34, 59-65.

67. A. S. Azmi, et al. Exosomes in cancer development, metastasis and drug resistance: A comprehensive review. *Cancer Metastasis Rev.* **2013**, 32, 10.1007/s10555-013-9441-9.

68. J. Marrugo-Ramirez, et al. Blood-based cancer biomarkers in liquid biopsy: A promising non-invasive alternative to tissue biopsy. *Int. J. Mol. Sci.* **2018**, 19, 2877.

69. A. Thind, and C. Wilson. Exosomal miRNAs as cancer biomarkers and therapeutic targets. *J. Extracell. Vesicles.* **2016**, 5, 10.3402/jev.v5.31292.

70. T. Kouwaki, et al. Extracellular vesicles deliver host and Virus RNA and regulate innate immune response. *Int. J. Mol. Sci.* **2017**, 18, 666.

71. D. G. Meckes, Jr. Exosomal communication goes viral. *J. Virol.* **2015**, 89, 5200-5203.

72. J. Z. Zaretsky, and D. H. Wreschner. Protein miltifunctionality: principles and mechanisms. *Transl. Oncogenomics*. **2008**, 3, 99-136.

73. K. Hanada, et al. Immune recognition of a human renal cancer antigen through post-translational protein splicing. *Nature.* **2004**, 427, 252-256.

74. J. F. Rehfeld, and J. P. Goetze. The posttranslational phase of gene expression: new possibilities in molecular diagnosis. *Curr. Mol. Med.* **2003**, 3, 25-38.

75. M. Danan-Gotthold, et al. Identification of recurrent regulated alternative splicing events across human solid tumors. *Nucleic Acids Res.* **2015**, 43, 5130-5144.

76. K. Scheffler, et al. High resolution top-down experimental strategies on the Orbitrap platform. *J. Proteomics*. **2018**, 175, 42-55.

77. L. Fornelli, et al. Top-down analysis of immunoglobulin G isotypes 1 and 2 with electron transfer dissociation on a high-field Orbitrap mass spectrometer. *J. proteomics*. **2017**, 159, 67-76.

78. J. K. Diedrich, et al. Energy dependence of HCD on peptide fragmentation: stepped collisional energy finds the sweet spot. *J. Am. Soc. Mass Spectrom*. **2013**, 24, 10.1007/s13361-013-0709-7.

80. C. Cui, et al. Comprehensive identification of protein disulphide bonds with pepsin/trypsin digestion, Orbitrap HCD and spectrum identification machine. *J. Proteomics*. **2019**, 198, 78-86.

81. H. Chi, et al. pNovo: de novo peptide sequencing and identification using HCD spectra. *J. Proteome Res.* **2010**, 9, 2713-2724.

82. S.T. Eshghi, et al. Classification of tandem mass spectra for identification of N- and O-linked glycopeptides. *Sci. Rep.* **2016**, 6, 37189.

83. G. Xu, and S. R. Jaffrey. Proteomic identification of protein ubiquitination events. *Biotechnol. Genet. Eng. Rev.* **2013**, 29, 73-109.

84. Z. Qu, et al. Proteomic quantification and site-mapping of S-nitrosylated proteins using isobaric iodo TMT reagent. *J. Proteome Res.* **2014**, 13, 3200-3211.

85. A. Michalski, et al. Ultra high resolution linear ion trap Orbitrap mass spectrometer (Orbitrap Elite) facilitates top down LC MS/MS and versatile peptide fragmentation modes. *Mol. Cell Proteomics.* **2012**, 11, O111.013698.

86. K. Ranganathan, and V. Sivasankar. MicroRNAs – biology and clinical applications. *J. Oral Maxillofac Pathol.* **2014**, 18, 229-234.

87. M. Kolanowska, et al. MicroRNA analysis using next-generation sequencing. *Methods Mol. Biol*. **2018**, 1823, 87-101.

88. Y-J. Su, et al. Next generation sequencing identifies miRNA-based panel for lupus nephritis. *Oncotarget.* **2018**, 9, 27911-27919.

89. P. Hartman, et al. Next generation sequencing for clinical diagnostics: Five year experience of an academic laboratory. *Mol. Genet. Metab. Rep.* **2019**, 19, 100464.

90. K. M. Danielson, et al. High throughput sequencing of extracellular RNA from human plasma. *PLoS One.* **2017**, 12, e0164644.

91. A. Gautam, et al. Identification of extracellular miRNA in archived serum samples by next-generation sequencing from RNA extracted using multiple methods. *Mol. Biol. Rep.* **2016**, 43, 1165-1178.

92. S. Ono, et al. Circulating microRNA biomarkers as liquid biopsy for cancer patients: pros and cons of current assay. *J. Clin. Med*. **2015**, 4, 1890-1907.

93. C. Manzoni, et al. Genome, transcriptome and proteome: the rise of omics data and their integration in biomedical sciences. *Brief Bioinform.* **2018**, 19, 286-302.

94. International HapMap Consortium. The international HapMap project. *Nature.* **2003**, 426, 789-796.

95. International Human Genom Sequencing Consortium. Finishing the euchromatic sequence of the human genome. *Nature.* **2004**, 431, 931-945.

96. G. S. Omenn. THE HUPO Human plasma proteome project. *Proteomics Clin. Appl.* **2007**, 1, 769-779.

97. T. K. Attwood, et al. A global perspective on evolving bioinformatics and data science training needs. *Brief Bioinform*. **2017**. doi: 10.1093/bib/bbx100.

98. C. Chen, et al. Protein bioinformatics databases and resources. *Methods Mol. Biol.* **2017**, 1558: 3-39.

99. M. S. Nobile, et al. Graphics processing units in bioinformatics, computational biology and system biology. *Brief Bioinform.* **2017**, 18, 870-885.

100. Y. Perez-Riverol, et al. OLS Client and OLS Dialog: open source tools to annotate public omics datasets. *Proteomics.* **2017**, 17. doi: 10.1002/pmic.201700244.

101. K. Kwon, et al. Improved software to browse the serial medical images for learning. J. *Korean Med. Sci.* **2017**, 32, 1195-1201.

102. S. Keerthikumar, et al. ExoCarta: a web-based compendium of exosomal cargo. *J. Mol. Biol.* **2016**, 428, 688-692.

103. M. Pathan, et al. Vesiclepedia 2019: a compendium of RNA, proteins, lipids and metabolites in extracellular vesicles. *Nucleic Acids Res.* **2019**, 47, D516-D519.

104. R. Goel, et al.Human protein reference database and human proteinpedia as resources for phosphoproteome analys. *Mol. Biosyst*. **2012**, 8, 453-463.

105. R. Oughtred, et al. The BioGRID interaction database: 2019 update. *Nucleic Acids Res.* **2019**, 47, D529-541.

106. B. Muthusamy, et al. Access guide to human Proteinpedia. *Curr. Protoc. Bioinformatics.* **2013**, 01, Unit-1.21.

107. Y. Perez-Riverol, et al. Making proteomics data accessible and reusable: Current state of proteomics databases and repositories. *Proteomics.* **2015**, 15, 930-950.

108. M. Pathan, et al. A novel community driven software for functional enrichment analysis of extracellular vesicles data. *J. Extracell. Vesicles.* **2017**, 6, 1321455.

109. The Gene Ontology Consortium. Gene Ontology Consortium: going forward. *Nucleic Acids Res.* **2015**, 43, D1049-D1056.

110. A. Fabregat, et al. The Reactome pathway knowledgebase. *Nucleic Acids Res*. **2018**, 46, D649-D655.

111. A. Kozomara, and S. Griffiths-Jones. miRBase: annotating high confidence microRNAs using deep sequencing data. *Nucleic Acids Res*. **2014**, 42, D68-D73.

112. C-H. Chou, et al. miRTarBase update 2018: a resource for experimentally validated microRNA-target interaction. *Nucleic Acids Res.* **2018**, 46, D296-D302.

113. V. Agarwal, et al. Predicting effective microRNA target sites in mammalian mRNA. *eLife.* **2015**, 4, e05005.

114. Z. Huang, et al. HMDD v3.0: a database for experimentally supported human microRNA-disease associations. *Nucleic Acids Res.* **2019**, 47, D1013-D1017.

115. D. H. Haft, et al. RefSeq: an update on prokaryotic genome annotation and curation. *Nucleic Acids Res*. **2018**, 46, D851-D860.

116. Z. Wang, et al. Mining data and metadata from the gene expression omnibus. *Biophys. Res*. **2019**, 11, 103-110.

117. J. N. Weinstein, et al. The Cancer Genome Atlas pan-cancer analysis project. *Nat. Genet.* **2013**, 45, 1113-1120.

118. M. Kanehisa, et al. KEGG: new perspectives on genomes, pathways, diseases and drugs. *Nucleic Acids Res.* **2017**, 45, D353-D361.

119. C. Fresno, and E. A. Fernández. RDAVIDWebService: a versatile R interface to DAVID. *Bioinformatics.* **2013**, 29, 2810-2811.

120. P. O. Williamson. Exploring PubMed as a reliable resource for scholarly communications services. *J. Med. Libr. Assoc.* **2019**, 107, 16-29.

121. S. Tyanova, et al. The MaxQuant computational platform for mass spectrometry-based shotgun proteomics. *Nat. Protoc*. **2016**, 11, 2301-2319.

122. J. Cox, et al. Andromeda: a peptide search engine integrated into the MaxQuant environment. *J. Proteome Res.* **2011**, 10, 1794-1805.

123. S. Tyanova, et al. The Perseus computational platform for comprehensive analysis of (prote)omics data. *Nat. Methods.* **2016**, 13, 731-740.

124. A. Schniers, et al. Ulcerative colitis: functional analysis of the in-depth proteome. *Clin. Proteomics.* **2019**, 16, 4.

125. S. Pundir, et al. UniProt tools. Curr. Protoc. *Bioinformatics.* **2017**, 53, 1.29.1-1,29.15.

126. The UniProt Consortium. UniProt: a hub for protein information. *Nucleic Acids Res.* **2015**, 43, D204-D 212.

127. P. Aiyetan, et al. M2Lite: An Open-source, Light-weight, Pluggable and Fast Proteome Discoverer MSF to mzldentML tool. *J. Bioinform.* **2014**, 1, 40-49.

128. W. R. Pearson. Finding protein and nucleotide similarities with FASTA. *Curr. Protoc. Bioinformatics.* **2016**, 53, 3.9.1-3.925.

129. The Gene Ontology Consortium. Expansion of the Gene Ontology knowledgebase and resources. *Nucleic Acids Res.* **2017**, 45, D331-D338.

130. Q. Shao, et al. A proteomic study of human Merkel cell carcinoma. *J. Proteomics Bioinform.* **2013**, 6, 275-282.

131. M. Kaspar, et al. Fibronectin as target for tumor therapy. *Int. J. Cancer* **2006**, 118, 1331-1339.

132. J. Labat-Robert, et al. Fibronectin in malignancy. *Semin. Cancer Biol.* **2002**, 12, 187-195.

133. S. Kazerounian, et al. Thrombospondins in cancer. *Cell. Mol. Life Sci.* **2008**, 65, 700-712.

134. N. Pouliot, and N. Kusuma. Laminin-511: A multi-functional adhesion protein regulating cell migration, tumor invasion and metastasis. *Cell. Adh. Migr.* **2013**, 7, 142-149.

135. P- F. Barcelona, and H. U. Saragovi. A pro-nerve growth factor (proNGF) and NGF binding protein, α2-macroglobulin, differentially regulates p75 and TrkA receptors and is relevant to neurodegeneration ex vivo and in vivo. *Mol. Cell. Biol.* **2015**, 35, 3396-3408.

136. Y. Fortenberry. The role of serpins in tumor cell migration. *Biol. Chem.* **2015**, 396, 205-213.

137. A. Saeed, et al. Mannan binding lectin-associated serine protease 1 is induced by hepatitis C virus infection and activates human hepatic stellate cells. *Clin. Exp. Immunol.* **2013**, 174, 265-273.

138. S. Dovrat, et al. 14-3-3 and beta-catenin are secreted on extracellular vesicles to activate the oncogenic Wnt pathway. *Mol. Oncol.* 2014, 8, 894-911.

139. A. M. Casper, et al. Sites of genetic instability in mitosis and cancer. *Ann. N. Y. Acad. Sci.* **2012**, 1267, 24-30.

140. C. Ciardiello, et al. Focus on extracellular vesicles: New frontiers of cell-to-cell communication in cancer. *Int. J. Mol. Sci.* **2016**, 17, E175.

141. I. Nakano, et al. Extracellular vesicles in the biology of brain tumour stem cells--Implications for inter-cellular communication, therapy and biomarker development. *Sem. Cell Dev. Biol.* **2015**, 40, 17-26.

142. M. Pook, et al. Platelets store laminins 411/421 and 511/521 in compartments distinct from a- or dense granules and secrete these proteins via microvesicles. *J. Thromb. Haemost.* **2014**, 12, 519-527.

143.T. F. McElrath, et al. Circulating microparticles proteins obtained in the late first trimester predict spontaneous preterm birth at less than 35 weeks' gestation: a panel validation with specific characterisation by parity. *Am. J. Obstet. Gynecol*. **2019**, S0002-9378(19)30250-9.

144. H. Cui, et al. Tissue inhibitor of metalloproteinases-1 induces a pro-tumourigenic increase of miR-210 in lung adenocarcinoma cells and their exosomes. *Oncogene*. **2015**, 34, 3640-3650.

145. C. O. Rodini, et al. Mesenchymal stem cells enhance tumorigenic properties of human glioblastoma through independent cell-cell communication mechanisms. *Oncotarget*. **2018**, 9, 24766-24777.

146. A. Vedeler, et al. Multiple roles of annexin A2 in post-transcriptional regulation of gene expression. *Curr. Protein Pept. Sci.* **2012**, 13, 401-412.

147. D. Xiao, et al. Identifying mRNA, microRNA and protein profiles of melanoma exosomes. *PLoS One*. **2012**, 7, e46874.

148. S. Maji, et al. Exosomal annexin II promotes angiogenesis and breast cancer metastasis. *Mol. Cancer Res.* **2017**, 15, 93-105.

149. T. Neill, et al. Decorin induces rapid secretion of thrombospondin-1 in basal breast carcinoma cells via inhibition of RAS homolog gene family, member A/Rho-associated coiled-coil containing protein kinase 1. FEBS J. 2013, 280, 2353-2368.

150. F. Wu, et al. Identification of biomarkers and potential molecular mechanisms of clear cell renal cell carcinoma. *Neoplasma.* **2018**, 65, 242-252.

151. S. Li, et al. Exosomes from hyperglycemia-stimulated vascular endothelial cells contain versican that regulate calcification/senescence in vascular smooth muscle cells. *Cell Biosci.* ***2019*****,** 9, 1.

152. R. Mirzaei, et al. Brain tumor-initiating cells export tenascin-C with exosomes to suppress T cell activity. *Oncoimmunology.* **2018**, 7, e1478647.

153. O. G. de Jong, et al. Exosomes from hypoxic endothelial cells have increased collagen crosslinking activity through up-regulation of lysyl oxidase-like 2. J. Cell. Mol. Med. 2016, 20, 342-350.

154. M. C. Sharma. Annexin A2 (ANX A2): An emerging biomarker and potential therapeutic target for aggressive cancers. *Int. J. Cancer.* **2019,** 144, 2074-2081.

155. B. Feldkoren, et al. Integrin signalling potentiates transforming grow factor-beta 1(TGF-beta) dependent down-regulation of E-Cadherin expression – Important implications for epithelial to mesenchymal transition (EMT) in renal cell carcinoma. *Exp. Cell Res.* **2017**, 355.

156. L. M. van Veenendaal, et al. Merkel cell carcinoma: Clinical outcome and prognostic factors in 351 patients. *J. Surg. Oncol.* **2018,** 117, 1768-1775.

157. A. S. Moshiri, et al. Polyomavirus-negative Merkel cell carcinoma: a more aggressive subtype based an analysis of 282 cases using multimodal tumor virus detection. *J. Invest. Dermatol.* **2017**, 137, 819-827.

158. C. Charoenviriyakul, et al. Preservation of exosomes at room temperature using lyophilisation. *Int. J. Pharm*. **2018**, 553, 1-7.

159. O. Zhao, et al. MicroRNA-222-3p promotes tumor cell migration and invasion and inhibits apoptosis, and is correlated with an unfavourable prognosis of patients with renal cell carcinoma. *Int. J. Mol. Med.* **2019**, 43, 525-534.

160. J. W. Tay, et al. Identification of reference miRNAs in plasma useful for the study of oestrogen-responsive miRNAs associated with acquired Protein S deficiency in pregnancy. *BMC Res. Notes.* **2017**, 10, 312.

161. F. Tian, et al. No significant difference between plasma miRNAs and plasma-derived exosomal miRNAs from healthy people. *Biomed. Res. Int.* **2017**, 2017, 1304816.

162. L. Deng, et al. Downregulation of miR-222-3p and upregulation of its target gene PARP1 are prognostic biomarkers for triple negative breast cancer patients and associated with poor prognosis. *Oncotarget.* **2017**, 8, 108712-108725.

163. N. Syn, et al. Exosome-mediated metastasis: From epithelial-mesenchymal transition to escape from immunosurveillance. *Trends Pharmacol. Sci.* **2016**, 37, 606-617.

164. M. P. Plebanek, et al. Pre-metastatic cancer exosomes induce immune surveillance by patrolling monocytes at the metastatic niche. *Nat. Commun.* **2017**, 8, 1319.

165. X. Ying, et al. Epithelial ovarian cancer-secreted exosomal miR-222-3p induce polarization of tumor-associated macrophages. *Oncotarget* **2016**, 7, 43076-43087.

166. F. Wei, et al. Exosomes derived from gemcitabine-resistant cells transfer malignant phenotypic traits via delivery of miRNA-222-3p. *Mol. Cancer* **2017**, 16, 132.

167. M. Jiang, et al. Dysregulation of SOCS-mediated negative feedback of cytokine signaling in carcinogenesis and its significance in cancer treatment. *Front. Immunol.* **2017**, 8, 70.

168. L. Santangelo, et al. Hepatitis C virus direct-acting antivirals therapy impacts on extracellular vesicles microRNAs content and on their immunomodulating properties. *Liver Int.* **2018**, 38, 1741-1750.

169. H. Xie, et al. MicroRNA expression patterns related to Merkel cell polyomavirus infection in human Merkel cell carcinoma. *J. Invest. Dermatol*. **2014**, 134, 507-517.

170. M. S. Ning, et al. Characterization of the Merkel cell carcinoma miRNome. *J. Skin Cancer.* **2014**, 2014, 289548.

171. T. Veija, et al. miRNA-34a underexpressed in Merkel cell polyomavirus-negative Merkel cell carcinoma. *Virchows Arch.* **2015**, 466, 289-295.

172. L. M. Knight, et al. Merkel cell polyomavirus small T antigen mediates microtubule destabilisation to promote cell motility and migration. *J. Virol.* **2015**, 89, 35-47.

173. A. Whitehouse, and A. Macdonald. Stathmin drives virus-induced metastasis. *Oncotarget.* **2015**, 6, 32289-32290.

174. N. Umegaki-Arao, et al. Karyopherin Alpha2 is essential for rRNA transcription and protein synthesis in proliferative keratinocytes. *PLoS One.* **2013**, 8, e76416.

175. A. Konstantinell, et al. Secretomic analysis of extracellular vesicles originating from polyomavirus-negative and polyomavirus-positive Merkel cell carcinoma cell lines. *Proteomics* **2016**, 16, 2587-2591.

176. S. Dovrat, et al. 14-3-3 and β-catenin are secreted on extracellular vesicles to activate the oncogenic Wnt pathway. *Mol. Oncol.* **2014**, 8, 894-911.

177. A. Castañeda, et al. pVHL suppresses Akt/β-catenin-mediated cell proliferation by inhibiting 14-3-3ζ expression. *Biochem. J.* **2017**, 474, 2679-2689.

178. Y. W. Chu, et al. MicroRNA-222 contributed to cell proliferation, invasion and migration via regulating YWHAG in osteosarcoma. *Eur. Rev. Med. Pharmacol. Sci.* **2018**, 22, 2588-2597.

179. L. Villabona, et al. Prognostic differences between male and female patients in virus-negative Merkel cell carcinoma. *J. Clin. Oncol.* **2018**, 36. doi: 10.1200/JCO.2018.36.15_suppl.e21601.

180. K. Daily, et al. Assessment of cancer cell line representativeness using microarray for Merkel cell carcinoma. *J. Invest. Dermatol.* **2015**, 135, 1138-1146.

181. P. W. Harms, et al. The distinctive mutational spectra of polyomavirus-negative Merkel cell carcinoma. *Cancer Res.* **2015**, 75, 3720-3727.

182. M. Mehrmohamadi, et al. Characterization of the usage of the serine metabolic network in human cancer. *Cell Rep*. **2014**, 9, 1507-1519.

183. Y. Zhu, et al. A critical role of glutamine and asparagine γ-nitrogen in nucleotide biosynthesis in cancer cells hijacked by an oncogenic virus. *MBio.* **2017**, 8, e01179-17.

184. C. Berrios, et al. merkel cell polyomavirus small T antigen promotes pro-glycolytic metabolic perturbations required for transformation. *PLoS Pathog.* **2016**, 12, e1006020.

185. J.H.G.M. van Beek. The dynamic side of the Warburg effect: glycolytic intermediate storage as buffer for fluctuating glucose and O2 supply in tumor cells. *F1000Res*. **2018**, 7, 1177.

186. S. Zhu, et al. The role of sirtuins family in cell metabolism during tumor development. *Semin Cancer Biol*. **2018**, S1044-579X(18)30107-X.

187. J. Marquez, et al. NADH dehydrogenase complex I is overexpressed in incipient metastatic murine colon cancer cells. *Oncol. Rep*. **2018**, 41, 742-752.

188. T. Murray Stewart, et al. Polyamine catabolism and oxidative damage. *J Biol Chem*. **2018**, 293, 18736-18745.

189. M. A. Dashty. A quick look at biochemistry: carbohydrate metabolism. *Clin Biochem.* **2013**, 46, 1339-1352.

190. W-J. Rappel, and L. Edelstein-Keshet. Mechanism of cell polarization. *Curr. Opin. Syst. Biol.* **2017**, 3, 43-53.

191. N. Taniguchi, and Y. Kizuka. Glycans and cancer: role of N-glycans in cancer biomarkers, progression and metastasis, and therapeutics. *Adv. Cancer Res*. **2015**, 126, 11-51.

192. G. Goh, et al. Mutational landscape of MCPyV-positive and MCPyV-negative Merkel cell carcinomas with implication for immunotherapy. *Oncotarget.* **2016**, 7, 3403-3415.

193. G. Hendriks, et al. Transcription and replication: far relatives make uneasy bedfellows. *Cell Cycle*. **2010**, 9, 2300-2304.

194. L. Savolainen, et al. The XPD subunit of TFIIH is required for transcription-associated but not DNA double-strand break-induced recombination in mammalian cells. *Mutagenesis*. **2010,** 25, 623-629.

195. K. Uchiyama, et al. VCIP135, a novel essential factor for p97/p47-mediated membrane fusion, is required for Golgi and ER assembly in vivo. *J. Cell Biol.* **2002**, 159, 855-866.

196. L. G. Ju, et al. Characterization of WDR20: A new regulator of the ERAD machinery. *Biochim Biophys Acta Mol Cell Res.* **2018**, 1865, 970-980.

197. S. J. Mishra, et al. Transformation of the non-selective aminocyclohexanol-based Hsp90 inhibitor into a Grp94-selective scaffold. *ACS Chem Biol.* **2017**, 12, 244-253.

198. T. Li, et al. Oncogenic Kaposi's sarcoma-associated herpesvirus upregulates argininosuccinate synthase 1, a rate-limiting enzyme of the citrulline-nitric oxide cycle, to activate the STAT3 pathways and promote growth transformation. *J. Virol.* **2019**, 93, e01599-18.

199. A. Silberman, et al. Acid-induced downregulation of ASS1 contributes to the maintenance of intracellular pH in cancer. *Cancer Res.* **2019**, 79, 518-533.

200. J. Wu, et al. Exosome in virus-associated cancer. *Cancer Lett.* **2018**, 438, 44-51.

DATASET BRIEF

Secretomic analysis of extracellular vesicles originating from polyomavirus-negative and polyomavirus-positive Merkel cell carcinoma cell lines

Aelita Konstantinell[1], Jack-Ansgar Bruun[1], Randi Olsen[1], Augusta Aspar[1], Nataša Škalko-Basnet[2], Baldur Sveinbjørnsson[1] and Ugo Moens[1]

[1] Department of Medical Biology, Faculty of Health Sciences, University of Tromsø, Tromsø, Norway
[2] Department of Pharmacy, Faculty of Health Sciences, University of Tromsø, Tromsø, Norway

Received: May 23, 2016
Revised: June 30, 2016
Accepted: July 7, 2016

Extracellular vesicles or exosomes constitute an evolutionarily conserved mechanism of intercellular signaling. Exosomes are gaining an increasing amount of attention due to their role in pathologies, including malignancy, their importance as prognostic and diagnostic markers, and their potential as a therapeutic tool. Merkel cell carcinoma (MCC) is an aggressive form of skin cancer with a poor prognosis. Because an effective systemic treatment for this cancer type is currently not available, an exosome-based therapy was proposed. However, comprehensive secretome profiling has not been performed for MCC. To help unveil the putative contribution of exosomes in MCC, we studied the protein content of MCC-derived exosomes. Since approximately 80% of all MCC cases contain Merkel cell polyomavirus (MCPyV), the secretomes of two MCPyV-negative and two MCPyV-positive MCC cell lines were compared. We identified with high confidence 164 exosome-derived proteins common for all four cell lines that were annotated in ExoCarta and Vesiclepedia databases. These include proteins implicated in motility, metastasis and tumor progression, such as integrins and tetraspanins, intracellular signaling molecules, chaperones, proteasomal proteins, and translation factors. Additional virus-negative and virus-positive MCC cell lines should be examined to identify highly representative exosomal proteins that may provide reliable prognostic and diagnostic biomarkers, as well as targets for treatment in the future. Data are available via ProteomeXchange with identifier PXD004198.

Keywords:
Cancer / Cell biology / Exosome / Merkel cell carcinoma / Polyomavirus

Additional supporting information may be found in the online version of this article at the publisher's web-site

Merkel cell carcinoma (MCC) is an aggressive skin cancer of neuroendocrine origin, with a mortality rate >50% [1]. Feng et al. identified a previously unknown polyomavirus that was integrated in eight out of ten examined MCC samples [2]. They referred to this novel virus as Merkel cell polyomavirus (MCPyV), and worldwide studies have confirmed that approximately 80% of MCC contain integrated viral DNA [3, 4]. Cell culture and animal studies have confirmed the oncogenic properties of MCPyV [5, 6], with MCPyV classified as a potential oncogenic biological agent in MCC [7]. Besides surgical excision and postoperative radiotherapy, no effective systemic treatment for this cancer type is yet available [8].

Exosomes are small bilayer proteolipid vesicles secreted by a variety of cell types [9]. Their sizes vary from 30 to 100 nm in diameter [10] or slightly larger up to 150 nm [11, 12]. Extracellular vesicles (EVs) contain cytosolic components [13]; however, the composition, biogenesis, and secretion of exosomes are influenced by the surrounding environment and cellular conditions [14].

Correspondence: Aelita Konstantinell, PhD Candidate, Department of Medical Biology, Faculty of Health Sciences, University of Tromsø, NO-9037 Tromsø, Norway
E-mail: aelita.g.konstantinell@uit.no
Fax: +47-776-251-40

Abbreviations: EV, extracellular vesicle; **MCC**, Merkel cell carcinoma; **MCPyV**, Merkel cell polyomavirus

Table 1. The exosomes ($n = 3$) size distributions were determined by photon correlation spectroscopy on a submicron particle sizer model 370, and are represented in intensity-weight distribution

Cell type	Size distribution				
	Mean diameter peak 1 (nm)	%	Mean diameter peak 2 (nm)	%	PA[a)]
MCC13	29 ± 3	32	104 ± 5	66	0.37
MCC26	29 ± 5	36	134 ± 8	63	0.33
MKL1	36 ± 5	55	126 ± 8	44	0.36
MKL2	31 ± 4	39	158 ± 7	61	0.38

a) Polydispersity index.

Exosomes have gained increasing attention for their involvement in the pathogenesis of several diseases, including cancer. Virus-infected cell-derived vesicles are not only packed with cellular compounds, but also contain viral proteins and nucleic acids [15]. This may help facilitate the transfer of viral compounds to new cells and promote pathogenic processes [16, 17]. Intercellular signaling mediated by EVs or exosomes is an evolutionarily conserved phenomenon [18, 19]. Furthermore, exosomes can also be recognized by antigen-presenting cells, and cell-to-cell mediated immune activation can result in antitumor responses [20,21]. Exosome-based vaccines have been developed for cancer therapeutics [22], and to help assess the possible role of MCC-generated exosomes in tumorigenesis we investigated whether MCC cell lines produce exosomes, and we compared the protein content of exosomes secreted by two different MCPyV-negative, such as MCC13 and MCC26, and two different MCPyV-positive cell lines, such as MKL-1 and MKL-2, respectively.

EVs were isolated from Merkel carcinoma cell lines by a series of differential centrifugation, filtration, and the use of the ExoQuick exosome precipitation reagent. All experiments were run in triplicate, while the collection of EVs and their characterization were done from 10 mL of supernatant. The Submicron Particle Size Analyzer showed the vesicular structures of these purified EVs with a diameter range of 30–150 nm (Table 1). The transmission electron microscopy confirmed this result, which is in agreement that EVs within the range of 30–150 nm are cup-shaped vesicles (Fig. 1A: in box and B: arrow heads), and that those smaller than 30 nm or larger than 150 nm EVs are apoptotic blebs and shedding microvesicles, respectively, as previously reported [12, 23]. More experimental details are provided in the Supporting Information.

For Merkel carcinoma cell lines, the identification of EV protein peptide mixtures containing formic acid was loaded onto a Thermo Fisher Scientific EASY system. Peptides were fractionated, and separated peptides were analyzed using a Thermo Scientific Q-Exactive mass spectrometer. Data were collected in a data-dependent mode using a Top10 method [24]. The fragmentation spectra were searched against the UniprotKB Homo Sapiens 2016/02/29 database using an in-house MASCOT server. The raw data were processed using Proteome Discoverer 1.4 software. Peptide ions were then filtered using a FDR set to 1% for further peptide identification. The secretome profiling of two MCPyV-negative cell lines, MCC13 and MCC26, and of the MCPyV-positive cell lines, MKL1 and MKL2 [25, 26], resulted in the identification of 172 common microvesicular proteins of 500, 325, 258, and 228 identified proteins from MCC13, MCC26, MKL1, and MKL2, respectively (Fig. 2A). The variables of identified proteins' number explain the proteins' expression variation between the cell lines [27], as well as the heterogeneity of human cancer [28], patient-to-patient variation [12], and the identification of proteins in our proteome derived from replicative Q-Exactive MS analyses ($n = 3$).

To compare our Merkel cell lines EV dataset with other studies, we performed an enrichment analysis using ExoCarta v5 [29], Vesiclepedia v3 [30] protein databases, and The FunRich v2.1.2 [31] open access tool. The total list of proteins from exosomes displayed an approximate 94% overlap with

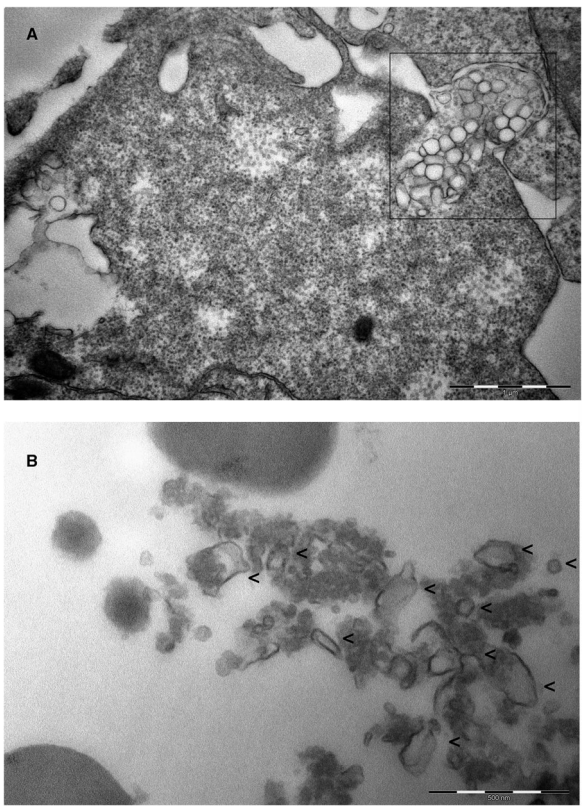

Figure 1. Characterization of Merkel cells and their exosomes by transmission electron microscopy, ×80 000 magnification. (A) Merkel cells releasing and exchanging vesicles (in box) via juxtacrine cell–cell communication. Scale bar = 1 μm. (B) A section of purified exosomes produced using the malachite green protocol and size was confirmed by EVs of 30–150 nm (arrow heads), which are displaying a cup-shaped morphology characteristic of exosomes. Scale bar = 500 nm.

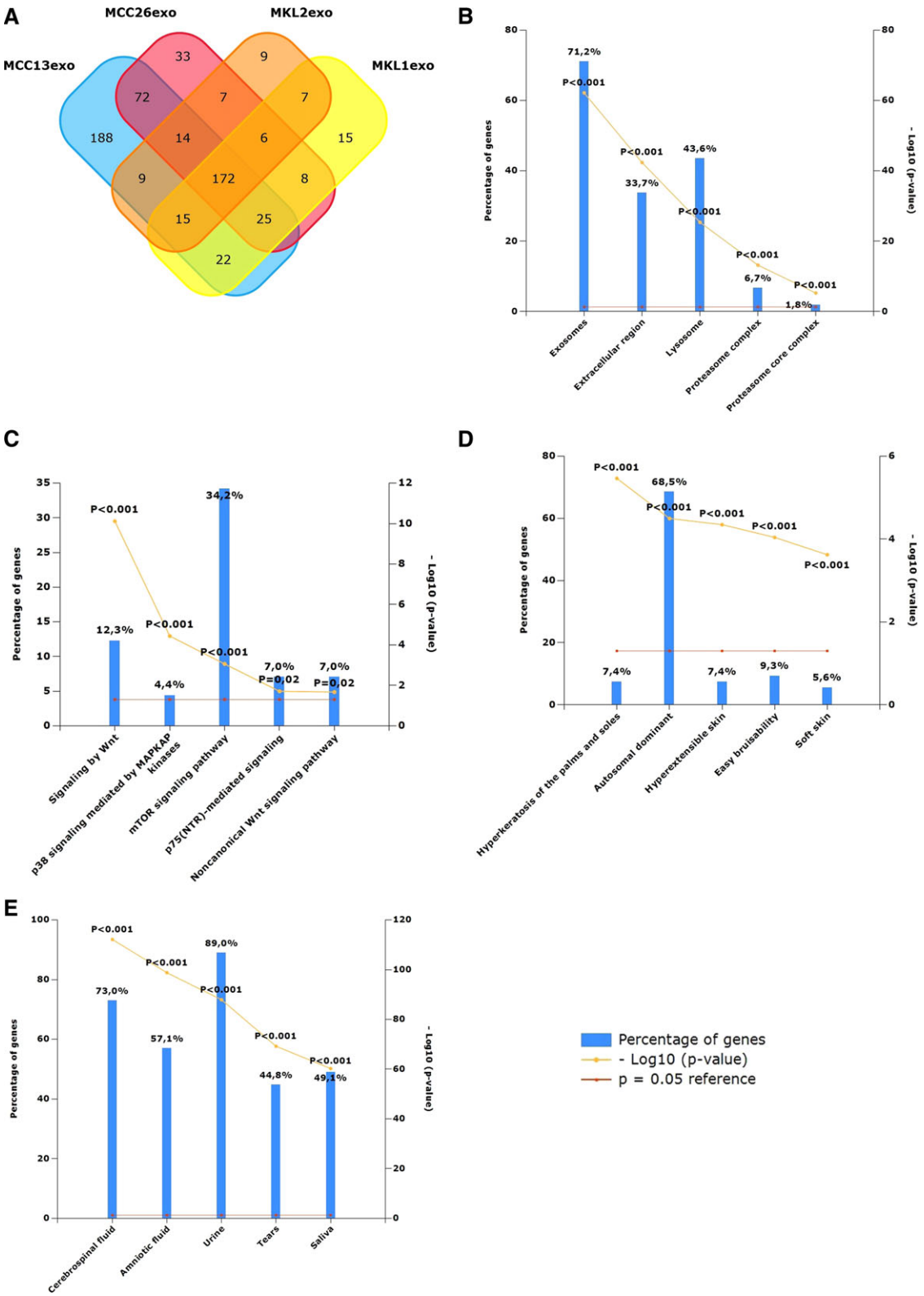

Figure 2. Comparison analysis of MCPyV-negative and MCPyV-positive Merkel cell lines secretomic proteins. (A) Venn diagram of the overlap between the four cell lines. Enrichment analysis of cellular components localization (B), biological pathways (C), clinical phenotypes (D), and site of expression (E) of common proteins from this study over FunRich database as background.

ExoCarta and an approximate 99% overlap with Vesiclepedia. The overlap with the top 100 protein markers is approximately 69% (MCC13), 49% (MCC26), 47% (MKL1) and 39% (MKL2), respectively.

From 172 proteins, 164 proteins were annotated in ExoCarta and Vesiclepedia databases (Supporting Information Table 1). These common cargo proteins include 37 exosomal markers (Supporting Information Table 2). Cellular components comprise exosomes (71.2%), lysosome (43.6%), proteasome complexes (6.7%) and a proteasome core complex (1.8%) with a significance level $p < 0.001$. Proteins from extracellular region (33.7%, $p < 0.001$) of Merkel carcinoma cell lines presuppose to be located on the surface of EVs (Fig. 2B and Supporting Information Table 3). They might be potential biomarkers of MCC surface and proteins that recipient cells recognize, which allow the design of targeted treatment. Many of the exosomal proteins are associated with metastasis and tumorigenesis/tumor progression, including fibronectin [32, 33], thrombospondin [34], and laminin β1 [35]. Several of the EVs proteins were exploited as a therapeutic target: alpha-2-macroglobulin [36] and serpin peptidase inhibitor, clade F, member 1 [37], while others such as mannan-binding lectin serine peptidase 1 have an impact on the severity of disease in, e.g. hepatitis C virus infections [38].

Interestingly, we identified the lactate dehydrogenase B at subnetwork mechanistic target of rapamycin pathway [39], and several 14-3-3 proteins at p75(NTR)-mediated signaling, p38 MAPK signaling, and the Wnt pathway [40] (Fig. 2C and Supporting Information Table 4). The majority of proteins displayed a positive association with autosomal-dominant, genetic processes ($p < 0.001$, Fig. 2D and Supporting Information Table 5). Chromosomal instability and a loss of heterozygosity are important steps in tumorigenesis [41]. The ranking of the EV proteins included in the network, according to the enrichment analysis secreted in urine (89.0%), cerebrospinal fluid (73.0%), amniotic fluid (57.1%), saliva (49.1%), and tears (44.8%), has a significance level $p < 0.001$ (Fig. 2E). The body fluids provide condition-specific biomarkers, with a potential source for the diagnosis and development of a targeted therapy [42, 43].

In conclusion, our results show that MCPyV-negative and MCPyV-positive Merkel cell lines' EVs contain several proteins associated with tumor cell motility and metastasis. Importantly, we identified a list of vesicular proteins derived from the extracellular region, which could reveal biomarkers specific for MCC identification and EVs' recognition proteins by recipient cells. Lastly, our comprehensive secretome profile stimulates further studies aiming at the differences and functions of EVs secreted by MCPyV-negative and MCPyV-positive Merkel cell lines, respectively.

The MS proteomics data have been deposited to the ProteomeXchange Consortium via the PRIDE [44] partner repository with the dataset identifier PXD004198.

We thank Professor Baki Akgül (University of Cologne, Germany) for the kind gift of the MCC cell lines. This work was supported by the Odd Fellow Medisinsk-Vitenskapelig Forskningsfond (A65216).

The authors have declared no conflict of interest.

References

[1] Albores-Saavedra, J., Batich, K., Chable-Montero, F., Sagy, N. et al., Merkel cell carcinoma demographics, morphology, and survival based on 3870 cases: a population based study. *J. Cutan. Pathol.* 2010, *37*, 20–27.

[2] Feng, H., Shuda, M., Chang, Y., Moore, P. S., Clonal integration of a polyomavirus in human Merkel cell carcinoma. *Science* 2008, *319*, 1096–1100.

[3] Tolstov, Y. L., Pastrana, D. V., Feng, H. C., Becker, J. C. et al., Human Merkel cell polyomavirus infection II. MCV is a common human infection that can be detected by conformational capsid epitope immunoassays. *Int. J. Cancer* 2009, *125*, 1250–1256.

[4] Chang, Y., Moore, P. S., Merkel cell carcinoma: a virus-induced human cancer. *Annu. Rev. Pathol.* 2012, *7*, 123–144.

[5] Verhaegen, M. E., Mangelberger, D., Harms, P. W., Vozheiko, T. D. et al., Merkel cell polyomavirus small T antigen is oncogenic in transgenic mice. *J. Invest. Dermatol.* 2015, *135*, 1415–1424.

[6] Arora, R., Shuda, M., Guastafierro, A., Feng, H. et al., Survivin is a therapeutic target in Merkel cell carcinoma. *Sci. Transl. Med.* 2012, *4*, 133ra56.

[7] Bouvard, V., Baan, R., Straif, K., Grosse, Y. et al., A review of human carcinogens—Part B: biological agents. *Lancet Oncol.* 2009, *10*, 321–322.

[8] Rabinowits, G., Systemic therapy for Merkel cell carcinoma: what's on the horizon? *Cancers* 2014, *6*, 1180–1194.

[9] Stoorvogel, W., Kleijmeer, M. J., Geuze, H. J., Raposo, G., The biogenesis and functions of exosomes. *Traffic* 2002, *3*, 321–330.

[10] Robbins, P. D., Morelli, A. E., Regulation of immune responses by extracellular vesicles. *Nat. Rev. Immunol.* 2014, *14*, 195–208.

[11] Colombo, M., Raposo, G., Thery, C., Biogenesis, secretion, and intercellular interactions of exosomes and other extracellular vesicles. *Annu. Rev. Cell Dev. Biol.* 2014, *30*, 255–289.

[12] Choi, D. S., Park, J. O., Jang, S. C., Yoon, Y. J. et al., Proteomic analysis of microvesicles derived from human colorectal cancer ascites. *Proteomics* 2011, *11*, 2745–2751.

[13] Simons, M., Raposo, G., Exosomes–vesicular carriers for intercellular communication. *Curr. Opin. Cell Biol.* 2009, *21*, 575–581.

[14] de Jong, O. G., Verhaar, M., Chen, Y., Vader, P. et al., Cellular stress conditions are reflected in the protein and RNA content of endothelial cell derived exosomes. *J. Extracell.*

Vesicles 2012, *16*, Available at: http://www.journalofextracellularvesicles.net/index.php/jev/article/view/18396. Date accessed: 25 Jul. 2016.

[15] Meckes, D. G. Jr., Raab-Traub N., Microvesicles and viral infection. *J. Virol.* 2011, *85*, 12844–12854.

[16] Schorey, J. S., Cheng, Y., Singh, P. P., Smith, V. L., Exosomes and other extracellular vesicles in host-pathogen interactions. *EMBO Rep.* 2015, *16*, 24–43.

[17] Jaworski, E., Narayanan, A., Van Duyne, R., Shabbeer-Meyering, S. et al., Human T-lymphotropic virus type 1-infected cells secrete exosomes that contain Tax protein. *J. Biol. Chem.* 2014, *289*, 22284–22305.

[18] Kanwar, S. S., Dunlay, C. J., Simeone, D. M., Nagrath, S., Microfluidic device (ExoChip) for on-chip isolation, quantification and characterization of circulating exosomes. *Lab Chip* 2014, *14*, 1891–1900.

[19] Fevrier, B., Raposo, G., Exosomes: endosomal-derived vesicles shipping extracellular messages. *Curr. Opin. Cell Biol.* 2004, *16*, 415–421.

[20] Wolfers, J., Lozier, A., Raposo, G., Regnault, A. et al., Tumor-derived exosomes are a source of shared tumor rejection antigens for CTL crosspriming. *Nat. Med.* 2001, *7*, 297–303.

[21] André, F., Chaput, N., Schartz, N. E., Flament, C. et al., Exosomes as potent cell-free peptide-based vaccine. I. Dendritic cell-derived exosomes transfer functional MHC class I/peptide complexes to dendritic cells. *J. Immunol.* 2004, *172*, 2126–2136.

[22] Hao, S., Moyana, T., Xiang, J., Cancer immunotherapy by exosomebased vaccines. *Cancer Biother. Radiopharm.* 2007, *22*, 692–703.

[23] Mathivanan, S., Ji, H., Simpson, R. J., Exosomes: extracellular organelles important in intercellular communication. *J. Proteomics* 2010, *73*, 1907–1920.

[24] Olsen, J. V., Schwartz, J. C., Griep-Raming, J., Nielsen, M. L. et al., A dual pressure linear ion trap orbitrap instrument with very high sequencing speed. *Mol. Cell. Proteomics* 2009, *8*, 2759–2769.

[25] Leonard, J. H., Cook, A. L., Van Gele, M., Boyle, G. M. et al., Proneural and proneuroendocrine transcription factor expression in cutaneous mechanoreceptor (Merkel) cells and Merkel cell carcinoma. *Int. J. Cancer* 2002, *101*, 103–110.

[26] Shuda, M., Feng, H., Kwun, H. J., Rosen, S. T. et al., T antigen mutations are a human tumor-specific signature for Merkel cell polyomavirus. *Proc. Natl. Acad. Sci. USA* 2008, *105*, 16272–16277.

[27] Geiger, T., Wehner, A., Schaab, C., Cox, J., Mann, M., Comparative proteomic analysis of eleven common cell lines reveals ubiquitous but varying expression of most proteins. *Mol. Cell. Proteomics* 2012, *11*, M111.

[28] Shao, Q., Byrum, S. D., Moreland, L. E., Mackintosh, S. G. et al., A proteomic study of human Merkel cell carcinoma. *J. Proteomics Bioinform.* 2013, *6*, 275–282.

[29] Keerthikumar, S., Chisanga, D., Ariyaratne, D., Al Saffar, H. et al., ExoCarta: a web-based compendium of exosomal cargo. *J. Mol. Biol.* 2016, *428*, 688–692.

[30] Kalra, H., Simpson, R. J., Ji, H., Aikawa, E. et al., Vesiclepedia: a compendium for extracellular vesicles with continuous community annotation. *PLoS Biol.* 2012, *10*, e1001450.

[31] Pathan, M., Keerthikumar, S., Ang, C. S., Gangoda, L. et al., FunRich: an open access standalone functional enrichment and interaction network analysis tool. *Proteomics* 2015, *15*, 2597–2601.

[32] Kaspar, M., Zardi, L., Neri, D., Fibronectin as target for tumor therapy. *Int. J. Cancer* 2006, *118*, 1331–1339.

[33] Labat-Robert, J., Fibronectin in malignancy. *Semin. Cancer Biol.* 2002, *12*, 187–195.

[34] Kazerounian, S., Yee, K. O., Lawler, J., Thrombospondins in cancer. *Cell. Mol. Life Sci.* 2008, *65*, 700–712.

[35] Pouliot, N., Kusuma, N., Laminin-511: a multi-functional adhesion protein regulating cell migration, tumor invasion and metastasis. *Cell. Adh. Migr.* 2013, *7*, 142–149.

[36] Barcelona, P. F., Saragovi H. U., A pro-nerve growth factor (proNGF) and NGF binding protein, α2-macroglobulin, differentially regulates p75 and TrkA receptors and is relevant to neurodegeneration ex vivo and in vivo. *Mol. Cell. Biol.* 2015, *35*, 3396–3408.

[37] Fortenberry, Y., The role of serpins in tumor cell migration. *Biol. Chem.* 2015, *396*, 205–213.

[38] Saeed, A., Baloch, K., Brown, R. J., Wallis, R. et al., Mannan binding lectin-associated serine protease 1 is induced by hepatitis C virus infection and activates human hepatic stellate cells. *Clin. Exp. Immunol.* 2013, *174*, 265–273.

[39] Shao, Q., Byrum, S., Moreland, L. E., Mackintosh, S. G. et al., A proteomic study of human Merkel cell carcinoma. *J. Proteomics Bioinform.* 2013, *6*, 275–282.

[40] Dovrat, S., Caspi, M., Zilberberg, A., Lahav, L. et al., 14-3-3 and betacatenin are secreted on extracellular vesicles to activate the oncogenic Wnt pathway. *Mol. Oncol.* 2014, *8*, 894–911.

[41] Casper, A. M., Rosen, D. M., Rajula, K. D., Sites of genetic instability in mitosis and cancer. *Ann. N. Y. Acad. Sci.* 2012, *1267*, 24–30.

[42] Ciardiello, C., Cavallini, L., Spinelli, C., Yang, J. et al., Focus on extracellular vesicles: new frontiers of cell-to-cell communication in cancer. *Int. J. Mol. Sci.* 2016, *17*, E175.

[43] Nakano, I., Garnier, D., Minata, M., Rak, J., Extracellular vesicles in the biology of brain tumour stem cells–implications for inter-cellular communication, therapy and biomarker development. *Sem. Cell Dev. Biol.* 2015, *40*, 17–26.

[44] Vizcaino, J. A., Csordas, A., Del-Toro, N., Dianes, J. A. et al., 2016 update of the PRIDE database and its related tools. *Nucleic Acids Res.* 2016, *44*, D447–D456.

Supporting Information

Materials and Methods

Cell Culture

The human Merkel cell polyomavirus-negative cell lines MCC13 and MCC26 and polyomavirus-positive Merkel cell carcinoma cell lines MKL-1 and MKL-2 were a kind gift from Dr B. Akgül (Institut für Virologie Uniklinik Köln, Köln, Germany). All cell lines were kept in culture medium RPMI-1640 (Sigma-Aldrich, Oslo, Norge) supplemented with 10% exosome depleted fetal bovine serum (Exosome-depleted FBS, System Biosciences, Cambridge, UK) for 72 hours. All cell types were incubated in a 5% CO_2 humidified incubator at 37^{o}C. FBS-associated-exosomes were stripped and were removed by dilution of FBS in RMPI-1640. Then, a cell suspension was collected and centrifuged for 5 minutes at 200 x *g* to removed whole cells. The collected supernatants were centrifuged for 15 minutes at 3000 x *g* to remove dead cells and stored in aliquots at -80 ^{0}C.

Extracellular Vesicles Isolation and Purification

The supernatants were thawed and centrifuged for 30 minutes at 10,000 x g in an centrifuge using a JA-25.50 rotor (Avanti J-26XP, Beckman Coulter Inc., Fullerton, CA, USA) to remove cell debris, and subsequently sterile-filtered using a 0.2 µm filter (Pall Corporation, Ann Arbor, MI, USA). Extracellular vesicles were isolated by ExoQuick-TC^{TM} Exosome Precipitation Solution (System Biosciences) according to the manufacture's instruction. Briefly, the appropriate volume of ExoQuick-TC Exosome Precipitation

Solution was added to the supernatant. The mixsture was incubated for 12 hours at 4 ºC and centrifuged at 1500 x *g* for 30 minutes at room temperature. The extracellular vesicles' pellet was centrifuged (Allegra® X-15R, Beckman Coulter Inc., Palo, CA, USA) for another 5 minutes at 1500 x *g* and the supernatant was removed without disturbing the precipitated extracellular vesicles in pellet.

Transmission Electron Microscopy

Cells and extracellular vesicles were fixed with 1x fixative consisting of 0.5% Glutaraldhyde (Sigma-Aldrich), 4% Formaldehyde (Sigma-Aldrich), and 0.05% Malachite Green (Sigma-Aldrich) in PHEM-buffer (Sigma-Aldrich) and microwaved 14 minutes following the Malachite Green Fix according to Valdivia's lab protocol [1]. After washing, cells and extracellular vesicles were dehydrated in graded ethanol solutions. Cells and extracellular vesicles were flat embedded with epoxy resin and cured on the coverslip at 60 °C for 24 h. The flat embedding was cut into small pieces to isolate the cells and extracellular vesicles of interest. The pieces were glued on spar resin blocs, trimmed close to the cells and extracellular vesicles of interest and mounted on an ultra-microtome (Leica, Germany) for sectioning as parallel as possible to the resin surface. Serial sections of 60 nm thickness were caught with a loop and set down on 75 lines/inch Hexagonal Mesh copper/0.7% formvar (Sigma-Aldrich)-coated grids (Electron Microscopy Sciences, Chemi-Teknik AS, Oslo, Norge). Sections were observed at 80 kV with a JEOL JEM-1010 (JEOL Ltd, Peabody, MA, USA), and images were

acquired with a digital camera Morada (Olympus Soft Imaging System, Münster, Germany).

Particle Size Analysis

The particle size distributions of extracellular vesicles was determined by photon correlation spectroscopy (Submicron particle sizer model 370, Nicomp, Santa Barbara, CA, USA). In order to avoid interference from dust particles, the test tubes to be used for the determination were filled with distilled water and sonicated for 10 min in ultrasonic bath, then rinsed with filtered water (using 0.2 µm filter) prior to the experiments. All formulations were prepared in a laminar airflow bench and analyses run in vesicle mode and the intensity-weight distribution at 23-24 °C [2]. Three parallels were determined (run time at least 25 min) for each sample measurement.

NuPage Gel Electrophoresis

Each protein concentration was determined by the Direct Detection method (Direct Detect Spectrometer, Merck Life Science AS, Oslo, Norway) as described previously [3]. Separation of the exosomal proteins from total lysates (30 µg) was performed by 4-12% NuPage Novex (Life Technologies, Oslo, Norway).

Liquid Chromatography-Tandem Mass Spectrometry

Gel pieces were subjected to in gel reduction, alkylation, and tryptic digestion using 6 ng/µl trypsin (V511A, Promega, Wisconsin, USA) [4]. OMIX C18 tips (Varian Inc., Palo Alto, CA, USA) were used for sample clean up and concentration. Peptide mixtures containing 0.1% formic acid were

loaded onto a Thermo Fisher Scientific EASY-nLC1000 system and EASY-Spray column (C18, 2µm, 100 Å, 50µm, 50 cm). Peptides were fractionated using a 2-100% acetonitrile gradient in 0.1 % formic acid over 50 min at a flow rate of 200 nl/min. The separated peptides was analysed using a Thermo Scientific Q-Exactive mass spectrometer. Data was collected in data dependent mode using a Top10 method [5]. The raw data were processed using the Proteome Discoverer 1.4 software. The fragmentation spectra were searched against the UniprotKB Homo Sapiens 2016/02/29 database using an in-house Mascot server (Matrix Sciences, UK). Peptide mass tolerances used in the search were 10 ppm, and fragment mass tolerance was 0.02 Da. Peptide ions was filtered using a false discovery rate (FDR) set to 1 % for peptide identifications.

Data Analysis

The Exocarta v5 [6] (www.exocarta.og) and Vesiclepedia v3 [7] (www.microvesicles.org) databases were used for analysis of MCC cell lines specific EVs proteins. The MCC cell lines specific EVs proteins annotated in ExoCarta and Vesiclepedia (n = 164) were analysed for enrichment by FunRich v2.1.2 [8, 9] (www.funrich.org) open access tool.

References

[1] Cocchiaro, J. L., Kumar, Y., Fischer, E. R., Hackstadt, T., Valdivia, R. H., Cytoplasmic lipid droplets are translocated into the lumen of the Chlamydia trachomatis parasitophorous vacuole. *Proc. Natl. Acad. Sci. U. S. A.* 2008, *105*, 9379-9384.

[2] Jøraholmen, M. W., Vanic, Z., Tho, I., Škalko-Basnet, N., Chitosan-coated liposomes for topical vaginal therapy: Assuring localized drug effect. *Int. J. Pharm.* 2014, *472*, 94-101.

[3] Strug, I., Utzat, C., Cappione, A., Gutierrez, S. et al., Development of a univariate membrane-based mid-infrared method for protein quantitation and total lipid content analysis of biological samples. *J. Anal. Methods Chem.* 2014, *2014*, 657079.

[4] Shevchenko A, Wilm M, Vorm O, Mann M. Mass spectrometric sequencing of proteins from silver stained polyacrylamide gels. *Anal. Chem.* 1996, *68*, 850-858.

[5] Olsen, J. V., Schwartz, J. C., Griep-Raming, J., Nielsen, M. L. et al., A dual pressure linear ion trap orbitrap instrument with very high sequencing speed. *Mol. Cell. Proteomics* 2009, *8*, 2759-2769.

[6] Keerthikumar, S., Chisanga, D., Ariyaratne, D.,Al Saffar, H. et.al., ExoCarta: A web-based compendium of exosomal cargo. *J. Mol. Biol.* 2016, *428,* 688-692.

[7] Kalra, H., Simpson, R. J., Ji, H., Aikawa E. et. al., Vesiclepedia: a compendium for extracellular vesicles with continuous community annotation. *PLoS Biol.* 2012, *10*, e1001450.

[8] Pathan, M., Keerthikumar, S., Ang, C. S., Gangoda, L. et. al., FunRich: An open access standalone functional enrichment and interaction network analysis tool. *Proteomics* 2015, *15*, 2597-2601.

[9] Benito-Martin, A., Peinado, H., FunRich proteomics software analysis, let the fun begin. *Proteomics* 2015, *15*, 2555-2556.

Research article

Comparative Analysis of microRNA Expression Profiles of Exosomes Derived from Polyomavirus-Negative and –Positive Merkel Cell Lines by Next Generation Sequencing

Aelita Konstantinell [1, #, *], Augusta Hlin Aspar Sundbø [1], Hao Shi[2], Nataša Škalko-Basnet [3], Weng-Onn Lui [2, #], Baldur Sveinbjørnsson [1] and Ugo Moens [1, #]

[1] Department of Medical Biology, University of Tromsø The Arctic University of Norway, Faculty of Health Sciences, Tromsø, Norway; aelita.g konstantinell@uit.no (A.K); augusta.h.a.sundbo@uit.no (A.A.S.); baldur.sveinbjornsson@uit.no (B.S.); ugo.moens@uit.no (U.M.);

[2] Department of Oncology-Pathology, Karolinska Institutet, Stockholm; Cancer Center Karolinska, Karolinska University Hospital, Stockholm, Sweden; hao.shi@ki.se (H.S.); weng-onn.lui@ki.se (W-O.L.);

[3] Department of Pharmacy, University of Tromsø The Arctic University of Norway, Faculty of Health Sciences, Tromsø, Norway; natasa.skalko-basnet@uit.no (N.S-B.);

# authors contributed equally to this work;

* Author to whom correspondence should be addressed:
e-mail: aelita.g.konstantinell@uit.no (A.K.), phone: +47 936 303 04

Received: date; Accepted: date; Published: date

Abstract: MicroRNAs (miRNAs) are small non-coding RNAs responsible for post-transcriptional regulation of gene expression through interaction with messenger RNAs (mRNAs). They are involved in important biological processes and dysregulated in a variety of diseases, including cancer and infections. Merkel cell carcinoma (MCC) is skin cancer of neuroendocrine origin. The major risk factors are ultraviolet light exposure and the presence of integrated Merkel cell polyomavirus (MCPyV) genome. In the past few years, evidence of the presence of cellular miRNAs in extracellular human body fluids such as serum, plasma, saliva, and urine has accumulated. miRNAs have been found in membrane-bound vesicles such as exosomes. Although little known about the role of exosomal miRNAs, it has demonstrated that miRNAs secreted by virus-infected cells are transferred to and act in uninfected recipient cells, thereby contributing to spreading the pathogenic properties of the virus. I this work, we sequenced exosomal miRNAs of MCPyV-negative and –positive MCC cell lines and validated on exosomal serum/plasma healthy donors and MCC patients. The result showed the miR-222-3p is present in exosomes from Merkel cell carcinoma cell culture, serum of healthy donors and plasma of MCC patients.

Keywords: microRNA, exosomal miRNA, Merkel cell carcinoma, Merkel cell polyomavirus, cell line.

1. Introduction

Merkel cell carcinoma (MCC) is an aggressive and lethal type of neuroendocrine skin cancer [1]. MCC is rare, but its incidence is increasing by 95% compared to melanoma and solid tumors [2]. The risk of developing Merkel cell carcinoma is greatly increased among a large number of immunosuppressed patients [3-6]. Integrated Merkel cell polyomavirus (MCPyV) genome is found in ~80% of MCC [1]. However, ~20% of MCC tumors do not have detectable MCPyV, which suggest alternative etiologies for this tumor type. UV exposure being a major risk factor. The pathogenesis, aggressiveness, metastatic potential and response to treatment can be different among individual patients with the same kind of cancer that suggest the role of genetic factors in cancer pathogenesis [7]. There are needs of personalized treatments of cancer patients. Highly specific biomarkers may provide valuable information for diagnosis, prognosis, and therapy [8]. The treatment of MCC depends on many factors, but traditionally is the surgical intervention and the adjuvant chemo- and radiation therapy [9]. Immune therapy based on monoclonal antibodies targeting the program cell death protein 1 (PD-1) and its ligand L1 (PD-1/PD-L1) axis represents a promising approach for cancer treatment in MCC patients [10-12]. However, PD-1/PD-L1 therapy has failed to arrest the cancer progression leading to identifying pre-existing and acquired mechanisms of resistance to the immune treatment [11-13].

It is clear that cell-to-cell communication serves an important role in cancer cells adaption and survival. Cells can communicate by direct contact via junctions or by secreting signaling molecules that are taken up by targets cells. Another mode of communication is by secreting extracellular vesicles packed with cargo which are taken up by recipient cells. One type of extracellular vesicles is exosomes [14]. Exosomes are membrane vesicles of an average 30 – 300 nm in diameter [15]. They are produced by most cells, are stable and can be detected in various body fluids such as serum, plasma, saliva and urine that are routinely examined in patients. Exosomes can carry proteins, lipids, sugars, RNA and DNA [16, 17]. However, the exosomal contents are unique for the different cell types from which they originate. Exosomes play an important role in non-pathogenic and pathogenic processes. The exosomal process is perturbed in cancer, and cancer cells secrete more exosomes compare to healthy cells [16]. Many studies confirmed that exosomes from different cells types contain a unique expression profile of microRNAs (miRNAs), which indicates selectivity of exosomal miRNAs [14, 18-23]. The miRNAs are modulators of gene expression. They are approximately 17-24 nucleotide long non-coding RNAs that function by targeting messenger RNA (mRNA) leading to their degradation and suppressing protein translation at the post-transcriptional level [23-25]. miRNAs involved in every aspect of cellular processes such as cell cycle control, proliferation, programmed cell death, immune responses, hormone secretions, and angiogenesis through the gene expression regulation [25-29].

Furthermore, aberrant expression of the miRNAs profile has been described in various diseases, including cancer that they associated with disease stage, cancer subtype and drug resistance [30-36]. Exosomes and miRNAs are detectable in various body fluids such as serum, plasma, saliva, and urine. Moreover, the levels of exosomes and miRNAs differ between healthy donors and cancer patients [24]. Thus, exosomal miRNAs are important as messengers in cell-to-cell-communication [37].

In the current study, the exosomal microRNAome from MCPyV-negative and –positive MCC cell lines compared by next-generation sequencing (NGS). The presence of one differentially expressed miRNA, miR-222-3p was validated in exosomes from Merkel cell carcinoma cell culture and in serum samples from healthy donors and plasma from MCC patients. Furthermore, putative target genes and the role of miR-222-3p as the messenger in cell-to-cell communication in the cancer environment and the circulation is discussed

2. Results

2.1. Characterization of Exosomes from MCPyV-Negative and -Positive Merkel Cell Carcinoma Cell Lines

Exosomes were isolated from the MCPyV-negative cell lines MCC13, MCC26, and UISO, and the MCPyV-positive cell lines MKL1, MKL2, and WaGa. The purified exosomes were evaluated by size, protein markers, and electron microscopic appearance.

The diameter of exosomes is considered to be between 30 and 300 nm [15, 38]. The size distribution of the exosomes isolated from the six MCC cell lines was determined by photon correlation spectroscopy and showed that the mean diameter size of exosomes from MCPyV-negative MCC cell lines was in the range between 25.1 ± 2.6 and 211.5 ± 38.3 nm, whereas those from MCPyV-positive MCC varied between 38.2 ± 4.3 and 227.0 ± 28.2 nm (**Table** 1). These results showed the size of the exosomes from MCC cell lines corresponds to the predicted size of exosomes. An exception was exosomes from the MCPyV-negative cell line, UISO, for which the mean size of the first peak (9.9% of the UISO-derived exosomes) in ranged between 25.1 ± 2.6 nm in diameter. This is somewhat smaller than exosomes usually are considered to be [15, 38]. For the MCPyV-positive cell line MKL2, 57.7% of exosomes had a mean diameter of 177.4 ± 21.3 nm, which was slightly larger as reported in our previous work, but still in the range of exosomes size [15, 39].

Table 1. The exosomes size distribution was determined by photon correlation spectroscopy on submicron particle sizer model 370 and represented in intensity-weight distribution.

Sample	Mean diameter peak 1 (nm)	%	Mean diameter peak 2 (nm)	%	PI[a]
MCC13	28.2 ± 3.1	16.8	112.9 ± 15.9	48.7	0.471
MCC26	48.2 ± 7.0	44.8	211.5 ± 38.3	55.2	0.375
UISO	25.1 ± 2.6	9.9	48.3 ± 20.19	91.1	0.689[b]
MKL1	38.8 ± 4.2	40.8	177.4 ± 21.3	59.2	0.373
MKL2	38.2 ± 4.3	42.3	227.0 ±28.2	57.7	0.408
WaGa	40.6 ± 3.8	14.3	137.3	85.7	0.373

[a]Polydispersity index. [b]Agglomerates were observed, high PI

The size of exosomes visualized by transmission electron microscopy was in agreement with the photon correlation spectroscopy measurement (**Figure 1**). The mean size range for exosomes from the MCPyV-negative MCC13 and MCPyV-positive MKL1 cell lines was observed between 30 and 180 nm in diameter.

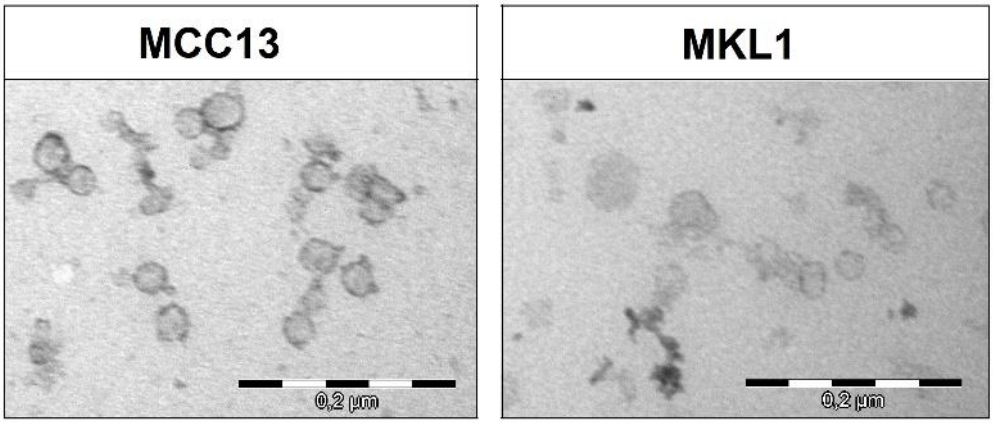

Figure 1. Characterizations of exosomes from supernatants of cell lines by transmission electron microscopy, x80 000 magnification. A section of purified exosomes produced using the negative contrast staining, the mean size range of observed exosomes was between 30 and 180 nm in diameter. Scale bar = 0.2 µm.

Common canonical exosomal proteins can be used as markers to identify exosomes. Western blot analysis of the isolated exosomes demonstrated that they were positive for the exosomal marker CD63 and negative for the cell contamination cis-Golgi marker, GM130 (**Figure 2a**) [40]. Total cell lysates were used as positive controls for the GM130 Golgi marker (**Figure 2b**).

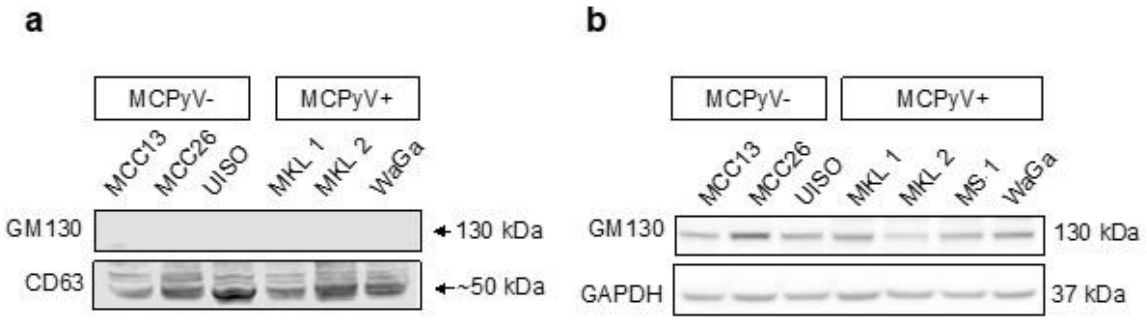

Figure 2. Characterizations of exosomal markers in exosome isolated from culture supernatants of MCC cell lines. (**a**) Evaluation of the negative protein GM130 (130 kDa), and the exosomal marker CD63 (50 kDa) present in exosomes from MCPyV-negative and –positive cell lines by Western blotting. (**b**) Western blot analysis of GM130 protein in total cell lysates of MCC cell lines. GAPDH was used as loading control.

2.2 Characterization of Exosomes from Healthy Donors and Patients Samples

Exosomes isolated from serum/plasma samples of healthy donors (HD) and MCC patients (ME) were evaluated by several methods (**Table 2**). Exosomes of healthy human donors had been isolated from the donors' pooled serum, prepared with quality and care. Each lot of exosomes was carefully characterized for particle size and concentration by NanoSight™ analysis, and expression of specific exosome protein markers CD9 and CD63 were validated by Western blot (not showed). On account of the small volumes of the patient samples two samples, ME18 and ME29 were chosen to study by Photon correlation spectroscopy and TEM as complementary methods to western blotting and qRT-PCR.

Table 2. Characterization of exosomes purified from healthy donors (n = 4) and patients samples (n = 8) by several methods.

			Analyzed by			
Sample no.	Age (year)	Diagnosis	Photon correlation spectroscopy	TEM	Western Blotting	qRT-PCR
HD1	-	-	+	+	+	+
HD2	-	-	+	+	+	+
HD3	-	-	-	-	+	+
HD4	-	-	-	-	+	+
ME18	74	MCC	+	+	+	+
ME20	76	MCC	-	-	+	+
ME21	62	MCC	-	-	+	+
ME22	66	MCC	-	-	+	+
ME29	80	MCC	+	+	+	+
ME31	72	MCC	-	-	+	+
ME33	71	MCC	-	-	+	+
ME36	71	MCC	-	-	+	+

The exosome size distribution was determined by photon correlation spectroscopy that showed the mean size of exosomes from HD in the range between 28.1 ± 1.8 and 168.2 ± 19.7 nm in diameter and the mean size of the exosomes from ME in the range between 26.4 ± 3.1 and 173.6 ± 8.9 nm in diameter (**Table 3**).

Table 3. The size distribution of exosomes isolated from a healthy donor and MCC patient samples.

	Size distribution				
Sample no.	Mean diameter peak 1 (nm)	%	Mean diameter peak 2 (nm)	%	PI[a]
HD1	28.1 ± 1.8	29.7	89.3 ± 10.4	70.3	0.429
HD2	35.8 ± 4.6	25.5	168.2 ±19.7	74.5	0.570
ME18	34.7 ± 3.3	17.6	173.6 ± 8.9	82.4	0.672[b]
ME29	26.4 ± 3.1	43.7	110.7 ± 12.5	56.3	0.358

[a]Polydispersity index. [b]Agglomerates were observed, high PI

Isolated exosomes were visualized by transmission electron microscopy (**Figure 3**). In spite of this small range, TEM confirmed the known size range of exosomes [15, 38]. The size distribution was in the range between 30 and 180 nm in diameter on HD and 25 and 200 nm in diameter on ME.

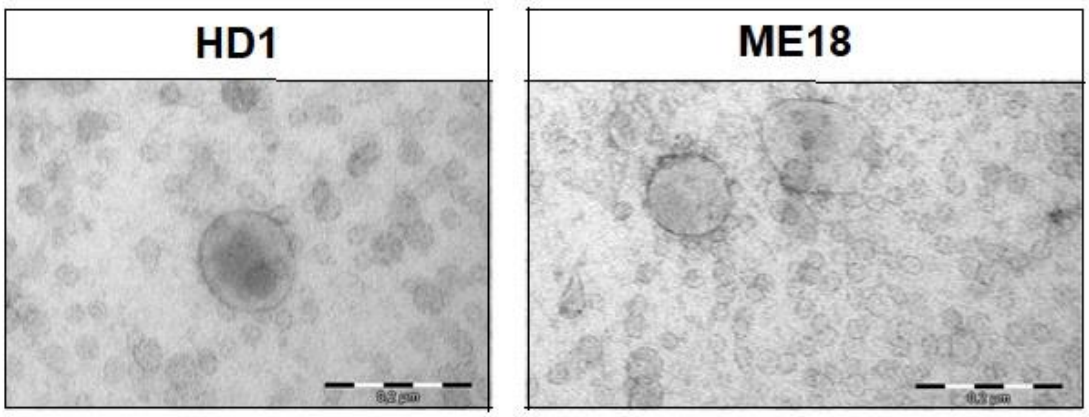

Figure 3. TEM of exosomes from the serum of healthy donor HD1 and plasma of MCC patient ME18, x 80 000 magnification. Scale bar = 0.2 μm.

As shown in **Figure 4**, the analysis performed by Western blot on lysates of the vesicles using antibodies against the exosomal marker CD63 and negative control for GM130 confirmed that isolated vesicles are exosomes without any cellular contamination. These results confirmed that the vesicles isolated from the serum/plasma samples were exosomes based on their size and marker protein expression.

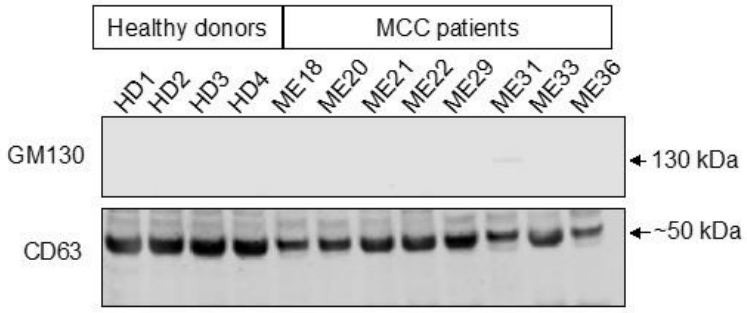

Figure 4. Detection of exosomal marker CD63 protein in exosomes purified from serum samples of healthy donors (HD) and plasma samples of MCC patients (ME). Top panel: the exosome negative marker protein CM130 (130 kDa), and bottom panel: the exosomal marker CD63 (50 kDa).

2.3. Exosomal miRNA Profiles Originated from Merkel Cell Carcinoma Cell Lines by Deep Sequencing

To assess the exosomal miRNA profiles of Merkel cell carcinoma, deep sequencing of miRNA purified from exosomes originated from the MCPyV-negative MCC13 and MCC26, and the MCPyV-positive MKL1 and MKL2 MCC cell lines was performed. Sequencing was performed with three independent exosomal RNA preparations for each cell lines. In total, 16 517 058 ± 5 527 592 reads for MCC13, 17 073 897 ± 1 603 976 reads for MCC26, 17 708 458 ± 5 192 408 reads for MKL1 and 30 364 588 ± 17 011 373 reads for MKL2, respectively were obtained. On average, 20.4 million reads obtained per sample.

After mapping the data and counting to relevant entries in miRBase 20 the numbers of known miRNAs calculated (**Figure 5**). Identified miRNAs across each sample were for transcripts per million (TPM) >1: 299 ± 47 for MCC13 exosomes, 346 ± 53 for MCC26 exosomes, 364 ± 40 for MKL1 exosomes and 357 ± 17 for MKL2 exosomes. Identified miRNAs across each sample were for TPM >10: 152 ± 28 for MCC13 exosomes, 175 ± 30 for MCC26 exosomes, 181 ± 21 for MKL1 exosomes and 172 ± 9 for MKL2 exosomes. In summary, the number of identified miRNAs with average TPM > 1 was 360 across all samples, and the number of identified miRNAs with average TPM > 10 was 198 across all samples. The reliability of the identified miRNAs increased with the number of identified fragments [41].

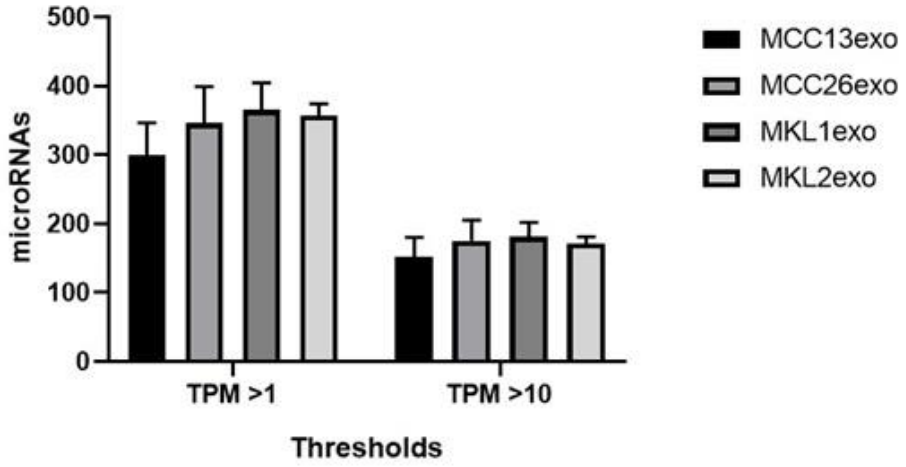

Figure 5. A number of identified known miRNA with the number of counts for each group of samples with average >1TPM and >10TPM.

The miRNAs prediction found 439 predicted miRNAs in the dataset based on putative precursor hairpin structures and these included in the subsequent supervised differential expression analysis that gives the 519 differentially expressed miRNAs (**Supplementary Material, Table S1**).

To illustrate the exosomal differentially expressed miRNA profiles of the four MCC cell lines unsupervised clustering of miRNAs and samples was performed. As shown in the dendrogram in Figure 6, MCPyV-negative and –positive cell lines were separated into two distinct clusters based on the exosomal miRNA profiles.

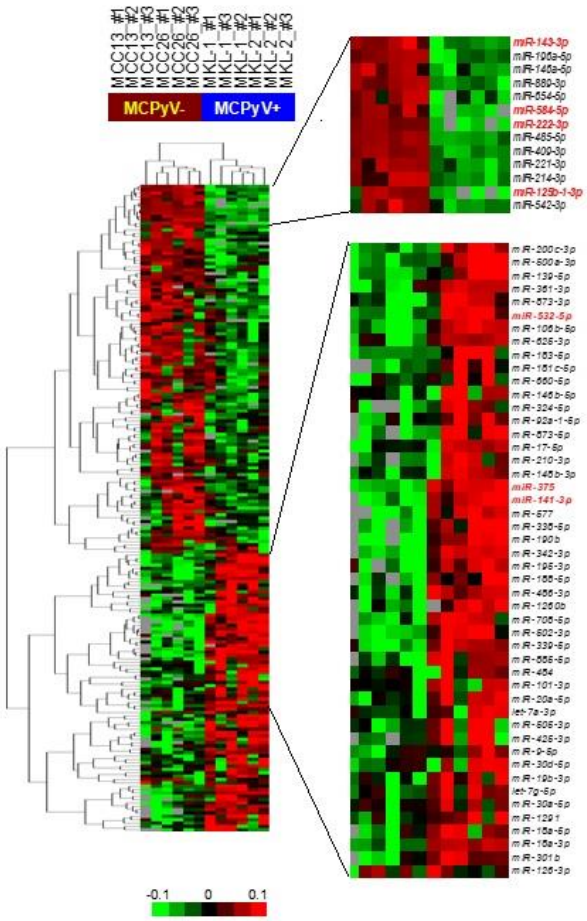

Figure 6. Heat Map and unsupervised hierarchical clustering by samples and miRNAs. miRNAs and samples were clustered using Euclidean distance and complete linkage. Red and green colors indicate relatively high and low expression, respectively. Missing values are shown in gray. #1-3 refers to different replicates with independent exosomal RNA isolations. miRNAs selected for qRT-PCR validation are highlighted in red.

Notably, several exosomal miRNAs were unique to specific MCC type. **Supplementary Material, Table S2** includes the miRNAs that were ≥2-fold upregulated when comparing the miRNAome from exosomes derived from the virus-negative and virus-positive MCC cell lines. For MCC MCPyV-negative and –positive cell lines, the miRNA existent pattern was not homogenous. Expression levels of *miR-21-3p/5p, miR-22-3p/5p, miR-142-3p/5p, miR-199a-3p/5p, miR-199b-3p/5p, miR-409-3p/5p, miR-125b-1-3p/5p* and *miR-3180-3p/5p* in the exosomes originated from both MCPyV-negative MCC cell lines and expression levels of *miR-532-3p/5p, miR-873-3p/5p and miR-6515-3p/5p* in the exosomes originated from both MCPyV-positive MCC cell lines differed two-fold or more.

2.4. Validation Analysis of miRNAs-Sequencing Data via qRT-PCR

Differential expression of eight miRNAs was validated by qRT-PCR (**Table 4**). These miRNAs were also selected based on their previously described involvement in MCC [42-48] and other tumor types

[49-54]. The five miRNAs upregulated in MCC MCPyV-negative cell lines compare to MCPyV-positive cell lines are miR-31-5p, miR-125b-1-3p, miR-143-3p, miR-222-3p and miR-584-5p. The three miRNAs upregulated in MCPyV-positive cell lines compare to MCPyV-negative cell lines are miR-141-3p, miR-375 and miR-532-5p. miR-30a-5p, which was stably expressed across all samples as showed the NGS analysis, was used as an internal control for the validation study.

Table 4. Validation of 8 selected microRNA from the exosomal microRNA sequencing result with qRT-PCR method. miRNA sequencing evaluation shows ≥2-fold upregulation or down-regulation of microRNA in exosomes from MCC MCPyV-negative vs. MCPyV-positive cell lines. The qRT-PCR result, differences in miRNAs presence in exosomes from MCPyV-negative and –positive were assessed using the paired t-test. A *P* value of less than 0.05 considered statistically significant.

miRNA	miRNA seq				miRNA qRT-PCR	
	MCPyV- vs. MCPyV+				MCPyV- vs. MCPyV+	
	LogFC	FDR	*P* Value	Mean MCPyV-	*P* Value	Mean MCPyV-
miR-31-5p	8.730	3.787e-14	1.16e-15	Higher	0.03*	Higher
miR-125b-1-3p	9.923	7.77e-20	8.98e-22	Higher	0.11	Higher
miR-141-3p	-7.237	1.64e-16	3.15e-18	Lower	0.15	Higher
miR-143-3p	7.764	9.28e-17	1.43e-18	Higher	0.09	Higher
miR-222-3p	9.753	5.23e-20	5.04e-22	Higher	0.002*	Higher
miR-375	-10.406	3.73e-47	7.18e-50	Lower	0.07	Higher
miR-532-5p	-4.870	7.15e-15	1.52e-16	Lower	0.88	Lower
miR-584-5p	9.452	3.62e-20	2.79e-22	Higher	0.42	Higher

LogFC, LogFoldChange; **FDR,** False Discovery Rate; *, statistically significant.

The selected miRNAs were detected in all samples. This presence of miR-31-5p and miR-222-3p was further investigated in exosomes purified from serum 4 healthy donors and plasma 8 MCC patient. The qRT-PCR result confirmed that only exosomal miR-222-3p expression agrees with the NGS result. The miR-222-3p was upregulated in MCPyV-negative MCC cell lines (**Figure 7a**). A Mann-Whitney U test performed to determine whether there were differences in miR-222-3p expression level between samples. There was a statistically significant difference between the miR-222-3p levels in the exosome samples between the median of MCPyV-negative (1.659) and -positive MCC cell lines (0.008), $U = 0$, $P = 0.0022$ (**Figure 7b**). The miR-222-3p was not statistically significant in exosome samples between the median of healthy donors (3.627) and patient (1.064), $U = 7$ (**Figure 7b**).

a.

miRNA	miRNA seq				miRNA qRT-PCR	
	MCPyV- vs MCPyV+				MCPyV- vs MCPyV+	
	LogFC	FDR	*P* Value	Mean MCPyV-	*P* Value	Mean MCPyV-
miR-222-3p	9.753	5.23e-20	5.04e-22	Higher	0.0022	Higher

LogFC, LogFoldChange; **FDR**, False Discovery Rate

b.

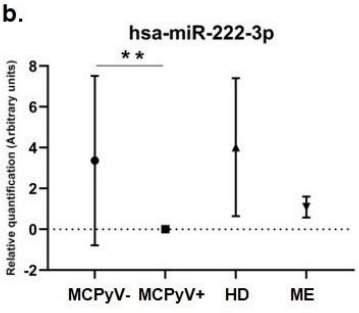

Figure 7. Validation of exosomal miR-222-3p expression by qRT-PCR methods in MCC cell lines and serum and plasma samples of healthy individuals and MCC patients. **a)** The sequencing result (miRNA seq) marked Higher means that the miRNA is upregulated (≥2-fold) in exosomes from MCC MCPyV-negative and down-regulated (≥2-fold) in exosomes from MCC MCPyV-positive. The qRT-PCR result, differences in miRNAs presence in exosomes from MCPyV-negative and –positive were assessed using the Mann-Whitney test. **b)** The relative miR-222-3p levels present in exosomes purified from MCC MCPyV-negative and –positive cell lines, serum from healthy donors (HD; n=4) and plasma from MCC patients (n=8). Differences in miR-222-3p presence in exosomes samples were assessed using the Mann-Whitney test. The *y*-axes show arbitrary units representing the relative miRNA expression levels, error bars ± SD, ***P*-value < 0.005.

To quote the exosomal miR-222-3p expression change in progress upon viral and cancer status in the circulatory system, healthy donors and patients' samples quantified in relation to MCPyV-negative and –positive cell lines. There were no statistically significant differences between the fold changes of miR-222-3p in healthy donors (median = 477.7) and patients (median = 250.6) in relation to MCC MCPyV-positive cell line (not showed). There was the statistically significant difference between the fold change in miR-222-3p expression in exosome samples from healthy donors (1.626) and patients (0.241), respectively in relation to MCC MCPyV-negative cell line, $U = 32.50$, $P = 0.0023$.

2.5. Prediction of putative miR-222-3p targets

To understand the exosomal miR-222-3p influence in health and disease, miRNA's target genes predicted using the ExoCarta, TargetScan, and miRTarBase [55-57]. As a result, 212 (ExoCarta), 245 (TargetScan) and 394 (miRTarBase) potential target genes for miR-222-3p were identified (**Supplementary Material, Table S3A: ExoCarta, S3B: TargetScan,** and **S3C: miRTarBase**). The enrichment analyses were done by FunRich3.1.3 (**Figure 8**) [58]. Only 20 were shared by all three databases (**Supplementary Material, Table S4**).

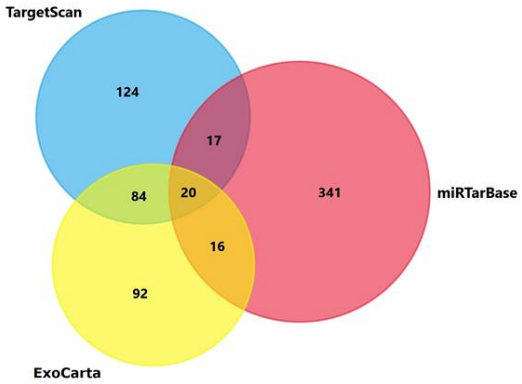

Figure 8. Venn-diagram of the overlap between the predicted target genes by ExoCarta, TargetScan, and miRTarBase, which shows 20 common targets of miR-222-3p (**Supplementary Material, Table S4**).

These include sorting nexin-4 (SNX4), SUN domain-containing protein 2 (SUN2), stathmin (STMN1), 14-3-3 gamma (YWHAG), RNA-binding protein with serine-rich domain 1 (RNPS1), and importin subunit alpha-1 (KPNA2) that differentially expressed proteins on MCC cell lines (our unpublished data; **Supplementary Material, Table S5**). The 14-3-3 gamma protein was detected in extracellular vesicles originated from MCC cell lines [39]. Expression of SNX4, SUN2 and RNPS1 in MCC not been reported before. Besides these, target genes expressed in leukocytes (55.0%, P = 0.046), according to the enrichment analysis (**Figure 9**).

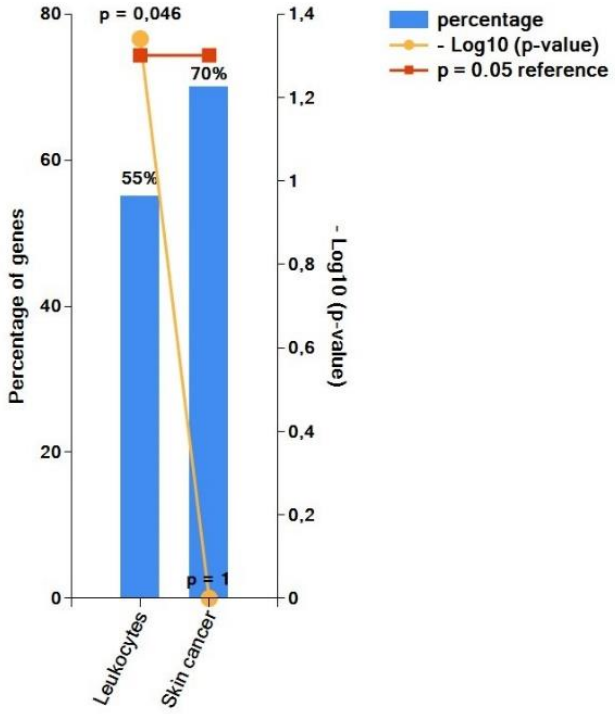

Figure 9. Enrichment analysis of 20 common miR-222-3p predicted targets' site of expression. The FunRich database as a background including only human genes and proteins, *P*-value < 0.05.

Eleven of these twenty target genes such as sorting nexin-4 (SNX4); SUN domain-containing protein 2 (SUN2); stathmin (STMN1); 14-3-3 gamma (YWHAG); tumor protein p53 binding protein 2 (TP53BP2); poly(A) binding protein interacting protein 2 (PAIP2); zinc finger FYVE-type containing 16 (ZFYVE16); suppressor of cytokine signaling 3 (SOCS3); proline-rich nuclear receptor coactivator 2 (PNRC2); dipeptidyl peptidase 8 (DPP8); and reversion inducing cysteine-rich protein with kazal motifs (RECK) expressed and were been reported before in leukocytes (**Supplementary Material, Table S6**) [59-68].

3. Discussion

The present study has demonstrated the secretion of exosomes by Merkel cell carcinoma cell lines and the presence of exosomes in serum or plasma samples from healthy donors and MCC patients. The exosomes were an average 30 – 250 nm in diameter. The exosomal miRNAs contents from MCPyV-negative and –positive MCC cell lines was investigated by high-throughput sequencing, showing differential expression in exosomes derived from virus-negative and virus-positive MCC cell lines. Results of this deep sequencing indicated that miR-222-3p was more abundant in exosomes generated by virus-negative MCC cells than in exosomes secreted by virus-positive MCC cell lines. RT-qPCR validation confirmed this finding. MiR-222-3p was also detected in exosomes purified from serum samples of healthy donors and plasma samples of MCC patients. The miR-222-3p presence at a higher level in exosomes in healthy condition than in pathophysiological condition. In the early studies, the plasma miR-222-3p identified as a strong intrinsic reference miRNA useful for the study of estrogen-responsive miRNAs in pregnancy, and the other study concluded that there was no significant difference on the designation of miRNAs between plasma and plasma-derived exosomal, but the frequency was higher in plasma in healthy people [69-72].

For the discussion, we focused on the role of exosomal miR-222-3p and their targets in cancer.

MiR-222-3p has been detected in exosomes from cancer such as epithelial ovarian cancer, non-small cell lung cancer and breast cancer [52, 69, 70]. MiR-222-3p has described neither in tissues nor in cells from MCCs. [42-45]. These support selectivity of exosomal miRNAs, particularly miR-222-3p.

The enrichment analysis showed 11 of predicted 20 common miR-222-3p targets expressed in leukocytes and six of them identified as differentially expressed proteins in MCC cell lines. The cancer cells and their exosomes likely interfere with the induction of an efficient immune response via several mechanisms inducing triggering T cell suppression mechanisms, attenuating NK cell cytotoxicity, and engaging pro-metastatic inflammatory processes and generating an immunosuppressive environment to escape from the immune system and eventually, treatment failure [73, 74].

Initially revealed that exosomal miR-222-3p derived from epithelial ovarian cancer induce polarization of tumor-associated macrophages [53]. Further, transferred miR-222-3p into subcellular

sites in recipient cells induced repression of expression target genes [69]. One of the miR-222-3p target genes is the SOCS family, which is a major negative regulator of cytokine signaling that regulates development, subsets profiling and function of immune cells in carcinogenesis [75]. Moreover, the exosomal miR-222-3p demonstrated malignant characteristics and features as a regulator of gemcitabine resistance by targeting suppressor of cytokine signaling 3 (SOCS3) [69]. Furthermore, miR-222-3p was found to be enriched in exosomes from patients with hepatitis C virus (HCV) related immuno-pathogenesis and miR-222-3p inhibited natural killer cells (NK) degranulation activity. Direct-acting antiviral (DAA) therapy markedly reduced the levels of exosomal miR-222-3p and restored NK function [76].

There can be a distinct implication of exosomal miR-222-3p in the immunopathogenesis of MCC. The sorting nexin-4, inner nuclear membrane protein SUN2, and RNA binding protein with serine-rich domain 1 were never mentioned to be associated with MCCs, but a stathmin 1 associated with MCPyV ST antigen, which mediates microtubule destabilization to promote cell motility and migration in MCCs [78, 79]. The karyopherin alpha 2 induced expression found in MCCs and it is essential for ribosomal RNA (rRNA) transcription and protein synthesis in proliferating keratinocytes [80]. Interestingly, MCC cell lines' exosomes content 14-3-3 protein gamma (YWHAG) [39]. 14-3-3 protein gamma is one of the oncogenic Wnt pathway's activation factor, and an additional factor of PI3/Akt/beta-catenin signaling on cell proliferation [81, 82]. Recently, Chu and colleagues showed that level of miR-222 was significantly lower in osteosarcoma tumor tissue samples than that in the group of samples from healthy individuals. MiR-222 over-expression decreased cell proliferation and invasion in osteosarcoma [83]. Moreover, reduced miR-222 promoted YWHAG expression and up-regulation of YWHAG restored the inhibiting effect of miR-222 mimics [83]. Wei and colleagues' study of exosomal miR-222-3p concluded that a higher level of these exosomal miRNAs in serum from non-small cell lung cancer (NSCLC) patients usually predicted a worse prognosis [69]. Thus, the exosomal miR-222-3p and its targets may play a pleiotropic role in MCC tumorigenesis and drug resistance.

A current limitation of this project is an exclusive pilot study of exosomes and exosomal miRNAs in plasma samples from MCC patient and the comprehensive exosomal miRNA analysis in MCC cell lines.

In conclusion, our results showed that the presence of exosomal miR-222-3p in exosomes derived from MCC cell lines, healthy donors and MCC patients. There was a statistically significant higher level of miR-222-3p in the exosome samples from MCPyV-negative compared with virus-positive MCC cell lines, suggesting higher levels of miR-222-3p in MCPyV-negative than MCPyV-positive MCC tumor. The miR-222-3p usefulness as a biomarker needs to be further explored and its role in MCC remains

elusive. The target genes' scanning indicates that the exosomal miR-222-3p play pleiotropic role dependent on recipient cells in health and disease.

4. Materials and Methods

4.1. Samples

4.1.1. Cell Culture

The human Merkel cell polyomavirus-negative cell lines MCC13, MCC26 and UISO, and polyomavirus-positive Merkel cell carcinoma cell lines MKL-1, MKL-2 were a kind gift from Dr. B. Akgül (Institut für Virologie Uniklinik Köln, Köln, Germany) and WaGa. All cell lines were kept in culture medium RPMI-1640 (Sigma-Aldrich, Oslo, Norge) supplemented with 10% exosome depleted fetal bovine serum (exosome-depleted FBS, SBI, CA, USA). All cell types were incubated in a 5% CO_2 humidified incubator at 37°C. FBS-associated-exosomes were stripped and were removed by dilution of FBS in RMPI-1640. Then, a cell suspension was collected and centrifuged for 5 minutes at 200 x *g* to remove whole cells. The collected supernatants stored in aliquots at -80 ^{0}C.

4.1.2. Donor and Clinical Samples

Purified Exosomes from serum from healthy donors were purchased from Sanbio B.V. (Uden, The Netherlands).

Whole blood samples from 8 MCC patients were collected in heparinized tubes at Karolinska University Hospital. The blood samples were centrifuged to separate plasma at 10,000 rpm for 10 min and store at -80 ˚C until use. The study was approved by the Ethics Committee of Karolinska Institutet. All patients provided informed consent in written form.

4.2. Extracellular Vesicles Isolation and Purification

The supernatants were thawed and centrifuged (Allegra® X-15R, Beckman Coulter Inc., Palo, CA, USA) for 15 minutes at 3000 x g to remove dead cells. Then, the supernatants were sterile-filtered using a 0.2 μm filter (Pall Corporation, Ann Arbor, MI, USA). Extracellular vesicles were isolated by ExoQuick-TCTM Exosome Precipitation Solution (SBI, CA, USA) according to the manufacturer's instruction. Briefly, the appropriate volume of ExoQuick-TC Exosome Precipitation Solution was added to the supernatant. The mixture was incubated for 12 hours at 4^{0}C and centrifuged (Beckman Coulter Inc.) twice at 1500 x g for 30 and 5 minutes at room temperature. The supernatant was removed without disturbing the precipitated extracellular vesicles. The exosomes were purified by ExoQuick® ULTRA EV Isolation kit (SBI). The pellet containing the exosomes was re-suspended in 200 μl buffer A. The purification column was washed two times and 100 μl of buffer B was applied on top of the resin to prep it for sample loading. The re-suspended extracellular vesicles were added to the column and mixed

at room temperature on a rotating shaker for 5 minutes. To obtain exosomes, the column was transferred to 2 ml Eppendorf tube and centrifuged at 1000 x g for 30 seconds.

The serum samples were thawed and centrifuged (Allegra® X-15R, Beckman Coulter Inc.) at 12000 x g for 10 minutes. The supernatant was transferred to a new tube. Then, extracellular vesicles were isolated by ExoQuick® ULTRA EV Isolation kit for serum and plasma (SBI) according to the manufacturer's instruction. Briefly, the appropriate volume of ExoQuick-TC Exosome Precipitation Solution was added to the supernatant. The mixture was incubated for 30 minutes at four ^{0}C and centrifuged at 3000 x g for 10 minutes at room temperature. The supernatant was removed, and the precipitated extracellular vesicles were purified by ExoQuick® ULTRA EV Isolation kit (SBI) as mentioned above.

4.3. Electron Microscopy Imaging

For negative staining, 5 µl drops of exosomes (in PBS) were adsorbed onto 75 lines/inch Hexagonal Mesh copper/0.7% formvar (Sigma-Aldrich)-coated grids (Electron Microscopy Sciences, Chemi-Teknik AS, Oslo, Norge) for 5 min, washed by dabbing the grid onto four drops of double distilled water, and stained with 0.3% uranyl acetate (Sigma-Aldrich) and 2% methylcellulose (Sigma-Aldrich) for 2 minutes. The grid was examined at 80 kV with a JEOL JEM-1010 (JEOL Ltd, Peabody, MA, USA), and images were acquired with a digital camera Morada (Olympus Soft Imaging System, Münster, Germany).

4.4. Photon Correlation Spectroscopy

The particle size distributions of extracellular vesicles were determined by photon correlation spectroscopy (Submicron particle sizer model 370, Nicomp, Santa Barbara, CA, USA). To avoid interference from dust particles, the test tubes to be used for the determination were filled with distilled water and sonicated for 10 min in an ultrasonic bath, then rinsed with filtered water (using 0.2 µm filter) prior to the experiments. All formulations were prepared in a laminar airflow bench, and analyses run in vesicle mode and the intensity-weight distribution at 23-24 °C [84]. Three parallels were determined (run time at least 25 min) for each sample measurement.

4.5. RNA Isolation

Total exosomal RNAs were extracted using the SeraMir Exosome RNA Purification kit (SBI), according to the manufacturer's instruction. Briefly, 350 µl of lysis buffer was added to EVs pellet and vortexed for 15 seconds. The re-suspended exosomes were then placed at RT for 5 minutes to allow complete lysis. Then 200 µl of 100% ethanol was added, and the solution was vortexed for 10 seconds. The lysed exosomes were then transferred to a spin column and centrifuged at 13000 rpm for 1 minute. The column was washed twice by adding 400 µl of wash buffer to the column followed by centrifugation

for 1 min at 13000 rpm. The flow-through was discarded, and the column was centrifuged at 13000 rpm for 2 minutes to ensure it was completely dry. The total RNAs were eluted in 30 µl elution buffer. The column was centrifuged at 2000 rpm for 2 min to allow the buffer to spread in the column and there after for 1 min at 13000 rpm to elute exosomal RNA.

4.6. microRNA Sequencing

The microRNA sequencing and analysis were ordered as a commercial service from Exiqon A/S (Vedbæk, Denmark). The library preparation and Next Generation sequencing were conducted at Exiqon. Briefly, the library preparation was done using the NEBNext® Small RNA Library preparation kit (New England Biolabs, Ipswich, MA, USA). A total of 100 ng of total RNA was converted into microRNA NGS libraries. Adapters were ligated to the RNA. Then RNA was converted to cDNA. The cDNA was amplified using PCR (15 cycles), and during the PCR indices were added. After PCR the samples were purified. Library preparation QC was performed using Bioanalyzer 2100 (Agilent, Santa Clara, CA, USA). Based on the quality of the inserts and the concentration measurements, the libraries were pooled in equimolar ratios. The pool was then size selected using the LabChipXT (PerkinElmer, Denmark) aiming to select the fraction with the size corresponding to microRNA libraries (~145 nt). The library pools were quantified using the qPCR KAPA Library Quantification Kit (KAPA Biosystems). The library pool was then sequenced on a NextSeq 500 sequencing instrument according to the manufacturer's instructions. Raw data was de-multiplexed, and FASTQ files for each sample were generated using the bcl2fastq software (Illumina Inc.). FASTQ data were checked using the FASTQC tool (Babraham Bioinformatics, London, UK).

An average of 20.4 million reads was obtained per samples. The numbers of known miRs were calculated after mapping the data and counting to relevant entries in miRBase 20. The reliability of the identified miRNAs increased with the number of identified fragments. Samples were grouped as per their type identifiers, and quantification of miRNAs abundance was done.

For clustering analysis, miRNAs counts were normalized by trimmed mean method (TMM) and the normalized expression value was log transformed and clustered based on Euclidean distance and complete linkage using the Cluster 3.0 software (http://bonsai.hgc.jp/~mdehoon/software/cluster/software.htm) and visualized with Java TreeView version 1.1.6 (http://jtreeview.sourceforge.net/).

4.7. NuPage Gel Electrophoresis and Western Blotting

Exosomes were purified, harvested in RIPA Lysis and Extraction Buffer containing Halt™ Protease (Thermo Fisher Scientific Inc.). The exosomal protein concentration was determined by the Direct Detection method (Direct Detect Spectrometer, Merck Life Science AS, Oslo, Norway) as described

previously [85]. Equal amounts of protein (30 μg) were loaded on a 4-12% NuPage Novex gel (Life Technologies, Oslo, Norway) and separated by electrophoreses. Then proteins from exosomes were transferred to an Immobilon-FL PVDF membrane. The blotting membrane was blocked with Odyssey Blocking Buffer (BB, Li-Cor Biosciences GmbH, Bad Homburg, Germany), mouse CD63 (1:1000, Abcam) and rabbit GM130 (1:10000, Abcam) followed by incubation with anti-mouse Alexa 680 (1:5000, Molecular Probes) and anti-rabbit IRD800 (1:5000, Rockland) IgG secondary antibody. The proteins were detected using an Odyssey scanner (Li-COR Inc., USA).

Cultured cells were washed briefly with phosphate-buffer saline (PBS, Biochrom GmbH) and harvested in RIPA Lysis and Extraction Buffer containing Halt™ Protease and Phosphatase Inhibitor Cocktail (Thermo Fisher Scientific Inc.). Following sonication, the protein concentration was determined using a Protein Quantification Assay (MACHEREY-NAGEL GmbH & Co. KG, Düren, Germany). The protein lysates (30 μg) were supplemented with NuPAGE® LDS Sample Buffer (4X) (Thermo Fisher Scientific Inc.) as well as 100mM DTT (Sigma-Aldrich Norway AS) and incubated for 10min at 70°C. Equal amounts of protein were separated on NuPAGE™ Novex™ 4-12% Bis-Tris Protein Gels (Thermo Fisher Scientific Inc.) and transferred onto a 0.45μm PVDF Membrane (Merck Life Science AS, Oslo, Norway) according to the XCell SureLock Mini-Cell technical guide (Thermo Fisher Scientific Inc.). The membranes were blocked in TBS-T (Tris-buffered saline (TBS) with 0.1% Tween-20; Sigma-Aldrich Norway AS) containing 5% (w/v) skimmed milk powder. Incubation with primary antibodies Anti-GM130 (1:2000, Abcam) and Anti-GAPDH (1:4000, Santa Cruz Biotechnology) was performed overnight at 4°C according to antibody supplier recommendation in either blocking buffer or 5% BSA (AppliChem, Darmstadt, Germany) in TBS-T. Following three washes in TBS-T, the membranes were incubated in the appropriate secondary antibody solutions Goat Anti-Rabbit IgG H&L (HPR, 1:50000, Abcam) and Rabbit Anti-Mouse IgG H&L (HPR, 1:20000, Abcam) for 1h at room temperature. After four washes, detection and visualization were performed using SuperSignal™ West Pico Chemiluminescent Substrate (Thermo Fisher Scientific Inc.) and the ImageQuant LAS 4000 imager (GE Healthcare, Oslo, Norway). MagicMark™ XP Western Protein Standard (Thermo Fisher Scientific Inc.) was used to estimate the molecular mass of the detected proteins.

4.8. Quantitative RT-PCR

For quantification of miR levels, total exosomal RNA was extracted using the SeraMir Exosome RNA Purification kit (SBI), according to the manufacturer's instruction. RNA concentrations were determined on a CLARIOstar (BMG Labtech Inc., Cary, NC, USA). The cDNA synthesis was performed using the High Capacity cDNA Reverse Transcriptase kit (Applied Biosystems, Life Technologies, USA), according to the manufacturer's instructions for TaqMan Small RNA Assays. MiRNAs cDNAs were quantified by qRT-PCR using LightCycler® 96(Roche Diagnostics, Indianapolis, IN, USA) with

the TaqMan Universal Master Mix II, no UNG (Applied Biosystems) and TaqMan Fast Advanced Master Mix (Applied Biosystems). The miR-specific primers and probes were obtained from Thermo Fisher Scientific (Waltham, MA, USA) listed in **Table 5**. To calculate the relative expression levels of target miRNAs, the delta-Cq and the delta-delta-Cq algorithm method was utilized [86]. MiR-30a-5p was stably expressed across all samples and was therefore used as an internal control for normalization.

Table 5. The miR-specific primers and probes for two steps qRT-PCR.

miR	Assay ID
miR-30a-5p	000417
miR-31-5p	002279
miR-125b-1-3p	002378
miR-141-3p	478501_mir
miR-143-3p	477912_mir
miR-222-3p	002276
miR-375	478074_mir
miR-532-5p	001518
miR-584-5p	001624

4.8. Prediction of Target Genes for miR-222-3p

The miR-222-3p target genes were predicted using the ExoCarta, TargetScan, and miRTarBase databases [55-57]. Targets genes were analyzed for enrichment by FunRich3.1.3 (www.funrich.org) open-access tool. The enrichment analysis of the site of expression was performed and graphs constructed by the FunRich3.1.3 [58].

4.9. Data Analysis

The distribution of observed data was determined using descriptive statistics. For the qRT-PCR, the average Cq for each triplicate from the qRT-PCR was calculated. The relative quantification was used to compare the presence of exosomal miR-222-3p in MCPyV-negative, MCPyV-positive, healthy donors and patients samples normalized with miR-30a-5p as an internal control. The fold change was calculated by the delta-delta-Cq method with miR-30a-5p as an internal control. All comparison was performed using the Mann-Whitney U test. All statistical analyses were conducted and graphs constructed by the Prism 8 (GraphPad Software Inc., San Diego, CA, USA). Data are presented in median and a P value less than 0.05 were considered statistically significant ($*P < 0.05$, $**P < 0.005$).

Acknowledgments: This project was supported by the Odd Fellow Medisinsk-Vitenskapelig Forskningsfond (A65216) and in part, by the Familien Blix' Fond (A65256). We thanks Professor Baki Akgül (University of Cologne, Germany) for the kind gift of the MCC cell lines, and Dag Coucheron for professional recommendations in the microRNA matter. We also thank Exiqon A/S team for their support for conducting microRNA sequencing and analysis.

Author Contributions: A.K., B.S., and U.M. conceived and designed the experiments; A.K., A.A., and N.B-S. performed the experiments; A.K., A.A., H.S., N.B-S., B.S., W-O.L. and U.M. contributed reagents/materials/analysis tools; A.K. and W-O.L. analyzed the data and A.K., W-O.L., B.S., U. M. wrote the paper.

Conflicts of Interest: The authors declare no conflict of interest.

Abbreviations

CD63	Cluster of differentiation 63
GM130	Anti-GM130 antibody
HCV	Hepatitis C virus
KPNA2	Importin subunit alpha-1
NK	Natural killer
PD-1	Program death-1
RNPS1	RNA-binding protein with serine-rich domain 1
SNX2	Sorting nexin-2
SOCS	Suppressor of cytokine signaling
STMN1	Stathmin 1
SUN2	SUN domain-containing protein 2
TMM	The trimmed mean of M-value normalization method
TPM	Tags per million
YWHAG	Tyrosine 3-monooxygenase/tryptophan 5-monooxygenase activation protein gamma

References

1. Feng, H.; Shuda, M.; Chang, Y.; Moore, P.S. Clonal integration of a polyomavirus in human Merkel cell carcinoma. *Science.* **2008**, 319, 1096-1100. doi: 10.1126/science.1152586.
2. Voelker, R. Why Merkel cell cancer is garnering more attention. *JAMA.* **2018**, 320, 18-20. doi: 10.1001/jama.2018.7042.
3. Ziprin, P.; Smith, S.; Salerno, G.; Rosin, R.D. Two cases of Merkel cell tumour arising in patients with chronic lymphocytic leukaemia. *Br. J. Dermatol.* **2000**, 142, 525-528.
4. Engels, E.A.; Frisch, M.; Goedert, J.J.; Biggar, R.J.; Miller, R.W. Merkel cell carcinoma and HIV infection. *Lancet.* **2002**, 359, 497-498. doi: 10.1016/S0140-6736(02)07668-7
5. Penn, I.; First, M.R. Merkel's cell carcinoma in organ recipience: report of 41 cases. *Transplantation* **1999**, 68, 1717-1721.
6. Garrett, G.L.; Blanc, P.D.; Boscardin, J.; Lloyd, A.A.; Ahmed, R.L.; Anthony, T.; Bibee, K.; Breithaupt, A.; Cannon, J.; Chen, A.; Cheng, J.Y.; Chiesa-Fuxench, Z.; Colegio, O.R.; Curiel-Lewandrowski, C.; Del Guzzo, C.A.; Disse, M.; Dowd, M.; Eilers, R. Jr.; Ortiz, A.E.; Morris, C.; Golden, S.K.; Graves, M.S.; Griffin, J.R.; Hopkins, R.S.; Huang, C.C.; Bae, G.H.; Jambusaria, A.; Jennings, T.A.; Jiang, S.I.; Karia, P.S.; Khetarpal, S.; Kim, C.; Klintmalm, G.; Konicke, K.; Koyfman, S.A.; Lam, C.; Lee, P.; Leitenberger, J.J.; Loh, T.; Lowenstein, S.; Madankumar, R.; Moreau, J.F.; Nijhawan, R.I.; Ochoa, S.; Olasz, E.B.; Otchere, E.; Otley, C.; Oulton, J.; Patel, P.H.; Patel, V.A.; Prabhu, A.V.; Pugliano-Mauro, M.; Schmults, C.D.; Schram, S.; Shih, A.F.; Shin, T.; Soon, S.; Soriano, T.; Srivastava, D.; Stein, J.A.; Sternhell-Blackwell, K.; Taylor, S.; Vidimos, A.; Wu, P.; Zajdel, N.; Zelac, D.; Arron, S.T. Incidence of and risk factors for skin cancer in organ transplant recipients in the United States. *JAMA Dermatol.* **2017**, 153, 296-303. doi: 10.1001/jamadermatol.2016.4920.
7. Broustas, C.G.; Lieberman, H.B. DNA damage response genes and the development of cancer metastasis. *Radiat. Res.* **2014**, 181, 111-130. doi: 10.1667/RR13515.1.
8. Shabani Azim, F.; Houri, H.; Ghalavand, Z.; Nikmanesh, B. Next generation sequencing in clinical oncology: Applications, challenges and promises: A review article. *Iran. J. Public. Health* **2018**, 47, 1453-1457.
9. Becker, J.C.; Stang, A.; Hausen, A.Z.; Fischer, N.; DeCaprio, J.A.; Tothill, R.W.; Lyngaa, R.; Hansen, U.K.; Ritte, C.; Nghiem, P.; Bichakjian, C.K.; Ugurel, S.; Schrama, D. Epidemiology, biology and therapy of Merkel cell carcinoma from the EU project IMMOMEC. *Cancer Immunol Immunother.* **2018**, 67, 341-351. doi: 10.1007/s00262-017-2099-3.
10. Miller, N.J.; Church, C.D.; Fling, S.P.; Kulikauskas, R.; Ramchurren, N.; Shinohara, M.M.; Kluger, H.M.; Bhatia, S.; Lundgren, L.; Cheever, M.A.; Topalian, S.L.; Nghiem, P. Merkel cell polyomavirus-specific immune

responses in patients with Merkel cell carcinoma receiving anti-PD-1 therapy. *J. Immunother. Cancer* **2018**, 6, 131. doi: 10.1186/s40425-018-0450-7.
11. Bellone, M; Elia, A.R. Constitutive and acquired mechanisms of resistance to immune checkpoint blockade in human cancer. *Cytokine Growth Factor Rev.* **2017**, 36, 17-24. doi: 10.1016/j.cytogfr.2017.06.002.
12. Samimi, M. Immune checkpoint inhibitors and beyond: An overview of immune-based therapies in Merkel cell carcinoma. *Am J Clin Dermatol.* **2019**. doi: 10.1007/s40257-019-00427-9.
13. Tang, J.; Yu, J.X.; Hubbard-Lucey, V.M.; Neftelinov, S.T.; Hodge, J.P.; Lin, Y. Trial watch: The clinical trial landscape for PD1/PDL1 immune checkpoint inhibitors. *Nat. Rev. Drug Discov.* **2018**, 17, 854-855. doi: 10.1038/nrd.2018.210.
14. Zhang, J.; Li, S.; Li, L.; Li, M.; Guo, C.; Yao, J.; Mi, S. Exosome and exosomal microRNA: trafficking, sorting, and function. *Genomics Proteomics Bioinformatics* **2015**, 13, 17-24. doi: 10.1016/j.gpb.2015.02.001.
15. Ciardiello, C.; Cavallini, L.; Spinelli, C.; Yang, J.; Reis-Sobrerio, M.; de Candia, P.; Minciacchi, V.R.; Di Vizio, D. Focus on extracellular vesicles: new frontier of cell-to-cell communication in cancer. *Int. J. Mol. Sci*. **2016**, 17, 175. doi: 10.3390/ijms17020175.
16. Azmi, A.S.; Bao, B.; Sarkar, F.H. Exosomes in cancer development, metastasis, and drug resistance: a comprehensive review. *Cancer Metastasis Rev.* **2013**, 32, 623-642. doi: 10.1007/s10555-013-9441-9.
17. Yuana, Y.; Sturk, A.; Nieuwland, R. Extracellular vesicles in physiological and pathological conditions. *Blood Rev.* **2013**, 27, 31-39. doi: 10.1016/j.blre.2012.12.002.
18. Haug, B.H.; Hald, Ø.H.; Utnes, P.; Roth, S.A.; Løkke, C.; Flægstad, T.; Einvik, C. Exosome-like extracellular vesicles from MYCN-amplified neuroblastoma cells contain oncogenic miRNAs. *Anticancer Res.* **2015**, 35, 2521-2530.
19. Devhare, P.B.; Sasaki, R.; Shrivastava, S.; Di Bisceglie, A.M.; Ray, R.; Ray, R.B. Exosome-mediated intercellular communication between hepatitis C virus-infected hepatocytes and hepatic stellate cells. *J. Virol.* **2017**, 91, e02225-16. doi: 10.1128/JVI.02225-16.
20. Richards, K.E.; Zeleniak, A.K.; Fishel, M.L.; Wu, J.; Littlepage, L.E.; Hill, R. Cancer-associated fibroblast exosomes regulate survival and proliferation of pancreatic cancer. *Oncogene* **2017**, 36, 1770-1778. doi: 10.1038/onc.2016.353.
21. Ferguson, S.; Kim, S.; Lee, C.; Deci, M.; Nguyen, J. The phenotypic effects of exosomes secreted from distinct cellular sources: a comparative study based on miRNA composition. *AAPS. J.* **2018**, 20, 67. doi: 10.1208/s12248-018-0227-4.
22. Yu, X.; Odenthal, M.; Fries, J.W.U. Exosomes as miRNA carriers: formation-function-future. *Int J. Mol Sci.* **2016**, 17, 2028. doi: 10.3390/ijms17122028.
23. Hannafon, B.N.; Ding, W-Q. Intercellular communication by exosome-derived microRNAs in cancer. *Int J. Mol Sci.* **2013**, 14, 14240-14269. doi: 10.3390/ijms140714240.
24. Felekkis, K.; Touvana, E.; Stefanou, Ch.; Deltas, C. microRNA: a newly described class of encoded molecules that play a role in healthy and disease. *Hippokratia.* **2010**, 14, 236-240.
25. Oliveto, S.; Mancino, M.; Manfini, N., Biffo, S. Role of microRNA in translation regulation and cancer. *World J. Biol Chem.* **2017**, 8, 45-56. doi: 10.4331/wjbc.v8.i1.45.
26. Kavitha, N.; Vijayarathna, S.; Jothy, S.L.; Oon, C.E.; Chen, Y.; Kanwar, J.R.; Sashidharan, S. MicroRNAs: biogenesis, roles for carcinogenesis and as potential biomarkers for cancer diagnosis and prognosis. *Asian Pac J. Cancer Prev.* **2014**, 15, 7489-7497.
27. Luan, A.; Hu, M.S.; Leavitt, T.; Brett, E.A.; Wang, K.C.; Longaker, M.T.; Wan, D.C. Noncoding RNAs in wound healing: a new and vast frontier. *Adv. Wound Care (New Rochelle),* **2018**, 7, 19-27. doi: 10.1089/wound.2017.0765.
28. Gozuacik, D.; Akkoc, Y.; Ozturk, D.G.; Kocak, M. Autophagy-regulating microRNAs and cancer. *Front Oncol.* **2017**, 7, 1-22. doi: 10.3389/fonc.2017.00065.
29. Li, X. MiR-375, a microRNA related to diabetes. *Gene.* **2014**, 533, 1-4. doi: 10.1016/j.gene.2013.09.105.
30. Takahashi, R-U.; Prieto-Vila, M.; Hironaka, A.; Ochiya, T. The role of extracellular vesicles microRNAs in cancer biology. *Clin Chem Lab Med.* **2017**, 55, 648-656. doi: 10.1515/cclm-2016-0708.
31. Kim, J.; Yao, F.; Xiao, Z.; Sun, Y.; Ma, L. MicroRNAs and metastasis: small RNAs play big roles. *Cancer Metastasis Rev.* **2018**, 5-15. doi: 10.1007/s10555-017-9712-y.
32. Aftab, M.N.; Dinger, M.E.; Perera, R.J. The role of microRNAs and long non-coding RNAs in the pathology, diagnosis, and management of melanoma. *Arch Biochem Biophys.* **2014**, 563, 60-70. doi: 10.1016/j.abb.2014.07.022.

33. Pakravan, K.; Babashah, S.; Sadeghizadeh, M.; Mowla, S.J.; Mossahebi-Mohammadi, M.; Ataei, F.; Dana, N.; Javan, M. MicroRNA-100 shuttled by mesenchymal stem cell-derived exosomes suppresses in vitro angiogenesis through modulating the mTOR/HIF-1α/VEGF signaling axis in breast cancer cells. *Cell Oncol (Dordr).* **2018**, 40, 457-470. doi: 10.1007/s13402-017-0335-7.
34. O'Connell, R.M.; Rao, D.S.; Chudhuri, A.A.; Baltimore, D. Physiological and pathological roles for microRNAs in the immune system. *Nat Rev Immunol.* **2010**, 10, 111-122. doi: 10.1038/nri2708.
35. Farug, O.; Vecchione A. microRNA: diagnostic perspective. *Front Med (Lausanne).* **2015**, 2, 51. doi: 10.3389/fmed.2015.00051.
36. Bayraktar, R.; Van Roosbroeck, K. miR-155 in cancer drug resistance and as target for miRNA-based therapeutics. *Cancer Metastasis Rev.* **2018**, 37, 33-44. doi: 10.1007/s10555-017-9724-7.
37. Denzer, K.; Kleijmeer, M.J.; Heijnen, H.F.; Stoorvogel, W.; Geuze, H.J. Exosome: from internal vesicle of the multivesicular body to intercellular signaling device. *J. Cell Sci.* **2000**, 113, 3365-3374.
38. Chernyshev, V.S.; Rachamadugu, R.; Tseng, Y.H.; Belnap, D.M.; Jia, Y.; Butterfield, A.E.; Pease, L.F. 3th; Bernard, P.S., Skliar, M. Size and shape characterization of hydrated and desiccated exosomes. *Anal Bioanal Chem.* **2015**, 407, 3285-3301. doi: 10.1007/s00216-015-8535-3.
39. Konstantinell, A.; Bruun, J-A.; Olsen, R.; Aspar, A.; Škalko-Basnet, N.; Sveinbjørnsson, B.; Moens, U. Secretomic analysis of extracellular vesicles originating from polyomavirus-negative and polyomavirus-positive Merkel cell carcinoma cell lines. *Proteomics* **2016**, 16, 2587-2591. doi: 10.1002/pmic.201600223.
40. Samaeekia, R.; Rabiee, B.; Putra, I.; Shen, X.; Paark, Y.J.; Hematti, P.; Eslani, M.; Djalilian, A.R. Effect of human corneal mesenchymal stromal cell-derived exosomes on corneal epithelial wound healing. *Invest Ophthalmol Vis Sci.* **2018**, 59, 5194-5200. doi: 10.1167/iovs.18-24803.
41. Backes, C.; Meder, B.; Hart, M.; Ludwig, N.; Leidinger, P.; Vogel, B.; Galata, V.; Roth, P.; Menegatti, J.; Grässer, F.; Ruprecht, K.; Kahraman, M.; Grossmann, T.; Haas, J.; Meese, E.; Keller, A. Prioritizing and selecting likely novel miRNAs from NGS data. *Nucleic Acids Res.* **2016**, 44, e53. doi: 10.1093/nar/gkv1335.
42. Xie, H.; Lee, L.; Caramuta, S.; Höög, A.; Browaldh, N.; Björnhagen, V.; Larsson, C.; Lui, W.O. MicroRNA expression patterns related to Merkel cell polyomavirus infection in human Merkel cell carcinoma. *J Invest Dermatol.* **2014**, 134, 507-517. doi: 10.1038/jid.2013.355.
43. Renwick, N.; Cekan, P.; Masry, P. A.; McGeary, S. E.; Miller, J. B.; Hafner, M.; Li, Z.; Mihailovic, A.; Morozov, P.; Brown, M.; Gogakos, T.; Mobin, M. B.; Snorrason, E. L.; Feilotter, H. E.; Zhang, X.; Perlis, C. S.; Wu, H.; Suárez-Fariñas, M.; Feng, H.; Shuda, M.; Moore, P. S.; Tron, V. A.; Chang, Y.; Tuschl, T. Multicolor microRNA FISH effectively differentiates tumor types. J Clin Invest. 2013, 123, 2694-2702. doi: 10. 1172/JCI68760.
44. Ning, M.S.; Kim, A.S.; Prasad, N.; Levy, S.E.; Zhang, H.; Andl, T. Characterization of the Merkel cell carcinoma miRNome. *J Skin Cancer* **2014**, 2014, 289548. doi: 10.1155/2014/289548.
45. Veija, T.; Sahi, H.; Koljonen, V.; Bohling, T.; Knuutila, S.; Mosakhani, N. miRNA-34a underexpressed in Merkel cell polyomavirus-negative Merkel cell carcinoma. *Virchows Arc.* **2015**, 466, 289-295. doi: 10.1007/s00428-014-1700-9.
46. Abraham, K.J.; Zhang, X.; Vidal, R.; Paré, G.C.; Feilotter, H.E.; Tron, V.A. Roles for miR-375 in neuroendocrine differentiation and tumor suppression via Notch pathway suppression in Merkel cell carcinoma. *Am J Pathol*. **2016,** 186, 1025-1235. doi: 10.1016/j.ajpath.2015.11.020.
47. Kumar, S.; Xie, H.; Scicluna, P.; Lee, L.; Björnhagen, V.; Höög, A.; Larsson, C.; Liu, W.O. MiR-375 regulation of LDHB plays distinct roles in polyomavirus-positive and –negative Merkel cell carcinoma. *Cancer (Basel).* **2018**, 10, E443. doi: 10.3390/cancers10110443.
48. Chteinberg, E.; Sauer, C.M.; Rennspiess, D.; Beumers, L.; Schiffelers, L.; Eben, J.; Haugg, A.; Winnepenninckx, V.; Kurz, A.K.; Speel, E.J.; Zenke, M.; Zur Hausen, A. Neuroendocrine key regulatory gene expression in Merkel cell carcinoma. *Neoplasia.* **2018**, 20, 1227-1235. doi: 10.1016/j.neo.2018.10.003.
49. Ghorbanmehr, N.; Gharbi, S.; Korsching, E.; Tavallaei, M.; Einollahi, B.; Mowla, S.J. miR-21-5p, miR-141-3p, and miR-205-5p levels in urine-promising biomarkers for the identification of prostate and bladder cancer. *Prostate* **2018**, 1-8. doi: 10.1002/pros.23714.
50. Bi, J.; Liu, H.; Cai, Z.; Dong, W.; Jiang, N.; Yang, M.; Huang, J.; Lin, T. Circ-BPTF promotes bladder cancer progression and recurrence through the miR-31-5p/RAB27A axis. *Aging (Albany NY)* **2018**, 10, 1964-1976. doi: 10.18632/aging.101520.
51. Panza, E.; Ercolano, G.; De Cicco, P.; Armogida, C.; Scognamiglio, G.; Botti, G.; Girino, G.; Ianaro, A. MicroRNA-143-3p inhibits growth and invasiveness of melanoma cells by targeting cyclooxygenase-2 and

inversely correlates with malignant melanoma progression. *Biochem Pharmacol*. **2018**, 156, 52-59. doi: 10.1016/j.bcp.2018.08.008.

52. Chen, Y.Y.; Ho, H.L.; Lin, S.C.; Ho, T.D.; Hsu, C.Y. Upregulation of miR-125b, miR-181d, and miR-221 predicts poor prognosis in MGMT promoter-unmethylated glioblastoma patients. *Am J Clin Pathol*. **2018**, 149, 412-417. doi: 10.1093/ajcp/aqy008.
53. Ying, X.; Wu, Q.; Wu, X.; Zhu, Q.; Wang, X.; Jiang, L.; Chen, X.; Wang, X. Epithelial ovarian cancer-secreted exosomal miR-222-3p induce polarization of tumor-associated macrophages. *Oncotarget* **2016**, 7, 43076-43087. doi: 10.18632/oncotarget.9246.
54. Zhou, X.; Wen, W.; Shan, X.; Zhu, W.; Xu, J.; Guo, R.; Cheng, W.; Wang, F.; Qi, L.W.; Chen, Y.; Huang, Z.; Wang, T.; Zhu, D.; Liu, P.; Shu, Y. A six-microRNA panel in plasma was identified as a potential biomarker for lung adenocarcinoma diagnosis. *Oncotarget* **2017**, 8, 6513-6525. doi: 10.18632/oncotarget.14311.
55. Keerthikumar, S.; Chisanga, D.; Ariyaratne, D.; Al Saffar, H.; Anand, S.; Zhao, K.; Samuel, M.; Pathan, M.; Jois, M.; Chilamkurti, N.; Gangoda, L.; Mathivanan, S. ExoCarta: A web-based compendium of exosomal cargo. *J. Mol. Biol*. **2015**, 428, 688-692. doi: 10.1016/j.jmb.2015.09.019.
56. Agarwal, V.; Bell, G.W.; Nam, J.W.; Bartel, D.P. Predicting effective microRNA target sites in mammalian mRNAs. *Elife*. **2015**, 4. doi: 10.7554/eLife.05005.
57. Chou, C.H.; Shrestha, S.; Yang, C.D.; Chang, N.W.; Lin, Y.L.; Liao, K.W.; Huang, W.C.; Sun, T.H.; Tu, S.J.; Lee, W.H.; Chiew, M.Y.; Tai, C.S.; Wei, T.Y.; Tsai, T.R.; Huang, H.T.; Wang, C.Y.; Wu, H.Y.; Ho, S.Y.; Chen, P.R.; Chuang, C.H.; Hsieh, P.J.; Wu, Y.S.; Chen, W.L.; Li, M.J.; Wu, Y.C.; Huang, X.Y., Ng, F.L.; Buddhakosai, W.; Huang, P.C.; Lan, K.C.; Huang, C.Y.; Weng, S.L.; Cheng, Y.N.; Liang, C.; Hsu, W.L.; Huang, H.D. miRTarBase update 2018: a resource for experimentally validated microRNA-target interactions. *Nucleic Acids Res.* **2018**, 46, D296-D302. doi: 10.1093/nar/gkx1067.
58. Pathan, M.; Keerthikumar, S.; Chisanga, D.; Alessandro, R.; Ang, C.S.; Askenase, P.; Batagov, A.O.; Benito-Martin, A.; Camussi, G.; Clayton, A.; Collino, F.; Di Viziko, D.; Falcon-Perez, J.M.; Fonseca, P.; Fonseka, P.; Fontana, S.; Gho, Y.S.; Hendrix, A.; Hoen, E.N.; Iraci, N.; Kastaniegaard, K.; Kislinger, T.; Kowal, J.; Kurochkin, I.V.; Leornardi, T.; Liang, Y.; Llorente, A.; Lunavat, T.R.; Maji, S.; Monteleone, F.; Øverbye, A.; Panaretakis, T.; Patel, T.; Peinado, H.; Pluchino, S.; Principe, S.; Ronquist, G.; Royo, F.; Sahoo, S.; Spinelli, C.; Stensballe, A.; Thery, C.; van Herwijnen, M.J.C.; Wauben, M.; Welton, J.L.; Zhao, K.; Mathivanan, S. A novel community driven software for functional enrichment analysis of extracellular vesicles data. *J. Extracell. Vesicles* **2017**, 6, 1321455. doi: 10.1080/20013078.2017.1321455.
59. Leprince, C.; Le Scolan, E.; Meunier, B.; Fraisier, V.; Brandon, N.; De Gunzburg, J.; Camonis, J. Sorting nexin 4 and amphiphysin2, a new partnership between endocytosis and intracellular trafficking. *J Cell Sci.* **2003**, 116, 1937-1948. doi: 10.1242/jcs.00403.
60. Donahue, D. A.; Porrot, F.; Couespel, N.; Schwartz, O. SUN2 silencing impairs CD4 T cell proliferation and alters sensitivity to HIV-1 infection independently of Cyclophilin A. *J Virol.* **2017**, 91, e02303-16. doi: 10.1128/JVI.02303-16.
61. Filbert, E. L.; Le Borgne, M.; Lin, J.; Heuser, J. E.; Shaw, A. S. Stathmin regulates microtubule dynamics and microtubule organizing center polarization in activated T cells. *J Immunol*. **2012**, 188, 5421-5427. doi: 10.4049/jimmunol.1200242.
62. Mohammad, D. K.; Nore, B. F.; Hussain, A.; Gustafsson, M. O.; Mohamed, A. J.; Smith, C. I. Dual phosphorylation of Btk by Akt/protein kinase b provides docking for 14-3-3 gamma, regulates shuttling, and attenuates both tonic and induced signalling in B cells. *Mol Cell Biol*. **2013**, 33, 3214-3226. doi: 10.1128/MCB.00247-13.
63. Wang, X.; Yu, M.; Zhao, K.; He, M.; Ge, W.; Sun, Y.; Wang, Y.; Sun, H.; Hu, Y. Upregulation of miR-205 under hypoxia promotes epithelial-mesenchymal transition by targeting ASPP2. Cell Death Dis. 2016, 7, e2517. doi: 10.1038/cddis.
64. Yoon, T. D.; Lee, H. W.; Kim, Y. S.; Choi, H. J.; Moon, J. O.; Yoon, S. Identification and analysis of expressed genes using a cDNA library from rat thymus during regeneration following cyclophosphamide-induced T cell depletion. Int J Mol Med. 2013, 31, 731-739. doi: 10.3892/ijmm.2013.1238.
65. Zhao, X.; Li, D.; Qui, Q.; Jiao, B.; Zhang, R.; Liu, P.; Ren, R. Zfyve16 regulates the proliferation of B-lymphoid cells. *Front Med.* **2018**, 12, 559-565. doi: 10.1007/s11684-017-0562-3.
66. Harling, K.; Adankwah, E.; Güler, A.; Afum-Adjei Awuah, A.; Adu-Amoah. L.; Mayatepek, E.; Owusu-Dabo, E.; Nausch, N.; Jacobsen, M. Constitutive STAT3 phosphorylation and IL-6/IL-10 co-expression are associated

with impaired T-cell function in tuberculosis patients. *Cell Mol Immunol*. **2019**, 16, 275-287. doi: 10.1038/cmi.2018.5.

67. Cho, H.; Park, O. H.; Park, J.; Ryu, I.; Kim, J.; Ko, J.; Kim, Y. K. Glucocorticoid receptor interacts with PNRC2 in a ligand-dependent manner to recruit UPF1 for rapid mRNA degradation. Proc Natl Acad Sci U. S. A. 2015, 112, E1540-E1549. doi: 10.1073/pnas.1409612112.
68. Johnson, D. C.; Taabazuing, C. Y.; Okondo, M. C.; Chui, A. J.; Rao, S. D.; Brown, F.C.; Reed, C.; Peguero, E.; de Stanchina, E.; Kentsis, A.; Bachovchin, D. A. DPP8/DPP9 inhibitor-induced pyroptosis for treatment of acute myeloid leukemia. Nat Med. 2018, 24, 1151-1156. doi: 10.1038/s41591-018-0082-y.
69. Wei, F.; Ma, C.; Zhou, T.; Dong, X.; Luo, Q.; Geng, L.; Ding, L.; Zhang, Y.; Zhang, L.; Li, N.; Li, Y.; Liu, Y. Exosomes derived from gemcitabine-resistant cells transfer malignant phenotypic traits via delivery of miRNA-222-3p. *Mol. Cancer* **2017**, 16, 132. doi: 10.1186/s12943-017-0694-8.
70. Yu, D. D.; Wu, Y.; Shen, H.Y.; Lv, M. M.; Chen, W. X.; Zhang, X. H.; Zhong, S. L.; Tang, J. H.; Zhao, J. H. Exosomes in development, metastasis and drug resistance of breast cancer. Cancer Sci. 2015, 106, 959-964. doi: 10.1111/cas.12715.
71. Tian, F.; Shen, Y.; Chen, Z.; Li, R.; Ge, Q. No significant difference between plasma miRNAs and plasma-derived exosomal miRNAs from healthy people. *Biomed. Res. Int.* **2017**, 2017, 1304816. doi: 10.1155/2017/1304816.
72. Hsu, S-H.; Ghoshal, K. MicroRNAs in liver health and disease. *Curr. Pathobiol. Rep.* **2013**, 1, 53-62. doi: 10.1007/s40139-012-0005-4.
73. Plebanek, M.P.; Angeloni, N.L.; Vinokour, E.; Li, J.; Henkin, A.; Martinez-Marin, D.; Filleur, S.; Bhowmick, R.; Henkin, J.; Miller, S.D.; Ifergan, I.; Lee, Y.; Osman, I.; Thaxton, C.S.; Volpert, O.V. Pre-metastatic cancer exosomes induce immune surveillance by patrolling monocytes at the metastatic niche. *Nat. Commun.* **2017**, 8, 1319. doi: 10.1038/s41467-017-01433-3.
74. Syn, N.; Wang, L.; Sethi, G.; Thiery, J.P.; Goh, B.C. Exosome-mediated metastasis: From epithelial-mesenchymal transition to escape from immunosurveillance. *Trends Pharmacol. Sci.* **2016**, 37, 606-617. doi: 10.1016/j.tips.2016.04.006.
75. Jiang, M.; Zhang, W. W.; Liu, P.; Yu, W.; Liu, T.; Yu, J. Dysregulation of SOCS-mediated negative feedback of cytokine signaling in carcinogenesis and its significance in cancer treatment. *Front. Immunol.* **2017**, 8, 70. doi: 10.3389/fimmu.2017.00070.
76. Santangelo, L.; Bordoni, V.; Montaldo, C.; Cimini, E.; Zingoni, A.; Battistelli, C.; D'Offizi, G.; Capobianchi, M.R.; Santoni, A.; Tripodi, M.; Agrati, C. Hepatitis C virus direct-acting antivirals therapy impacts on extracellular vesicles microRNAs content and on their immunomodulating properties. *Liver Int.* **2018**, 38, 1741-1750. doi: 10.1111/liv.13700.
77. Dovrat, S.; Caspi, M.; Zilberberg, A.; Lahav, L.; Firsow, A.; Gur, H.; Rosin-Arbesfeld, R. 14-3-3 and β-catenin are secreted on extracellular vesicles to activate the oncogenic Wnt pathway. *Mol. Oncol.* **2014**, 8, 894-911. doi: 10.1016/j.molonc.2014.03.011.
78. Knight, L. M.; et al. Merkel cell polyomavirus small T antigen mediates microtubule destabilization to promote cell motility and migration. *J. Virol.* **2015**, 89, 35-47.
79. Whitehouse, A.; Macdonald, A. Stathmin drives virus-induced metastasis. *Oncotarget.* **2015**, 6, 32289-32290.
80. Umegaki-Arao, N.; et al. Karyopherin Alpha2 is essential for rRNA transcription and protein synthesis in proliferative keratinocytes. *PLoS One.* **2013**, 8, e76416.
81. Dovrat, S.; Caspi, M.; Zilberberg, A.; Lahav, L.; Firsow, A.; Gur, H.; Rosin-Arbesfeld, R. 14-3-3 and β-catenin are secreted on extracellular vesicles to activate the oncogenic Wnt pathway. *Mol. Oncol.* **2014**, 8, 894-911. doi: 10.1016/j.molonc.2014.03.011.
82. Castañeda, A.; Serrano, C.; Hernández-Trejo, J.A.; Gutiérrez-Martínez, I.Z.; Montejo-López, W.; Gómez-Suárez, M.; Hernández-Ruiz, M.; Betanzos, A.; Candelario-Martínez, A.; Romo-Parra, H.; Arias-Montaño, J.A.; Schnoor, M.; Meraz Ríos, M.A.; Gutierrez-Castillo, M.E.; Martínez-Dávila, I.A.; Villegas-Sepúlveda, N.; Martinez-Fong, D.; Nava, P. pVHL suppresses Akt/β-catenin-mediated cell proliferation by inhibiting 14-3-3ζ expression. *Biochem. J.* 2017, 474, 2679-2689. doi: 10.1042/BCJ20161097.
83. Chu, Y.W.; Wang, C.R.; Weng, F.B.; Yan, Z.J.; Wang, C. MicroRNA-222 contributed to cell proliferation, invasion and migration via regulating YWHAG in osteosarcoma. *Eur. Rev. Med. Pharmacol. Sci.* **2018**, 22, 2588-2597. doi: 10.26355/eurrev_201805_14952.

84. Jøraholmen, M. W.; Vanic, Z.; Tho, I.; Škalko-Basnet, N. Chitosan-coated liposomes for topical vaginal therapy: Assuring localized drug effect. *Int. J. Pharm.* **2014**, 472, 94-101. doi: 10.1016/j.ijpharm.2014.06.016.
85. Strug, I.; Utzat, C.; Cappione, A.; Gutierrez, S.; Amara, R.; Lento, J.; Capito, F.; Scudas, R.; Chernokalskaya, E.; Nadler, T. Development of a univariate membrane-based mid-infrared method for protein quantitation and total lipid content analysis of biological samples. *J. Anal. Methods Chem.* **2014**, 2014, 657079. doi: 10.1155/2014/657079.
86. Rao, X.; Huang, X.; Zhou, Z.; Lin, X. An improvement of the 2^(-delta delta CT) method for quantitative real-time polymerase chain reaction data analysis. *Biostat Bioinform Biomath.* **2013**, 3, 71-85.

COMPARATIVE AND INTEGRATED ANALYSES OF POLYOMAVIRUS-NEGATIVE AND –POSITIVE MERKEL CELL CARCINOMA CELL LINES AND THEIR EXOSOMES PROTEOMIC STUDIES

Aelita Konstantinell[1,*,#], Jack-Ansgar Bruun[1,#], Weng-Onn Lui[2], Baldur Sveinbjørnsson[1] and Ugo Moens[1,#]

[1]Department of Medical Biology, University of Tromsø, The Arctic University of Norway, Faculty of Health Sciences NO-9037 Tromsø, Norway

[2]Department of Oncology-Pathology, Karolinska Institutet, Stockholm; Cancer Center Karolinska, Karolinska University Hospital, Stockholm, Sweden;

E-mails: jack-ansgar.bruun@uit.no (J-A.B.), weng-onn.lui@ki.se (W-O.L.), baldur.sveinbjornsson@uit.no (B.S.), ugo.moens@uit.no (U.M.)

[#] authors contributed equally to this work

*Author to whom correspondence should be addressed; e-mail: aelita.g.konstantinell@uit.no (A.K.), phone: +47 936 303 04

Abbreviations: MCC, Merkel cell carcinoma; MCPyV, Merkel cell polyomavirus, LT, Large T-antigen; ST, Small T-antigen; VP1, major capsid; VP2 and VP3, minor capsids; ALTO, Alternative Large T open reading frame

Keywords: proteomics, polyomavirus, Merkel cell carcinoma, Merkel cell carcinoma cell lines, exosome

Abstract

Proteomics have become an important tool in discovery and understanding pathological processes at cellular level. Comparing the proteome of normal cells with diseased (malignant and other pathological conditions) or pathogen-infected cells allows identification of proteins and processes involved in the disease, and recognition of possible biomarkers and targets for treatment. Merkel cell carcinoma (MCC) is an aggressive type of cutaneous cancer that affects mostly elderly people. Approximately 80% of the tumors are caused by Merkel cell polyomavirus (MCPyV), while the remaining are caused by UV-induced mutations in the DNA of the cell. To understand the underlying mechanisms of virus-independent and virus-dependent MCC, we compared the proteome of MCPyV-negative (MCC13, MCC26, and USIO) and MCPyV-positive (MKL-1, MKL-2, MS-1, and WaGa) MCC cell lines. In total 4898 proteins were identified, of which 3312 were differentially expressed between the virus-negative and virus-positive cell lines. The viral oncoproteins large T- and small t-antigens were detected in the MCPyV-positive cells, but also in exosomes derived from these cells. Our proteomic data may identify unique biomarkers for MCPyV-negative and –positive MCCs and may allow the design of specific therapeutic strategies against the two types of MCC with different origin. Moreover, our results suggest that exosomal transmission of MCPyV oncoproteins to recipient cells in the tumor microenvironment contributes to tumorigenesis.

Data are available via ProteomeXchange with identifier PXD012909.

Introduction

Merkel cell carcinoma (MCC) is a rare, but aggressive neuroendocrine form of skin cancer with poor prognosis. About 20% of all MCC cases are associated with chronic UV light exposure, while the remaining 80% caused by Merkel cell polyomavirus [1, 2]. A hallmark for MCPyV-positive MCC is the integration of the viral genome [3]. This viral genome encodes the regulatory proteins large T antigen (LT), small T antigen (ST), 57 KT and alternative to Large T Open reading frame (ALTO) [4]. While the function of the latter two proteins remains unknown, LT and ST have oncogenic potentials in cell culture and animal models [5-14]. Another characteristic of MCPyV-positive MCC is the expression of a C-terminal truncated LT [3]. Despite the oncogenic properties of LT and ST, it is unclear if the presence or absence of integrated MCPyV alters the course or/and outcome of MCC [13, 15]. To understand the underlying mechanisms by which MCPyV contributes to MCC tumorigenesis and to identify potential biomarkers and therapeutic targets, we compared for the first time the proteomes of MCPyV-negative and -positive MCC cell lines. We also analyzed our previously published proteomic data of extracellular vesicles derived from MCC cell lines (PXD004198; [16]) for the presence of viral proteins. We found that more than 3000 proteins differentially expressed between virus-negative and virus-positive MCC cell lines and that MCPyV may use exosomes to transmit its oncoproteins LT and ST to recipient cells in the tumor microenvironment.

Results and Discussion

Proteins were isolated from the MCPyV-negative MCC13, MCC26, and UISO cell lines (group 1) and the virus-positive MKL-1, MKL-2, MS-1, and WaGa cell lines (group 2) by differential centrifugation and gel separation and subjected to mass spectrometry-based proteomics. All experiments run in triplicate. In total, 4898 proteins (**Supplementary Table 1**) identified, of which 3312 (**Supplementary Table 2**) showed differential expression between the two groups. We performed hierarchical clustering to determine groups of samples with similar global protein expression profiles (**Figure 1**). The MCPyV-negative cell line samples formed a group divergent from the MCPyV-positive cell line, indicating that these cell lines are distinct from each other.

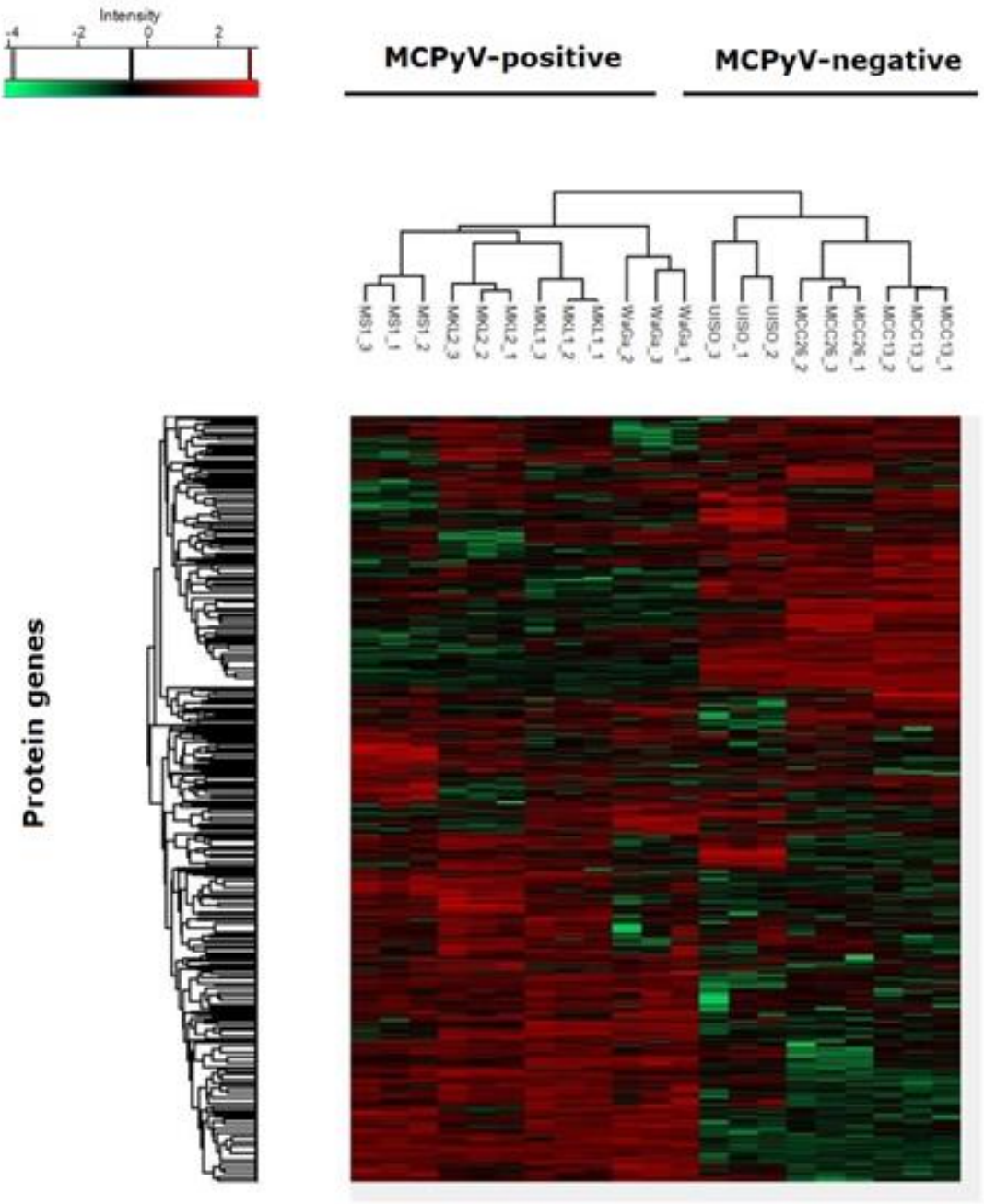

Figure 1. The dendrogram shows the hierarchical relationship between the samples with similar global protein expression profiles. The MCPyV-negative cell lines are MCC13, MCC26 and UISO, and the MCPyV-positive MCC cell lines are MKL-1, MKL-2, MS-1, and WaGa. All samples analyzed in triplicate. Each horizontal line represents one protein/protein gene.

The differences in protein expression can also be visualized in a principal components analysis (PCA) projection and with Volcano plot (**Figure 2A and 2B**). Again, these analyses indicate that the two groups of cells are distinct from each other.

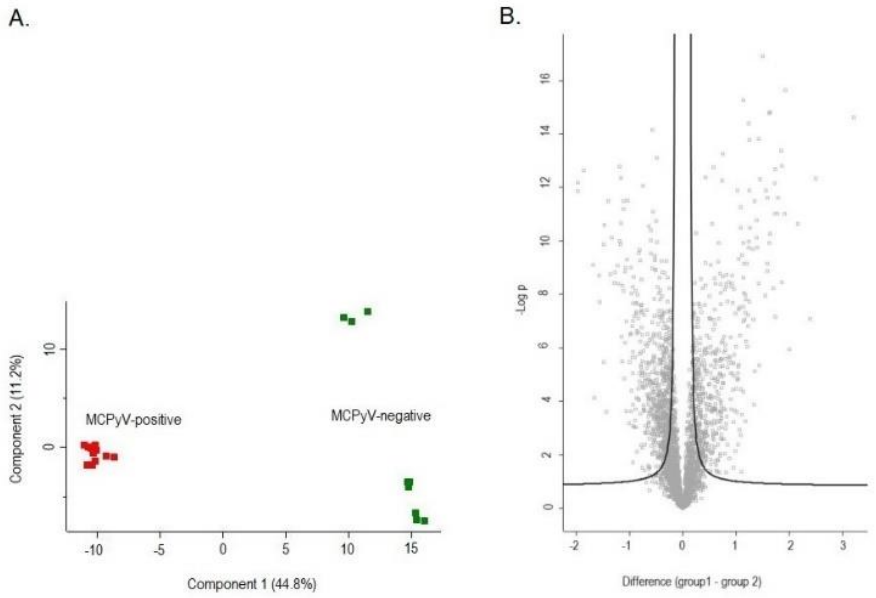

Figure 2. Two groups of divergent samples are the MCPyV-negative and -positive cell lines, which depicted **A.** Principal components (PCA) projection. **B.** Volcano plot.

Distinctions between the two groups of cells are expected by the PCA and Volcano plot because of morphological and genotypic differences between the cell lines and their grow conditions [17-20]. Comparing virus-negative and –positive cell lines identified proteins with significantly increased and decreased expression (**Supplementary Table 2**). To quantify the overall similarity in protein expression, Spearman's rank correlation coefficients between individual expressions profiles of MCC cell lines were computed (**Supplementary Table 3**). A strong, positive correlation (r = 0.70, n = 9, P = 0.0433) in protein expression between MCPyV-negative and MCPyV-positive MCC cell lines was found (**Figure 3**).

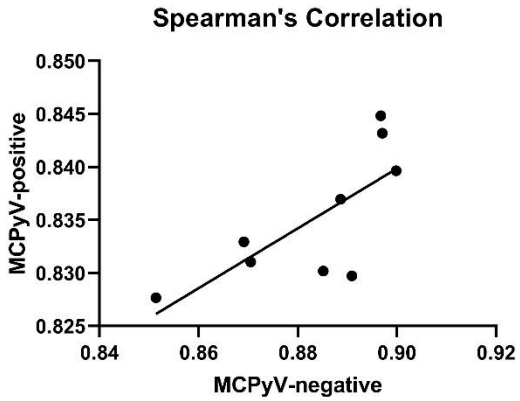

Figure 3. Spearman's correlation showing the relationship between protein expression in MCPyV-negative and –positive MCC cell lines (r =0.70, n = 9, P = 0.0433). Each dot represents one MCC cell line. The closer r is to ±1 the stronger the monotonic relationship. The strength of the correlation: r = 0.00-0.19 is "very weak"; r = 0.20-0.39 is "weak"; r = 0.40-0.59 is "moderate"; r = 0.60-0.79 is "strong"; and r = 0.80-1.00 is "very strong".

The fifty most increased and decreased proteins in MCC cell lines are given in **Table 1** and **Table 2**. The expression level for these proteins in other tumors compared to healthy tissue is included.

Table 1. Fifty proteins with most increased expression in virus-negative MCC cell lines compared to virus-positive MCC cell lines and their expression in other tumors. The number in parenthesis refers to the row number in **Supplementary Table 2**.

Protein name	**abbreviation**	**function**	**expression in cancer and in MCC cell line**	**reference**
Annexin A2	ANXA2 (1071)	cellular growth, cell motility, exocytosis, signal transduction,	Increased/Increased in MCPyV-negative MCC cell lines	[21]
Annexin A1	ANXA1 (1035)	anti-inflammatory activity, innate immune response, regulates transcription factors and miRNAs	Increased/Increased in MCPyV-negative MCC cell lines	[22]

Neuroblast differentiation-associated protein (desmoyokin)	AHNAK (1894)	Scaffold protein, cell architecture, and migration	Increased/Increased in MCPyV-negative MCC cell lines	[23]
Transgelin	TAGLN (1844)	architecture cytoskeleton	Increased/ Expressed poor	[24]
Major vault protein	MVP (2040)	nucleo-cytoplasmic transport, scaffold in signal transduction pathways	Increased/Increased in MCPyV-negative MCC cell lines	[25]
Myoferlin	MYOF (3052)	membrane regeneration and repair, endocytosis, lipid metabolism	Increased/Increased in MCPyV-negative MCC cell lines	[26]
Calpain-2 catalytic subunit	CAPN2 (1220)	Protease that cleaves substrates involved in cytoskeletal remodeling and signal transduction	Increased/Increased in MCPyV-negative MCC cell lines	[27]
Fermitin family homolog 2 (kindlin-2)	FERMT2 (2603)	Participates in the connection between extracellular matrix adhesion sites and the actin cytoskeleton, architecture cytoskeleton	Increased/Increased in MCPyV-negative MCC cell lines	[28]
Caldesmon 1	CALD1 (459)	Stabilizes actin, role in migration, invasion, and proliferation	Increased/Expressed poor	[29]
Galectin-1	LGALS1 (1101)	modulation cell-cell and cell-matrix interactions, cell proliferation	Increased/Increased in MCPyV-negative MCC cell lines	[30]
Perilipin-3 (TIP47)	PLIN3 (853)	Involved in endosome-to-Golgi transport, the formation of lipid droplets	Increased/Increased in MCPyV-negative MCC cell lines	[31, 32]
Plectin	PLEC (2074)	architecture cytoskeleton, scaffold protein in signaling pathways, intermediate filament networks	Increased/Increased in MCPyV-positive MCC cell lines	[33]

Serpin B6 (Hsp47)	SERPINB6 (1408)	prevents cellular damage by inhibiting leaking lysosomal serine proteases	Decreased/ Increased in MCPyV-negative MCC cell lines	[34]
NAD(P)H quinone dehydrogenase 1	NQO1 (1193)	Vitamin K metabolism, detoxification, cellular homeostasis, stabilization p53	Increased/ Increased in MCPyV-negative MCC cell lines	[35]
Serpin H1	SERPINH1 (1582)	Collagen biosynthesis	Increased/ Increased in MCPyV-negative MCC cell lines	[36]
Adenylyl cyclase-associated protein 2	CAP2 (1455)	Actin remodeling	Increased/ Increased in MCPyV-negative MCC cell lines	[37]
PDZ and LIM domain protein 7	PDLIM7 (2963)	Gene transcription, a scaffold protein, assembling proteins at actin	Increased/ Increased in MCPyV-negative MCC cell lines	[38]
Calponin-2	CNN2 (327)	structural organization of actin filaments	Increased/ Increased in MCPyV-negative MCC cell lines	[39]
A-kinase anchor protein 12	AKAP12 (1852)	anchoring protein in signal transduction	Increased and decreased/ Increased in MCPyV-negative MCC cell lines	[40]
Actin, aortic smooth muscle	ACTA2 (1754)	Cell motility, cytoskeleton structure and integrity, and intercellular signaling	Increased/Expressed poor	[41]
Ribosome-binding protein 1	RRBP1 (3074)	the interaction between the ribosome and the endoplasmic reticulum membrane, protein transport	Increased/ Increased in MCPyV-negative MCC cell lines	[42]
Zyxin	ZYX (2128)	Cell-cell signaling, cell-matrix adhesion, modulate cytoskeletal organization	Increased or decreased/ Increased in MCPyV-negative MCC cell lines	[43]

UDP-glucose 6-dehydrogenase	UGDH (856)	biosynthesis of glycosaminoglycans, which play roles in signal transduction and cell migration	Increased/ Increased in MCPyV-negative MCC cell lines	[44]
vimentin	VIM (1092)	Cytoskeleton compound responsible for cell shape and integrity of the cytoplasm, and stabilization of cytoskeletal interactions	Increased/Increased in MCPyV-negative MCC cell lines	[45] [46-49]
Collagen alpha-1(I) chain	COL1A1 (1023)	extracellular matrix structural constituent	Increased/ Increased in MCPyV-negative MCC cell lines	[50]
Lipoma-preferred partner	LPP (2590)	cell-cell adhesion and cell motility, gene transcription, signal transduction	Increased/Increased in MCPyV-positive MCC cell lines	[51]
Glycogen phosphorylase, liver form; α-1,4 glucan phosphorylase	PYGL (1063)	carbohydrate metabolism	Increased/ Increased in MCPyV-negative MCC cell lines	[52]
α-parvin	PARVA (627)	reorganization of the actin cytoskeleton, cell adhesion, motility and survival	Increased/ Increased in MCPyV-negative MCC cell lines	[53]
Coactosin-like protein	COTL1 (1995)	Architecture cytoskeleton, chaperone	Increased/ Increased in MCPyV-negative MCC cell lines	[54]
Caveolae Associated Protein 1 or Polymerase I and transcript release factor	CAVIN1=PTRF (2276)	caveolae formation, rRNA transcription	Increased/ Increased in MCPyV-negative MCC cell lines	[55]
Peptidyl-prolyl cis-trans isomerase	FKBP10 (2605)	Protein folding	Increased/ Increased in MCPyV-negative MCC cell lines	[56]
Utrophin	UTRN (1519)	anchoring the cytoskeleton to the plasma membrane	Not investigated/ Increased in MCPyV-negative MCC cell lines	

Integrin-linked protein kinase	ILK (114)	regulation integrin-mediated signal transduction, essential in the epithelial to mesenchymal transition	Increased/ Increased in MCPyV-negative MCC cell lines	[57]
Integrin α-2	ITGA2 (1217)	organization of extracellular matrix, adhesion cells to collagens	Increased/ Increased in MCPyV-negative MCC cell lines	[58]
LIM and calponin homology domains-containing protein 1	LIMCH1 (3190)	Architecture cytoskeleton, a negative regulator of cell migration	Not investigated/ Increased in MCPyV-negative MCC cell lines	
Gamma-interferon-inducible protein 16	IFI16 (2147)	Transcriptional regulation, modulates p53 function, cellular senescence	Decreased/ Increased in MCPyV-negative MCC cell lines	[59, 60]
Serum paraoxonase/arylesterase 2	PON2 (169)	protecting cells against oxidative stress	Increased/ Increased in MCPyV-negative MCC cell lines	[61]
EH domain-containing protein 4	EHD4 (2860)	Participates in the endocytic pathway, controls membrane reorganization/tubulation	Not investigated/ Increased in MCPyV-negative MCC cell lines	
Procollagen-lysine,2-oxoglutarate 5-dioxygenase 3	PLOD3 (851)	Post translational modifications necessary for stability of intermolecular crosslinks, matrix remodeling	Increased/ Increased in MCPyV-negative MCC cell lines	[62]
Tropomyosin beta chain	TPM2 (2233)	stabilizing cytoskeleton actin filaments	Decreased/Expressed poor	[63]
Y-box-binding protein 3	YBX3 (1210)	Transcriptional and translational repressor	Decreased/ Increased in MCPyV-negative MCC cell lines	[64]
Vinculin	VCL (1230)	Architecture cytoskeleton, cell-matrix adhesion and cell-cell	Increased/ Increased in MCPyV-negative MCC cell lines	[65]

		adhesion, cell locomotion		
Integrin alpha-V; Integrin alpha-V heavy chain; Integrin alpha-V light chain	ITGAV (1065)	cell surface adhesion and signaling	Increased/ Increased in MCPyV-negative MCC cell lines	[66]
Nicotinate phosphoribosyltransferase	NAPRT (2307)	prevent cellular oxidative stress	Decreased/ Increased in MCPyV-negative MCC cell lines	[67]
Tropomyosin α-4 chain	TPM4 (1789)	Architecture cytoskeleton	Increased and decreased/ Increased in MCPyV-negative MCC cell lines	[68, 69]
ATP-dependent 6-phosphofructokinase, muscle type	PFKM (237)	glycolysis	Not investigated/ Increased in MCPyV-negative MCC cell lines	
EH domain-containing protein 2	EHD2 (3053)	Participates in the endocytic pathway, controls membrane reorganization/tubulation	Decreased/ Increased in MCPyV-negative MCC cell lines	[70]
Flavine reductase (NADPH) or Biliverdin Reductase B	BLVRB (1358)	cellular redox regulator regulates activities in the insulin/IGF-1/IRK/PI3K/MAPK pathways	Increased/ Increased in MCPyV-negative MCC cell lines	[71, 72]
Ephrin type-A receptor 2	EPHA2 (1348)	Signaling pathways involved in migration, integrin-mediated adhesion, proliferation and differentiation of cells	Increased/ Increased in MCPyV-negative MCC cell lines	[73, 74]
Nicotinamide N-methyltransferase	NNMT (1458)	N-methylation of pyridines; regulation of multiple metabolic pathways	Increased/ Increased in MCPyV-negative MCC cell lines	[75]

Table 2. Fifty proteins with most increased expression in MCPyV-positive MCC cells compared to virus-negative MCC cells and their expression in other tumors. The number in parenthesis refers to the row number in **Supplementary Table 2**.

Protein name	**abbreviation**	**function**	**expression in cancers**	**reference**
Nesprin-2	SYNE2 (2534)	Cytoskeletal organization and cell motility	Increased/ Increased in MCPyV-positive MCC cell lines	[76]
Carboxypeptidase E	CPE (1208)	production of neuropeptides and role in the secretory pathway	Increased/ Increased in MCPyV-positive MCC cell lines	[77]
Kinesin-like protein	KIF1A (263)	transports membranous organelles	Decreased/Expressed poor	[78]
Creatine kinase U-type, mitochondrial	CKMT1A (1159)	catalyzes phosphorylation of creatine	Increased/ Increased in MCPyV-positive MCC cell lines	[79]
Advillin	AVIL (883)	Actin-binding protein involved in morphogenesis of neuronal cells which form ganglia	Not investigated/ Increased in MCPyV-positive MCC cell lines	
Neurofilament medium polypeptide	NEFM (433)	intracellular transport to axons and dendrites	Decreased/ Increased in MCPyV-positive MCC cell lines	[80]
Cellular retinoic acid-binding protein 1	CRABP1 (1352)	Binding and transport retinoid acid	Decreased/ Increased in MCPyV-positive MCC cell lines	[81]
14-3-3σ or stratifin	SFN (1389)	Cell cycle checkpoint protein and prevents DNA errors during mitosis	Decreased/ Increased in MCPyV-positive MCC cell lines	[82]

Dihydropyrimidinase-related protein 5	DPYSL5 (2746)	Neural development	Not investigated/ Increased in MCPyV-positive MCC cell lines	
Spectrin beta chain, non-erythrocytic 2	SPTBN2 (752)	glutamate signaling pathway	Not investigated/ Increased in MCPyV-positive MCC cell lines	
Kinesin-like protein KIF21A	KIF21A (192)	microtubule-dependent transport	Decreased/ Increased in MCPyV-positive MCC cell lines	[83]
Kinesin heavy chain isoform 5C	KIF5C (840)	intracellular transport	Decreased/ Increased in MCPyV-positive MCC cell lines	[83]
Tumor protein D52	TPD52 (1672)	regulator of lipid metabolism and Ca^{2+}-dependent protein secretion	Increased/Expressed similarly	[84]
Pyridoxal phosphatase	PDXP (2637)	cofilin-dependent actin cytoskeleton reorganization, required for normal progress through mitosis and normal cytokinesis, vitamin metabolic process	Not investigated/ Increased in MCPyV-positive MCC cell lines	
Erythrocyte Membrane Protein Band 4.1	EPB41 (1132)	Organizer of membrane and cytoskeleton	Decreased/Expressed poor	[85]
Synapsin-2	SYN2 (2566)	neurotransmitter transport and secretion	Not investigated/ Increased in MCPyV-positive MCC cell lines	
Insulinoma-associated protein 1	INSM1 (1834)	The transcription factor, a regulator of cell differentiation and cell cycle	Increased/ Increased in MCPyV-positive MCC cell lines	[86]

Epithelial splicing regulatory protein 1	ESRP1 (2275)	mRNA splicing factor	Increased/ Increased in MCPyV-positive MCC cell lines	[87]
ELAV-like protein 2	ELAVL2 (96)	Regulation mRNA splicing	not investigated/ Increased in MCPyV-positive MCC cell lines	
Neurofilament light polypeptide	NEFL (1068)	Cytoskeleton organization, intracellular transport to axons and dendrites	Decreased/ Increased in MCPyV-positive MCC cell lines	[88]
Dachshund homolog 1	DACH1 (3131)	Transcription factor, regulation cell proliferation	Increased/ Increased in MCPyV-positive MCC cell lines	[89]
2',5'-oligoadenylate synthase 3	OAS3 (3302)	inhibition of cellular protein synthesis and viral infection resistance	Not investigated/ Increased in MCPyV-positive MCC cell lines	
Guanine nucleotide-binding protein subunit α O1	GNAO1 (1104)	signal transduction	Decreased/ Increased in MCPyV-positive MCC cell lines	[90]
Transmembrane protein 97 (Sigma 2 receptor)	TMEM97=MAC30 (636)	regulator cellular cholesterol homeostasis and apoptosis	Increased/Expressed poor	[91]
Peroxiredoxin Like 2A (Redox-regulatory protein FAM213A)	PRXL2A=FAM213A (2764)	redox regulation protects cells from oxidative stress	Increased/ Increased in MCPyV-positive MCC cell lines	[92]
Coenzyme Q Protein 8A (Atypical kinase ADCK3, mitochondrial)	COQ8A=ADCK3 (2484)	biosynthesis of coenzyme Q10, function in the respiratory chain	Not investigated/ Increased in MCPyV-positive MCC cell lines	
α-internexin	INA (2133)	Intracellular transport,	Decreased/Expressed similarly	[93]

		cytoskeleton formation		
Unconventional myosin-VI	MYO6 (92)	Vesicle transport	Increased/ Increased in MCPyV-positive MCC cell lines	[94]
Unconventional myosin-Id	MYO1D (944)	endosomal protein trafficking	Not investigated/ Increased in MCPyV-positive MCC cell lines	
Epithelial cell adhesion molecule	EPCAM (332)	cell signaling, migration, proliferation, and differentiation	Increased/Increased in MCPyV-positive cell lines	[95]
Transmembrane protein 205	TMEM205 (664)	Secretion or vesicular trafficking	Increased/Expressed similarly	[96]
γ-enolase	ENO2 (1097)	Involved in glycolysis	Increased/Expressed similarly	[97]
ELAV-like protein 3	ELAVL3 (2027)	RNA stability and splicing	not investigated/ Increased in MCPyV-positive MCC cell lines	
Rab-3A-interacting protein	RAB3IP (2686)	Modulates actin organization and vesicular transport	Increased/ Increased in MCPyV-positive MCC cell lines	[98]
Dynamin-1	DNM1 (151)	Vesicular trafficking processes and receptor-mediated endocytosis	Increased/Expressed poor	[99]
Methyltransferase-like protein 7A	METTL7A (580)	Tumor suppressor, recruit cellular proteins for lipid droplet formation	Increased/ Increased in MCPyV-positive MCC cell lines	[100]

Zinc finger protein 385A	ZNF385A (2681)	Transcription factor and RNA-binding protein that affects the localization and the translation of a subset of mRNA	Not investigated/ Increased in MCPyV-positive MCC cell lines	
Ribosomal protein S6 kinase α-1 (RSK1/MAPKAPK1)	RPS6KA1 (458)	Signal transduction and controlling cell growth and differentiation	Increased/ Increased in MCPyV-positive MCC cell lines	[101]
Heat shock-related 70 kDa protein 2	HSPA2 (1655)	Molecular chaperone implicated, e.g. in the protection of the proteome from stress, correct folding, and transport of proteins, activation of proteolysis of misfolded proteins and the formation and dissociation of protein complexes	Increased/ Increased in MCPyV-positive MCC cell lines	[102]
Phosphoenolpyruvate carboxykinase [GTP], mitochondrial	PCK2 (2157)	Involved in the metabolic pathway that produces glucose from lactate and other precursors derived from the citric acid cycle	Decreased/ Increased in MCPyV-positive MCC cell lines	[103]

NADH-cytochrome b5 reductase 1	CYB5R1 (3122)	involved in desaturation and elongation of fatty acids, cholesterol biosynthesis, drug metabolism	Increased/ Increased in MCPyV-positive MCC cell lines	[104]
Lipopolysaccharide-responsive and beige-like anchor protein	LRBA (1591)	coupling signal transduction and vesicle trafficking	Increased/Expressed poor	[105]
Galectin-7	LGALS7 (1525)	modulating cell-cell and cell-matrix interactions	Increased/ Increased in MCPyV-positive MCC cell lines	[106]
V-type proton ATPase subunit isoform 1	ATP6V0A1 (2589)	assembly and activity of the vacuolar ATPase, protein sorting, receptor-mediated endocytosis, intracellular transport	Increased/ Increased in MCPyV-positive MCC cell lines	[107]
Syntaxin-1A	STX1A (2144)	Vesicle fusion	Increased/ Increased in MCPyV-positive MCC cell lines	[108]
Vacuolar protein sorting-associated protein 13A	VPS13A (2693)	Trans Golgi transport	Increased/ Increased in MCPyV-positive MCC cell lines	[109]
Ganglioside induced differentiation associated protein 1	GDAP1 (2489)	Signal transduction, promoting mitochondrial fission	Not investigated/ Increased in MCPyV-positive MCC cell lines	
Ribosomal protein S6 kinase alpha-5	RPS6KA5 = Msk1 (901)	signal transduction, phosphorylation and activation of	Increased/ Increased in MCPyV-positive MCC cell lines	[110]

		transcription factors		
HIV Tat-specific factor 1	HTATSF1 (818)	Transcription-splicing factor	not investigated/ Increased in MCPyV-positive MCC cell lines	
Isochorismatase domain-containing protein 1	ISOC1 (2613)	unknown	Not investigated/ Increased in MCPyV-positive MCC cell lines	

The proteomic analysis shows that MCPyV-positive MCC cell lines have a high number of unique peptides for the medium molecular weight neurofilament protein (NF-M) and neuronal intermediate filament proteins, α-internexin, than the MCPyV-negative cell lines, and that the latter are negative for the high molecular weight neurofilament protein (FN-H). Peripherin was not detected in MCC13, MCC26, and WaGa, but was abundant in MKL2. A high number of neuronal intermediate filament protein, nestin, found in MCC13 and UISO. The results underscore the neuroendocrine origin of the cell lines [111].

Two major clusters with a size of 1510 (**Supplementary Table 4**) and 1170 (**Supplementary Table 5**) proteins differentially expressed between MCPyV-negative and –positive MCC cell lines included 63 and 83 components of cellular compartments and biological pathways that up-regulated in MCPyV-positive and -negative MCC cell lines, respectively. The proteomic profile also revealed that MCPyV-positive MCC cell line cells had up-regulated expression of proteins involved in cellular pathways among epigenetic regulation of gene expression (*P* = 5.83E-07), histone modification (*P* = 2.82E-04), gene silencing (*P* = 6.45E-04), and RNA polymerase II-mediated transcription (*P* = 5.15E-06). In addition, data from virus-positive cells revealed increased expression of proteins involved in DNA replication (*P* = 1.89E-12), DNA recombination (*P* = 8.15E-09), DNA modification (*P* = 1.11E-03), DNA-dependent transcription termination (*P* = 1.73E-04), DNA repair (*P* = 3.52E-07), and DNA ligation (*P* = 8.94E-03). The increased demand for DNA synthesis requires enhanced metabolic activity of one-carbon (*P* = 3.01E-03), nucleobase-containing (*P* = 1.11E-21), cellular nitrogen compound (*P* = 7.08E-22), and nitrogen compounds (*P* = 1.43E-20). Moreover, cancer cell rewires their metabolic processes [112, 113]. E.g., cancer cells enhance "aerobic" glycolysis, known as the Warburg effect, to support rapid cell proliferation [114]. This Warburg effect seems to apply for MCPyV-positive MCC cell lines because they had upregulated expression of proteins involved in oxidative phosphorylation (*P* = 4.06E-03), particularly the NADH dehydrogenase

complex (*P* = 1.87E-05). An active transforming cell phenotype requires high energy. Lactate dehydrogenase B (LDHB) catalyzes the reversible conversion of lactate to pyruvate, and NAD to NADH, in the glycolytic pathway. With NADH accumulation, decreased mitochondrial oxidative phosphorylation occurs [115]. Cells that have a greater impairment of oxidative phosphorylation and high NADH production become more aggressive and metastatic [116], which is typical for the MCPyV-positive MCC. In contrast, the MCPyV-negative MCC cell lines profiles indicate that cells' metabolism switched to amine (*P* = 1.57E-03), polysaccharide (*P* = 8.61E-03) and carbohydrate (*P* = 4.20E-03) metabolic processes for cell growth (*P* = 1.05E-02), proliferation (*P* = 4.99E-03) and differentiation (*P* = 1.64E-03). Polyamines play a pleiotropic role, from modulating nucleic acid conformation to promoting cellular proliferation and signaling (signal transduction, *P* = 6.73E-06) [117]. Proteins implicated in cell motility (*P* = 4.04E-04), establishment or maintenance of cell polarity (*P* = 5.47E-03), cell surface (*P* = 4.05E-09), locomotion (*P* = 9.57E-05), and cellular membrane organization (*P* = 7.49E-04) were upregulated in MCPyV-negative MCC cells, indicating high invasiveness and metastasis of these cells. Differential expression of proteins involved in post-translational modification such as protein glycosylation (*P* = 1.04E-05), peptidyl-amino acid modification (*P* = 2.05E-04), protein folding (*P* = 4.86E-03), and protein modification process regulation (*P* = 5.24E-03) was observed. Upregulation of protein glycosylation of surface molecules showed a key feature of cancer cells, which use the endoplasmic reticulum (ER, *P* =1.35E-08)/Golgi apparatus (*P* = 1.28E-03) to add carbohydrates to their cumulative glycoproteins [118]. Thus, data indicates that the MCPyV-negative MCC cells, compared to virus-positive MCC cell lines, have a lower expression of proteins that participate in DNA, RNA and protein synthesis and regulation, but have upregulated expression of proteins engaged in post-translational modification. Hence, cancer progression and high cell proliferation may lead to transcription-associated mutation (TAM) and transcription-associated recombination (TAR) that gave a rise a high mutational burden of MCPyV-negative MCC.

Other proteins that were expressed at higher levels in virus-negative cell lines compared to virus–positive cell lines included proteins involved in endocytosis (*P* = 4.06E-06), exocytosis (*P* = 8.44E-03), intra- and extracellular vesicle-mediated-transport (*P* = 4.93E-10), Golgi vesicles (*P* = 1.25E-05), protein sorting (*P* = 3.66E-03). An exception was valosin-containing protein (VCP), aconitase 1 (ACO1) and argininosuccinate synthase 1 (ASS1), which were only detected in extracellular vesicles from MCPyV-positive cell lines. VCP is a membrane ATPase involved in ER homeostasis and ubiquitination and is required for the fusion of ER and Golgi

membranes [119, 120]. ACO1 is the moonlighting protein based on its ability to perform mechanistically distinct functions. One of the ACO1's ability is to bind glucose-regulated protein 94 kDa (Grp94), which is the ER-localized isoform of heat shock protein 90 (Hsp90). Hsp90 is responsible for trafficking and maturation of Toll-like receptors, immunoglobulins, and integrins [121]. ASS1 is a key enzyme in the citrulline-nitric oxide (NO) cycle, which can be upregulated by nitrogen efflux at Kaposi's sarcoma-associated herpesvirus (KSHV) infection and acid-induced downregulation contributes to the maintenance of intracellular pH in cancer [122, 123]. Evolutionary, exosomes maintain cellular homeostasis by carrying cellular remains from the misfolded proteins loaded on the ER through the Golgi and subsequently removing these waste products by exocytosis to prevent genotoxic conditions [124].

To validate some of our results, we compared our proteomic data with proteins that had been previously reported to be differentially expressed in these virus-negative and virus-positive cells [125, 126]. Guastafierro and colleagues had used immunohistochemistry (IHC) to investigate the expression of the positive MCC markers cytokeratin 1 (CK1), CK8, CK18 and CK20, and neuron-specific enolase (NSE), chromogranin A and synaptophysin, and the negative markers CK7, leukocyte common antigen (LCA) and thyroid transcription factor 1 (TTF-1) in the MCC13, MCC26, and UISO and in MKL-1, MKL-2 and MS-1 cell lines [125]. There were discrepancies between their results and our results (**Table 3**). IHC and proteomic analysis confirmed the absence of the negative markers CK7, LCA and TTF1 in all cell lines tested, except for MCC13 cells and confirmed the expression of CK20 on virus-positive, but not virus-negative MCC cell lines (**Table 3**). CK1 was detected in MCC13 and virus-positive cell lines by IHC, whereas mass spectrometry (MS) revealed expression in all cell lines tested. CK7, CK8, and CK18 give similar results with both methods, except that CK18 was also detected in MCC26 by MS. All cell lines were negative for chromatin A with both methods, except MKL2 which was positive by IHC. Synaptophysin was only discovered in MKL2 and MS1 cells by IHC. NSE detected in all cell lines, no expression was found by IHC in MCC26 cells. IHC of 52 MCC biopsies (28 virus-positive and 24 virus-negative) showed that >90% of all tumors expressed CK20 and chromogranin A with no significant difference between MCPyV-negative and MCPyV-positive MCCs [126].

Table 3. Expression of biomarkers on virus-negative and virus-positive MCC cell lines by immunohistochemistry [125] and mass spectrometry (this work). The number of unique peptides detected by tandem mass spectrometry is shown. - : protein not detected by IHC; + = protein detected by IHC.

Markers	IHC						MS/MS						
	MCPyV-negative			MCPyV-positive			MCPyV-negative			MCPyV-positive			
	MCC13	MCC26	UISO	MKL1	MKL2	MS1	MCC13	MCC26	UISO	MKL1	MKL2	MS1	WaGa
CK20	–	–	–	+	+	+	2	1	1	20	17	21	24
CK1 (AE1/AE3)	+	–	–	+	+	+	20	22	24	23	22	18	22
CK8 (CAM5.2)	+	–	–	+	+	+	26	4	1	27	24	28	29
CK18 (CAM5.2)	+	–	–	+	+	+	18	13	2	15	17	17	15
CK7	+	–	–	–	–	–	23	1	1	–	1	1	1
Chromogranin A	–	–	–	–	+	–	1	1	1	1	1	2	7
Synaptophysin	–	–	–	–	+	+	–	–	–	2	2	2	2
NSE	+	–	+	+	+	+	10	6	11	16	17	16	17
LCA	–	–	–	–	–	–	–	–	–	–	–	–	–
TTF-1	–	–	–	–	–	–	–	–	–	–	–	–	–

IHC, Immunohistochemistry; **MS/MS**, Mass tandem spectrometry; **MCPyV**, Merkel cell polyomavirus; **CK20**, Cytokeratin 20; **CK1**, Cytokeratin 1; **AE1/AE3**, Pan-cytokeratin antibody; **CK8**, Cytokeratin 8; **CK18**, Cytokeratin 18; **CAM5.2**, Pan-cytokeratin antibody; **CK7**, Cytokeratin 7; **NSE**, Neuron-specific enolase; **LCA**, Leukocyte common antigen; **TTF-1**, Thyroid transcription factor 1.

Our comparative proteomic analysis detected insulinoma-associated 1, a transcription factor expressed in tissues undergoing terminal neuroendocrine differentiation, in virus-positive MCC cell lines, but not in virus-negative cells. This protein was previously shown to be expressed in MCC, but the viral status of the tumors was not described [127]. Our proteomic analysis revealed that cell adhesion molecule 1 (CAM1) was unique for virus-positive cell lines. However, Iwasaki et al. using immunohistochemistry found that CAM1 was significantly higher expressed in MCPyV-negative MCCs [128]. The different source of material may explain this discrepancy.

Next, the presence of viral proteins in the viral-positive MKL-1, MKL-2, MS-1, and WaGa cell lines was investigated. Peptide fragments of LT and ST detected in all these cells, except for MKL-1 where no ST was found. ALTO seems to be expressed at detectable levels in MKL-1 and WaGa cells (**Table 4**). Previous qRT-PCR and IHC staining have confirmed the expression of LT in MKL-1, MKL-2 and MS-1 cells [125]. Peptide fragments of VP1 were present in all cell lines. MCPyV-positive cell lines are characterized by the integration of the viral genome

with interruption of the late region encoding the capsid proteins VP1 and VP2. As a consequence, no viral particles are produced [3, 129]. However, disruption of the late region of the viral genome may prevent the production of full-length capsid proteins, but 3' end truncated transcript may be synthesized, which can be translated in C-terminal truncated VP1 polypeptide.

Finally, we re-examined our previously published proteomic data of extracellular vesicles purified from MKL-1 and MKL-2 cells (PXD004198; [16]). LT and VP1 peptide fragments were detected in exosomes derived from both cell lines, whereas ST and VP2 fragments were only found in MKL-2. Guastafiero and collaborators could not detect VP2 transcripts by qRT-PCR [125]. The primers they used were located in the 3' end of the *VP2* gene and integration may have disrupted the region between the primers. Our proteomic data detected N-terminal fragments of VP2 which probably originate from the translation of the uninterrupted 5'end of the *VP2* gene. The discrepancy in the detection of VP2 in MKL-2- derived exosomes but not in the cell line remains elusive. The presence of LT and ST in exosomes suggests that viruses may use extracellular vesicles to spread their oncoproteins to target cells in the tumor microenvironment thereby contributing to the tumorigenic process.

Table 4. Viral protein fragments detected in MCPyV-positive MCC cell lines and extracellular vesicles purified from MKL-1 and MKL-2 cells. The number of fragments detected by MS/MS for each protein is shown. Accession number of proteins from The Protein database collection (https://www.ncbi.nlm.nih.gov/protein).

Cell Line	Protein	Number	Coverage (%)	Accession Number
MKL1	Truncated LT	11	46	207705716
		11	28	597569241
	LT	10	18	531990543
		9	16	1384959903
	LT, partial	5	29	557785972
	VP1, partial	1	8	1043615333
		1	4	1384960283
	ALTO	1	3	1384959909
MKL2	Truncated LT	3	15	471181001
		4	10	597569241
	Truncated LT, partial	3	16	597914272
	LT	4	7	220979589
		4	7	531990543
	LT, partial	5	11	557785946
		6	14	557785915
	ST	2	19	557785936
	VP1, partial	1	4	1384960269
MS1	truncated LT	2	16	557785906
		3	21	207705716
		1	8	307752571
	LT	1	3	557785962
	ST	2	22	289623109
	ST, partial	2	27	242254094
		2	44	557785991
	VP1, partial	2	16	1384960358
		1	6	597914268
		1	7	1384960273
		1	50	292658907
WaGa	Truncated LT	4	15	307752585
		1	15	471181009
	LT	5	10	220979601
		5	10	220979595
	ST, partial	2	11	242254082
	VP1, partial	1	11	610499559
		1	8	224576454
	ALTO	1	8	1144330406

Extracellular vesicles	Protein	Number	Coverage (%)	Accession Number
MKL1exo	Truncated LT	2	8	343183497
	LT	3	6	220979589
		2	2	220979589
		1	4	1028223539
	LT, chain E	1	11	330689596
	VP1	1	4	1029978634
		1	3	1029978618
	VP1, partial	1	3	1384960358
		1	7	224576452
		1	22	320118849
		1	9	189458640
		1	11	1384960388
MKL2exo	Truncated LT	1	6	378744307
	LT	4	5	220979589
		2	4	220979589
		2	5	610499700
	LT, partial	1	2	557785915
		1	13	610499506
		4	10	354683951
	LT, chain E	1	21	330689596
	ST, partial	1	12	242254091
		1	23	557785998
	VP1	2	4	1029978634
	VP1, partial	1	3	1384960358
		1	7	1384960347
		1	7	1384960386
		1	3	1384960358
	VP2	1	3	164664909

LT, Large T antigen;
ST, Small T antigen;
VP1, Major capsid protein;
VP2, Minor capsid protein;
ALTO, Alternative to Large T Open read frame

In conclusion, we have for the first time compared the proteomes of virus-negative and –positive MCC cell lines thereby identifying differentially expressed proteins that may be used as biomarkers for prognosis, diagnosis, and disease progression, and as potential therapeutic

targets. Our data indicate that different tumorigenic mechanisms are operating in virus-negative and virus-positive MCC. Moreover, MCPyV seems to spread its oncoproteins to target cells in the tumor microenvironment by extracellular vesicles.

Materials and Methods

Cell lines

The human Merkel cell carcinoma polyomavirus-negative cell lines MCC13, MCC26, and UISO and polyomavirus-positive cell lines MKL-1, MKL-2, MS-1, and WaGa were cultured as described previously [130]. Briefly, all cell lines were kept in culture medium RPMI-1640 supplemented with 10% fetal bovine serum. All cell types were incubated in a 5% CO2 humidified incubator at 37ºC.

Proteomic analysis

Cells were lysed by RIPA buffer, and cell debris was removed by centrifugation. The protein concentration for each sample was determined by the Direct Detection method as described previously [131]. Separation of cellular proteins from total lysates (30 µg) was performed by 4-12% NuPAGE Novex gel electrophoresis. All experiments were run in triplicate. Gel pieces were subjected to in-gel reduction, alkylation, and tryptic digestion using 6 ng/µl trypsin [132]. OMIX C18 tips were used for sample clean-up and concentration. Peptide mixtures containing 0.1% formic acid were loaded onto a Thermo Fisher Scientific EASY-nLC1200 system with an EASY-Spray column (C18, 2µm, 100 Å, 50µm, 50 cm). Peptides were fractionated using a 4-80% acetonitrile gradient in 0.1 % formic acid over 140 min at a flow rate of 300 nl/min. The separated peptides were analyzed using a Thermo Scientific Q-Exactive HF-X mass spectrometer.

Data processing

Data from three biological replicates of each sample were collected in the data-dependent mode using a Top5 method. Raw data were processed using MaxQuant (v 1.6.0.16) with the integrated Andromeda search engine. Label-free protein quantification was performed using the LFQ intensities. MS/MS data were searched against the current UniProt human database. A false discovery rate (FDR) of 0.01 was needed to yield a protein identification. Statistical validation of protein regulation was performed using the Perseus (v 1.6.0.7) software [133]. All contaminants were filtered out, and LFQ intensity values were log10-transformed. Quantitation values in at least 8 samples had to be observed for consideration in further analysis. Missing values were replaced from a normal distribution using a downshift of 1.8. Hierarchical clustering was performed on Z-score normalized data.

Virus proteins were identified using the Proteome Discoverer 2.2 software. Fragmentation spectra were searched against NCBInr Merkel Cell Polyomavirus proteome. Peptide mass tolerances used in the search were 10 ppm, and fragment mass tolerance was 0.1 Da. Peptide ions were filtered using a false discovery rate (FDR) set to 5 % for peptide identifications.

The mass spectrometry proteomics data have been deposited to the ProteomeXchange Consortium (http://proteomecentral.proteomexchange.org) via the PRIDE partner repository [134] with the dataset identifier PXD012909.

Author's contributions

A.K., W-O.L., B.S., and U.M. conceived and designed the experiments; A.K. and J-A.B. performed the experiments and analyzed the data; A.K., J-A.B, W-O.L., B.S., and U.M., wrote the paper.

Disclosure statement

The authors declare no conflict of interest.

Acknowledgments

This project was supported by the Olav and Erna Aakre Foundation (A…), the Odd Fellow Medisinsk-Vitenskapelig Forskningsfond (A65216) and in part, by the Familien Blix' Fond (A65256). We thank Professor Baki Akgül (University of Cologne, Germany) for the kind gift of the MCC cell lines.

References

1. Becker, J. C.; Stang, A.; DeCaprio, J. A.; Cerroni, L.; Lebbe, C.; Veness, M.; Nghiem, P., Merkel cell carcinoma. *Nat. Rev. Dis. Primers.* **2017,** 3, 17077.

2. Harms, P. W.; Harms, K. L.; Moore, P. S.; DeCaprio, J. A.; Nghiem, P.; Wong, M. K. K.; Brownell, I., The biology and treatment of Merkel cell carcinoma: current understanding and research priorities. *Nat. Rev. Clin. Oncol.* **2018,** 15, 763-776.

3. Feng, H.; Shuda, M.; Chang, Y.; Moore, P. S., Clonal integration of a polyomavirus in human Merkel cell carcinoma. *Science (New York, N.Y.)* **2008,** 319, 1096-1100.

4. Wendzicki, J. A.; Moore, P. S.; Chang, Y., Large T and small T antigens of Merkel cell polyomavirus. *Cur.r Opin. Virol* **2015,** 11, 38-43.

5. Borchert, S.; Czech-Sioli, M.; Neumann, F.; Schmidt, C.; Wimmer, P.; Dobner, T.; Grundhoff, A.; Fischer, N., High-affinity Rb binding, p53 inhibition, subcellular localization, and transformation by wild-type or tumor-derived shortened Merkel cell polyomavirus large T antigens. *J. Virol* **2014,** 88, 3144-3160.

6. Cheng, J.; Rozenblatt-Rosen, O.; Paulson, K. G.; Nghiem, P.; DeCaprio, J. A., Merkel cell polyomavirus large T antigen has growth-promoting and inhibitory activities. *J. Virol.* **2013,** 87, 6118-6126.

7. Demetriou, S. K.; Ona-Vu, K.; Sullivan, E. M.; Dong, T. K.; Hsu, S. W.; Oh, D. H., Defective DNA repair and cell cycle arrest in cells expressing Merkel cell polyomavirus T antigen. *Int. J. Cancer.* **2012,** 131, 1818-1827.

8. Knight, L. M.; Stakaityte, G.; Wood, J. J.; Abdul-Sada, H.; Griffiths, D. A.; Howell, G. J.; Wheat, R.; Blair, G. E.; Steven, N. M.; Macdonald, A.; Blackbourn, D. J.; Whitehouse, A., Merkel cell polyomavirus small T antigen mediates microtubule destabilization to promote cell motility and migration. *J. Virol.* **2015,** 89, 35-47.

9. Kwun, H. J.; Wendzicki, J. A.; Shuda, Y.; Moore, P. S.; Chang, Y., Merkel cell polyomavirus small T antigen induces genome instability by E3 ubiquitin ligase targeting. *Oncogene.* **2017,** 36, 6784-6792.

10. Shuda, M.; Kwun, H. J.; Feng, H.; Chang, Y.; Moore, P. S., Human Merkel cell polyomavirus small T antigen is an oncoprotein targeting the 4E-BP1 translation regulator. *J. Clin. Invest.* **2011,** 121, 3623-3634.

11. Shuda, M.; Guastafierro, A.; Geng, X.; Shuda, Y.; Ostrowski, S. M.; Lukianov, S.; Jenkins, F. J.; Honda, K.; Maricich, S. M.; Moore, P. S.; Chang, Y., Merkel Cell Polyomavirus Small T Antigen Induces Cancer and Embryonic Merkel Cell Proliferation in a Transgenic Mouse Model. *PLoS One.* **2015,** 10, e0142329.

12. Spurgeon, M. E.; Cheng, J.; Bronson, R. T.; Lambert, P. F.; DeCaprio, J. A., Tumorigenic activity of merkel cell polyomavirus T antigens expressed in the stratified epithelium of mice. *Cancer Res.* **2015,** 75, 1068-1079.

13. Verhaegen, M. E.; Mangelberger, D.; Harms, P. W.; Vozheiko, T. D.; Weick, J. W.; Wilbert, D. M.; Saunders, T. L.; Ermilov, A. N.; Bichakjian, C. K.; Johnson, T. M.; Imperiale, M. J.;

Dlugosz, A. A., Merkel cell polyomavirus small T antigen is oncogenic in transgenic mice. *J. Invest. Dermatol.* **2015,** 135, 1415-1424.

14. Verhaegen, M. E.; Mangelberger, D.; Harms, P. W.; Eberl, M.; Wilbert, D. M.; Meireles, J.; Bichakjian, C. K.; Saunders, T. L.; Wong, S. Y.; Dlugosz, A. A., Merkel Cell Polyomavirus Small T Antigen Initiates Merkel Cell Carcinoma-like Tumor Development in Mice. *Cancer Res.* **2017,** 77, 3151-3157.

15. Higaki-Mori, H.; Kuwamoto, S.; Iwasaki, T.; Kato, M.; Murakami, I.; Nagata, K.; Sano, H.; Horie, Y.; Yoshida, Y.; Yamamoto, O.; Adachi, K.; Nanba, E.; Hayashi, K., Association of Merkel cell polyomavirus infection with clinicopathological differences in Merkel cell carcinoma. *Human pathology* **2012,** 43, (12), 2282-91.

16. Konstantinell, A.; Bruun, J. A.; Olsen, R.; Aspar, A.; Skalko-Basnet, N.; Sveinbjornsson, B.; Moens, U., Secretomic analysis of extracellular vesicles originating from Polyomavirus-negative and Polyomavirus-positive merkel cell carcinoma cell lines. *Proteomics.* **2016**, 2587-2591.

17. Leonard, J.H.; Bell, J.R.; Kearsley, J.H., Characterization of cell lines established from Merkel-cell ("small-cell") carcinoma of the skin. *Int. J. Cancer.* **1993**, 55, 803-810.

18. Ronan, S.G.; Green, A.D.; Shilkaitis, A.; Huang, T.S.; Das Gupta, T.K., Merkel cell carcinoma: in vitro and in vivo characteristics of a new cell line. *J. Am. Acad. Dermatol.* **1993**, 29, 715-722.

19. Leonard, J.H.; Dash, P.; Holland, P.; Kearsley, J.H.; Bell, J.R. Characterisation of four Merkel cell carcinoma adherent cell lines. *Int. J. Cancer.* **1995**, 60, 100-107.

20. Houben, R.; Shuda, M.; Weinkam, R.; Schrama, D.; Feng, H.; Chang, H.; Chang, Y.; Moore, P.S.; Becker, J.C., Merkel cell polyomavirus-infected Merkel cell carcinoma cells require expression of viral T antigens. *J. Virol.* **2010**, 84, 7064-7072.

21. Sharma, M. C., Annexin A2 (ANX A2): An emerging biomarker and potential therapeutic target for aggressive cancers. *Int. J. Cancer.* **2019,** 144, 2074-2081.

22. Foo, S. L.; Yap, G.; Cui, J.; Lim, L. H. K., Annexin-A1 - A Blessing or a Curse in Cancer? *Trends Mol. Med.* **2019**, S1471-4914(19)30039-5.

23. Lee, H.; Kim, K.; Woo, J.; Park, J.; Kim, H.; Lee, K. E.; Kim, H.; Kim, Y.; Moon, K. C.; Kim, J. Y.; Park, I. A.; Shim, B. B.; Moon, J. H.; Han, D.; Ryu, H. S., Quantitative Proteomic

Analysis Identifies AHNAK (Neuroblast Differentiation-associated Protein AHNAK) as a Novel Candidate Biomarker for Bladder Urothelial Carcinoma Diagnosis by Liquid-based Cytology. *Mol. Cell. Proteomics: MCP.* **2018,** 17, 1788-1802.

24. Zou, C.; Zhao, P.; Xiao, Z.; Han, X.; Fu, F.; Fu, L., Gamma-delta T cells in cancer immunotherapy. *Oncotarget.* **2017,** 8, 8900-8909.

25. Lee, H. M.; Joh, J. W.; Seo, S. R.; Kim, W. T.; Kim, M. K.; Choi, H. S.; Kim, S. Y.; Jang, Y. J.; Sinn, D. H.; Choi, G. S.; Kim, J. M.; Kwon, C. H. D.; Chang, H. J.; Kim, D. S.; Ryu, C. J., Cell-surface major vault protein promotes cancer progression through harboring mesenchymal and intermediate circulating tumor cells in hepatocellular carcinomas. *Sci. Rep.* **2017,** 7, 13201.

26. Rademaker, G.; Costanza, B.; Bellier, J.; Herfs, M.; Peiffer, R.; Agirman, F.; Maloujahmoum, N.; Habraken, Y.; Delvenne, P.; Bellahcene, A.; Castronovo, V.; Peulen, O., Human colon cancer cells highly express myoferlin to maintain a fit mitochondrial network and escape p53-driven apoptosis. *Oncogenesis.* **2019,** 8, 21.

27. Liu, B.; Zhou, Y.; Lu, D.; Liu, Y.; Zhang, S. Q.; Xu, Y.; Li, W.; Gu, X., Comparison of the protein expression of calpain-1, calpain-2, calpastatin and calmodulin between gastric cancer and normal gastric mucosa. *Oncol. Lett.* **2017,** 14, 3705-3710.

28. Liu, S.; Chen, S.; Ma, K.; Shao, Z., Prognostic value of Kindlin-2 expression in patients with solid tumors: a meta-analysis. *Cancer Cell Int.* **2018,** 18, 166.

29. Kim, K. H.; Yeo, S. G.; Kim, W. K.; Kim, D. Y.; Yeo, H. Y.; Hong, J. P.; Chang, H. J.; Park, J. W.; Kim, S. Y.; Kim, B. C.; Yoo, B. C., Up-regulated expression of l-caldesmon associated with malignancy of colorectal cancer. *BMC Cancer.* **2012,** 12, 601.

30. Thijssen, V. L.; Heusschen, R.; Caers, J.; Griffioen, A. W., Galectin expression in cancer diagnosis and prognosis: A systematic review. *Biochim. Biophys. Acta.* **2015,** 1855, 235-247.

31. Wang, K.; Ruan, H.; Song, Z.; Cao, Q.; Bao, L.; Liu, D.; Xu, T.; Xiao, H.; Wang, C.; Cheng, G.; Tong, J.; Meng, X.; Yang, H.; Chen, K.; Zhang, X., PLIN3 is up-regulated and correlates with poor prognosis in clear cell renal cell carcinoma. *Urol. Oncol.* **2018,** 36, 343.e9-343.e19.

32. Muthusamy, K.; Halbert, G.; Roberts, F., Immunohistochemical staining for adipophilin, perilipin and TIP47. *J. Clin. Pathol.* **2006,** 59, 1166-1170.

33. Katada, K.; Tomonaga, T.; Satoh, M.; Matsushita, K.; Tonoike, Y.; Kodera, Y.; Hanazawa, T.; Nomura, F.; Okamoto, Y., Plectin promotes migration and invasion of cancer cells and is a novel prognostic marker for head and neck squamous cell carcinoma. *J. Proteomics.* **2012,** 75, 1803-1815.

34. Ha, E. S.; Choi, S.; In, K. H.; Lee, S. H.; Lee, E. J.; Lee, S. Y.; Kim, J. H.; Shin, C.; Shim, J. J.; Kang, K. H.; Phark, S.; Sul, D., Identification of proteins expressed differently among surgically resected stage I lung adenocarcinomas. *Clin. Biochem.* **2013,** 46, 369-377.

35. Lin, L.; Qin, Y.; Jin, T.; Liu, S.; Zhang, S.; Shen, X.; Lin, Z., Significance of NQO1 overexpression for prognostic evaluation of gastric adenocarcinoma. *Exp. Mol. Pathol.* **2014,** 96, 200-205.

36. Qi, Y.; Zhang, Y.; Peng, Z.; Wang, L.; Wang, K.; Feng, D.; He, J.; Zheng, J., SERPINH1 overexpression in clear cell renal cell carcinoma: association with poor clinical outcome and its potential as a novel prognostic marker. *J. Cell. Mol. Med.* **2018,** 22, 1224-1235.

37. Masugi, Y.; Tanese, K.; Emoto, K.; Yamazaki, K.; Effendi, K.; Funakoshi, T.; Mori, M.; Sakamoto, M., Overexpression of adenylate cyclase-associated protein 2 is a novel prognostic marker in malignant melanoma. *Pathol. Int.* **2015,** 65, 627-634.

38. Kang, S.; Xu, H.; Duan, X.; Liu, J. J.; He, Z.; Yu, F.; Zhou, S.; Meng, X. Q.; Cao, M.; Kennedy, G. C., PCD1, a novel gene containing PDZ and LIM domains, is overexpressed in several human cancers. *Cancer Res.* **2000,** 60, 5296-5302.

39. Qiu, Z.; Chu, Y.; Xu, B.; Wang, Q.; Jiang, M.; Li, X.; Wang, G.; Yu, P.; Liu, G.; Wang, H.; Kang, H.; Liu, J.; Zhang, Y.; Jin, J. P.; Wu, K.; Liang, J., Increased expression of calponin 2 is a positive prognostic factor in pancreatic ductal adenocarcinoma. *Oncotarget.* **2017,** 8, 56428-56442.

40. Goeppert, B.; Schmidt, C. R.; Geiselhart, L.; Dutruel, C.; Capper, D.; Renner, M.; Vogel, M. N.; Zachskorn, C.; Zinke, J.; Campos, B.; Schmezer, P.; Popanda, O.; Wick, W.; Weller, M.; Meyermann, R.; Schittenhelm, J.; Harter, P. N.; Simon, P.; Weichert, W.; Schirmacher, P.; Plass, C.; Mittelbronn, M., Differential expression of the tumor suppressor A-kinase anchor protein 12 in human diffuse and pilocytic astrocytomas is regulated by promoter methylation. *J. Neuropathol. Exp. Neurol.* **2013,** 72, 933-941.

41. Fujita, H.; Ohuchida, K.; Mizumoto, K.; Nakata, K.; Yu, J.; Kayashima, T.; Cui, L.; Manabe, T.; Ohtsuka, T.; Tanaka, M., alpha-Smooth Muscle Actin Expressing Stroma Promotes an Aggressive Tumor Biology in Pancreatic Ductal Adenocarcinoma. *Pancreas.* **2010,** 39, 1254-1262.

42. Wang, L.; Wang, M.; Zhang, M.; Li, X.; Zhu, Z.; Wang, H., Expression and significance of RRBP1 in esophageal carcinoma. *Cancer Manag. Res.* **2018,** 10, 1243-1249.

43. Kotb, A.; Hyndman, M. E.; Patel, T. R., The role of zyxin in regulation of malignancies. *Heliyon.* **2018,** 4, e00695.

44. Huang, D.; Casale, G. P.; Tian, J.; Lele, S. M.; Pisarev, V. M.; Simpson, M. A.; Hemstreet, G. P., 3rd, Udp-glucose dehydrogenase as a novel field-specific candidate biomarker of prostate cancer. *Int. J. Cancer.* **2010,** 126, 315-327.

45. Toiyama, Y.; Yasuda, H.; Saigusa, S.; Tanaka, K.; Inoue, Y.; Goel, A.; Kusunoki, M., Increased expression of Slug and Vimentin as novel predictive biomarkers for lymph node metastasis and poor prognosis in colorectal cancer. *Carcinogenesis.* **2013,** 34, 2548-2557.

46. Goto, K.; Anan, T.; Fukumoto, T.; Kimura, T.; Misago, N., Carcinoid-Like/Labyrinthine Pattern in Sebaceous Neoplasms Represents a Sebaceous Mantle Phenotype: Immunohistochemical Analysis of Aberrant Vimentin Expression and Cytokeratin 20-Positive Merkel Cell Distribution. *Am. J. Dermatopathol.* **2017,** 39, 803-810.

47. Shah, I. A.; Netto, D.; Schlageter, M. O.; Muth, C.; Fox, I.; Manne, R. K., Neurofilament immunoreactivity in Merkel-cell tumors: a differentiating feature from small-cell carcinoma. *Mod. Pathol.* **1993,** 6, 3-9.

48. van Muijen, G. N.; Ruiter, D. J.; Warnaar, S. O., Intermediate filaments in Merkel cell tumors. *Hum. Pathol.* **1985,** 16, 590-595.

49. Balaton, A. J.; Capron, F.; Baviera, E. E.; Meyrignac, P.; Vaury, P.; Vuong, P. N., Neuroendocrine carcinoma (Merkel cell tumor?) presenting as a subcutaneous tumor. An ultrastructural and immunohistochemical study of three cases. *Pathol.Res. Pract.* **1989,** 184, 211-216.

50. Zhang, Z.; Wang, Y.; Zhang, J.; Zhong, J.; Yang, R., COL1A1 promotes metastasis in colorectal cancer by regulating the WNT/PCP pathway. *Mol. Med. Rep.* **2018,** 17, 5037-5042.

51. Ngan, E.; Kiepas, A.; Brown, C. M.; Siegel, P. M., Emerging roles for LPP in metastatic cancer progression. *J. Cell Commun. Signal.* **2018,** 12, 143-156.

52. Chen, J.; Cao, S.; Situ, B.; Zhong, J.; Hu, Y.; Li, S.; Huang, J.; Xu, J.; Wu, S.; Lin, J.; Zhao, Q.; Cai, Z.; Zheng, L.; Wang, Q., Metabolic reprogramming-based characterization of circulating tumor cells in prostate cancer. *J. Exp. Clin. Cancer Res.* **2018,** 37, 127.

53. Bravou, V.; Antonacopoulou, A.; Papanikolaou, S.; Nikou, S.; Lilis, I.; Giannopoulou, E.; Kalofonos, H. P., Focal Adhesion Proteins alpha- and beta-Parvin are Overexpressed in Human Colorectal Cancer and Correlate with Tumor Progression. *Cancer Invest.* **2015,** 33, 387-397.

54. Jeong, H. C.; Kim, G. I.; Cho, S. H.; Lee, K. H.; Ko, J. J.; Yang, J. H.; Chung, K. H., Proteomic analysis of human small cell lung cancer tissues: up-regulation of coactosin-like protein-1. *J. Proteome Res.* **2011,** 10, 269-276.

55. Nassar, Z. D.; Hill, M. M.; Parton, R. G.; Parat, M. O., Caveola-forming proteins caveolin-1 and PTRF in prostate cancer. *Nat. Rev. Urol.* **2013,** 10, 529-536.

56. Ge, Y.; Xu, A.; Zhang, M.; Xiong, H.; Fang, L.; Zhang, X.; Liu, C.; Wu, S., FK506 binding protein 10 is overexpressed and promotes renal cell carcinoma. *Urol. Int.* **2017,** 98, 169-176.

57. Dai, D. L.; Makretsov, N.; Campos, E. I.; Huang, C.; Zhou, Y.; Huntsman, D.; Martinka, M.; Li, G., Increased expression of integrin-linked kinase is correlated with melanoma progression and poor patient survival. *Clin. Cancer Res.* **2003,** 9, 4409-4414.

58. Yang, Q.; Bavi, P.; Wang, J. Y.; Roehrl, M. H., Immuno-proteomic discovery of tumor tissue autoantigens identifies olfactomedin 4, CD11b, and integrin alpha-2 as markers of colorectal cancer with liver metastases. *J. Proteomics.* **2017,** 168, 53-65.

59. Alimirah, F.; Chen, J.; Davis, F. J.; Choubey, D., IFI16 in human prostate cancer. *Mol. Cancer Res.* **2007,** 5, 251-259.

60. Matuszczak, E.; Oksiuta, M.; Hermanowicz, A.; Debek, W., Traumatic pneumatocele in an 11-year-old boy - report of a rare case and review of the literature. *Kardiochir. Torakochirurgia Pol.* **2017,** 14, 59-62.

61. Shakhparonov, M. I.; Antipova, N. V.; Shender, V. O.; Shnaider, P. V.; Arapidi, G. P.; Pestov, N. B.; Pavlyukov, M. S., Expression and Intracellular Localization of Paraoxonase 2 in Different Types of Malignancies. *Acta Naturae.* **2018,** 10, 92-99.

62. Tsai, C. K.; Huang, L. C.; Tsai, W. C.; Huang, S. M.; Lee, J. T.; Hueng, D. Y., Overexpression of PLOD3 promotes tumor progression and poor prognosis in gliomas. *Oncotarget.* **2018,** 9, 15705-15720.

63. Ma, Y.; Xiao, T.; Xu, Q.; Shao, X.; Wang, H., iTRAQ-based quantitative analysis of cancer-derived secretory proteome reveals TPM2 as a potential diagnostic biomarker of colorectal cancer. *Front. Med.* **2016,** 10, 278-285.

64. Wong, J. J.; Lau, K. A.; Pinello, N.; Rasko, J. E., Epigenetic modifications of splicing factor genes in myelodysplastic syndromes and acute myeloid leukemia. *Cancer Sci.* **2014,** 105, 1457-1463.

65. Ruiz, C.; Holz, D. R.; Oeggerli, M.; Schneider, S.; Gonzales, I. M.; Kiefer, J. M.; Zellweger, T.; Bachmann, A.; Koivisto, P. A.; Helin, H. J.; Mousses, S.; Barrett, M. T.; Azorsa, D. O.; Bubendorf, L., Amplification and overexpression of vinculin are associated with increased tumour cell proliferation and progression in advanced prostate cancer. *J. Pathol.* **2011,** 223, 543-552.

66. Linhares, M. M.; Affonso, R. J., Jr.; Viana Lde, S.; Silva, S. R.; Denadai, M. V.; de Toledo, S. R.; Matos, D., Genetic and Immunohistochemical Expression of Integrins ITGAV, ITGA6, and ITGA3 As Prognostic Factor for Colorectal Cancer: Models for Global and Disease-Free Survival. *PLoS One.* **2015,** 10, e0144333.

67. Duarte-Pereira, S.; Pereira-Castro, I.; Silva, S. S.; Correia, M. G.; Neto, C.; da Costa, L. T.; Amorim, A.; Silva, R. M., Extensive regulation of nicotinate phosphoribosyltransferase (NAPRT) expression in human tissues and tumors. *Oncotarget.* **2016,** 7, 1973-1983.

68. Kabbage, M.; Trimeche, M.; Ben Nasr, H.; Hammann, P.; Kuhn, L.; Hamrita, B.; Chahed, K., Tropomyosin-4 correlates with higher SBR grades and tubular differentiation in infiltrating ductal breast carcinomas: an immunohistochemical and proteomics-based study. *Tumour Biol.* **2013,** 34, 3593-3602.

69. Yang, R.; Zheng, G.; Ren, D.; Chen, C.; Zeng, C.; Lu, W.; Li, H., The clinical significance and biological function of tropomyosin 4 in colon cancer. *Biomed. Pharmacother.* **2018,** 101, 1-7.

70. Liu, J.; Ni, W.; Qu, L.; Cui, X.; Lin, Z.; Liu, Q.; Zhou, H.; Ni, R., Decreased Expression of EHD2 Promotes Tumor Metastasis and Indicates Poor Prognosis in Hepatocellular Carcinoma. *Dig. Dis. Sci.* **2016,** 61, 2554-2567.

71. Kubickova, K. N.; Subhanova, I.; Konickova, R.; Matousova, L.; Urbanek, P.; Parobkova, H.; Kupec, M.; Pudil, J.; Vitek, L., Predictive role BLVRA mRNA expression in hepatocellular cancer. *Ann. Hepatol.* **2016,** 15, 881-887.

72. Pallua, J. D.; Schaefer, G.; Seifarth, C.; Becker, M.; Meding, S.; Rauser, S.; Walch, A.; Handler, M.; Netzer, M.; Popovscaia, M.; Osl, M.; Baumgartner, C.; Lindner, H.; Kremser, L.; Sarg, B.; Bartsch, G.; Huck, C. W.; Bonn, G. K.; Klocker, H., MALDI-MS tissue imaging identification of biliverdin reductase B overexpression in prostate cancer. *J. Proteomics.* **2013,** 91, 500-514.

73. Chen, L. F.; Ito, K.; Murakami, Y.; Ito, Y., The capacity of polyomavirus enhancer binding protein 2alphaB (AML1/Cbfa2) to stimulate polyomavirus DNA replication is related to its affinity for the nuclear matrix. *Mol. Cell Biol.* **1998,** 18, 4165-4176.

74. Dunne, P. D.; Dasgupta, S.; Blayney, J. K.; McArt, D. G.; Redmond, K. L.; Weir, J. A.; Bradley, C. A.; Sasazuki, T.; Shirasawa, S.; Wang, T.; Srivastava, S.; Ong, C. W.; Arthur, K.; Salto-Tellez, M.; Wilson, R. H.; Johnston, P. G.; Van Schaeybroeck, S., EphA2 Expression Is a Key Driver of Migration and Invasion and a Poor Prognostic Marker in Colorectal Cancer. *Clin. Cancer Res.* **2016,** 22, 230-242.

75. Xu, J.; Moatamed, F.; Caldwell, J. S.; Walker, J. R.; Kraiem, Z.; Taki, K.; Brent, G. A.; Hershman, J. M., Enhanced expression of nicotinamide N-methyltransferase in human papillary thyroid carcinoma cells. *J. Clin. Endocrinol. Metabol.* **2003,** 88, 4990-4996.

76. Liggett, J. L.; Choi, C. K.; Donnell, R. L.; Kihm, K. D.; Kim, J. S.; Min, K. W.; Noegel, A. A.; Baek, S. J., Nonsteroidal anti-inflammatory drug sulindac sulfide suppresses structural protein Nesprin-2 expression in colorectal cancer cells. *Biochim. Biophys. Acta.* **2014,** 1840, 322-331.

77. Shen, H. W.; Tan, J. F.; Shang, J. H.; Hou, M. Z.; Liu, J.; He, L.; Yao, S. Z.; He, S. Y., CPE overexpression is correlated with pelvic lymph node metastasis and poor prognosis in patients with early-stage cervical cancer. *Arch. Gynecol. Obstet.* **2016,** 294, 333-342.

78. Guerrero-Preston, R.; Hadar, T.; Ostrow, K. L.; Soudry, E.; Echenique, M.; Ili-Gangas, C.; Perez, G.; Perez, J.; Brebi-Mieville, P.; Deschamps, J.; Morales, L.; Bayona, M.; Sidransky, D.; Matta, J., Differential promoter methylation of kinesin family member 1a in plasma is associated with breast cancer and DNA repair capacity. *Oncol. Rep.* **2014,** 32, 505-512.

79. Cimino, D.; Fuso, L.; Sfiligoi, C.; Biglia, N.; Ponzone, R.; Maggiorotto, F.; Russo, G.; Cicatiello, L.; Weisz, A.; Taverna, D.; Sismondi, P.; De Bortoli, M., Identification of new genes associated with breast cancer progression by gene expression analysis of predefined sets of neoplastic tissues. *Int. J. Cancer.* **2008,** 123, 1327-1338.

80. Calmon, M. F.; Jeschke, J.; Zhang, W.; Dhir, M.; Siebenkas, C.; Herrera, A.; Tsai, H. C.; O'Hagan, H. M.; Pappou, E. P.; Hooker, C. M.; Fu, T.; Schuebel, K. E.; Gabrielson, E.; Rahal, P.; Herman, J. G.; Baylin, S. B.; Ahuja, N., Epigenetic silencing of neurofilament genes promotes an aggressive phenotype in breast cancer. *Epigenetics.* **2015,** 10, 622-632.

81. Celestino, R.; Nome, T.; Pestana, A.; Hoff, A. M.; Goncalves, A. P.; Pereira, L.; Cavadas, B.; Eloy, C.; Bjoro, T.; Sobrinho-Simoes, M.; Skotheim, R. I.; Soares, P., CRABP1, C1QL1 and LCN2 are biomarkers of differentiated thyroid carcinoma, and predict extrathyroidal extension. *BMC Cancer.* **2018,** 18, 68.

82. Ren, H. Z.; Pan, G. Q.; Wang, J. S.; Wen, J. F.; Wang, K. S.; Luo, G. Q.; Shan, X. Z., Reduced stratifin expression can serve as an independent prognostic factor for poor survival in patients with esophageal squamous cell carcinoma. *Dig. Dis. Sci.* **2010,** 55, 2552-2560.

83. Lucanus, A. J.; Yip, G. W., Kinesin superfamily: roles in breast cancer, patient prognosis and therapeutics. *Oncogene.* **2018,** 37, 833-838.

84. Ha, M.; Han, M. E.; Kim, J. Y.; Jeong, D. C.; Oh, S. O.; Kim, Y. H., Prognostic role of TPD52 in acute myeloid leukemia: A retrospective multicohort analysis. *J. Cell. Biochem.* **2019,** 120, 3672-3678.

85. Yang, X.; Yu, D.; Ren, Y.; Wei, J.; Pan, W.; Zhou, C.; Zhou, L.; Liu, Y.; Yang, M., Integrative functional genomics implicates EPB41 dysregulation in hepatocellular carcinoma risk. *Am. J. Hum. Genet.* **2016,** 99, 275-286.

86. Xin, Z.; Zhang, Y.; Jiang, Z.; Zhao, L.; Fan, L.; Wang, Y.; Xie, S.; Shangguan, X.; Zhu, Y.; Pan, J.; Liu, Q.; Huang, Y.; Dong, B.; Xue, W., Insulinoma-associated protein 1 is a novel

sensitive and specific marker for small cell carcinoma of the prostate. *Hum. Pathol.* **2018,** 79, 151-159.

87. Jeong, H. M.; Han, J.; Lee, S. H.; Park, H. J.; Lee, H. J.; Choi, J. S.; Lee, Y. M.; Choi, Y. L.; Shin, Y. K.; Kwon, M. J., ESRP1 is overexpressed in ovarian cancer and promotes switching from mesenchymal to epithelial phenotype in ovarian cancer cells. *Oncogenesis.* **2017,** 6, e391.

88. Peng, G.; Yuan, X.; Yuan, J.; Liu, Q.; Dai, M.; Shen, C.; Ma, J.; Liao, Y.; Jiang, W., miR-25 promotes glioblastoma cell proliferation and invasion by directly targeting NEFL. *Mol. Cell. Biochem.* **2015,** 409, 103-111.

89. Liang, F.; Lu, Q.; Sun, S.; Zhou, J.; Popov, V. M.; Li, S.; Li, W.; Liu, Y.; Jiang, J.; Kong, B., Increased expression of dachshund homolog 1 in ovarian cancer as a predictor for poor outcome. *Int. J. Gynecol. Cancer.* **2012,** 22, 386-393.

90. Pei, X.; Zhang, J.; Wu, L.; Lu, B.; Zhang, X.; Yang, D.; Liu, J., The down-regulation of GNAO1 and its promoting role in hepatocellular carcinoma. *Biosci. Rep.* **2013,** 33, e00069.

91. Han, K. Y.; Gu, X.; Wang, H. R.; Liu, D.; Lv, F. Z.; Li, J. N., Overexpression of MAC30 is associated with poor clinical outcome in human non-small-cell lung cancer. *Tumour Biol.* **2013,** 34, 821-825.

92. Nicolussi, A.; D'Inzeo, S.; Capalbo, C.; Giannini, G.; Coppa, A., The role of peroxiredoxins in cancer. *Mol. Clin. Oncol.* **2017,** 6, 139-153.

93. Wang, Y.; Chen, Y.; Li, X.; Hu, W.; Zhang, Y.; Chen, L.; Chen, M.; Chen, J., Loss of expression and prognosis value of alpha-internexin in gastroenteropancreatic neuroendocrine neoplasm. *BMC Cancer.* **2018,** 18, 691.

94. You, W.; Tan, G.; Sheng, N.; Gong, J.; Yan, J.; Chen, D.; Zhang, H.; Wang, Z., Downregulation of myosin VI reduced cell growth and increased apoptosis in human colorectal cancer. *Acta Biochim. Biophys. Sin. (Shanghai).* **2016,** 48, 430-436.

95. Wen, K. C.; Sung, P. L.; Chou, Y. T.; Pan, C. M.; Wang, P. H.; Lee, O. K.; Wu, C. W., The role of EpCAM in tumor progression and the clinical prognosis of endometrial carcinoma. *Gynecol. Oncol.* **2018,** 148, 383-392.

96. Schmit, K.; Michiels, C., TMEM Proteins in Cancer: A Review. *Front. Pharmacol.* **2018,** 9, 1345.

97. Vizin, T.; Kos, J., Gamma-enolase: a well-known tumour marker, with a less-known role in cancer. *Radiol. Oncol.* **2015,** 49, 217-226.

98. Guo, W.; Chen, Z.; Chen, Z.; Yu, J.; Liu, H.; Li, T.; Lin, T.; Chen, H.; Zhao, M.; Li, G.; Hu, Y., Promotion of Cell Proliferation through Inhibition of Cell Autophagy Signalling Pathway by Rab3IP is Restrained by MicroRNA-532-3p in Gastric Cancer. *J. Cancer.* **2018,** 9, 4363-4373.

99. Meng, J., Distinct functions of dynamin isoforms in tumorigenesis and their potential as therapeutic targets in cancer. *Oncotarget.* **2017,** 8, 41701-41716.

100. Zhou, S.; Shen, Y.; Zheng, M.; Wang, L.; Che, R.; Hu, W.; Li, P., DNA methylation of METTL7A gene body regulates its transcriptional level in thyroid cancer. *Oncotarget.* **2017,** 8, 34652-34660.

101. Houles, T.; Roux, P. P., Defining the role of the RSK isoforms in cancer. *Semin. Cancer Biol.* **2018,** 48, 53-61.

102. Zhai, L. L.; Xie, Q.; Zhou, C. H.; Huang, D. W.; Tang, Z. G.; Ju, T. F., Overexpressed HSPA2 correlates with tumor angiogenesis and unfavorable prognosis in pancreatic carcinoma. *Pancreatology.* **2017,** 17, 457-463.

103. Luo, S.; Li, Y.; Ma, R.; Liu, J.; Xu, P.; Zhang, H.; Tang, K.; Ma, J.; Liu, N.; Zhang, Y.; Sun, Y.; Ji, T.; Liang, X.; Yin, X.; Liu, Y.; Tong, W.; Niu, Y.; Wang, N.; Wang, X.; Huang, B., Downregulation of PCK2 remodels tricarboxylic acid cycle in tumor-repopulating cells of melanoma. *Oncogene.* **2017,** 36, 3609-3617.

104. Woischke, C.; Blaj, C.; Schmidt, E. M.; Lamprecht, S.; Engel, J.; Hermeking, H.; Kirchner, T.; Horst, D., CYB5R1 links epithelial-mesenchymal transition and poor prognosis in colorectal cancer. *Oncotarge.t* **2016,** 7, 31350-3160.

105. Wang, J. W.; Gamsby, J. J.; Highfill, S. L.; Mora, L. B.; Bloom, G. C.; Yeatman, T. J.; Pan, T. C.; Ramne, A. L.; Chodosh, L. A.; Cress, W. D.; Chen, J.; Kerr, W. G., Deregulated expression of LRBA facilitates cancer cell growth. *Oncogene.* **2004,** 23, 4089-4097.

106. Menkhorst, E.; Griffiths, M.; Van Sinderen, M.; Rainczuk, K.; Niven, K.; Dimitriadis, E., Galectin-7 is elevated in endometrioid (type I) endometrial cancer and promotes cell migration. *Oncol. Lett.* **2018,** 16, 4721-4728.

107. Antonacopoulou, A. G.; Grivas, P. D.; Skarlas, L.; Kalofonos, M.; Scopa, C. D.; Kalofonos, H. P., POLR2F, ATP6V0A1 and PRNP expression in colorectal cancer: new molecules with prognostic significance? *Anticancer Res.* **2008,** 28, 1221-1227.

108. Raja, S. A.; Abbas, S.; Shah, S. T. A.; Tariq, A.; Bibi, N.; Yousuf, A.; Khawaja, A.; Nawaz, M.; Mehmood, A.; Khan, M. J.; Hussain, A., Increased expression levels of Syntaxin 1A and Synaptobrevin 2/Vesicle-Associated Membrane Protein-2 are associated with the progression of bladder cancer. *Genet. Mol. Biol.* **2019,** 42, 40-47.

109. Honisch, S.; Yu, W.; Liu, G.; Alesutan, I.; Towhid, S. T.; Tsapara, A.; Schleicher, S.; Handgretinger, R.; Stournaras, C.; Lang, F., Chorein addiction in VPS13A overexpressing rhabdomyosarcoma cells. *Oncotarget.* **2015,** 6, 10309-10319.

110. Fu, X.; Fan, X.; Hu, J.; Zou, H.; Chen, Z.; Liu, Q.; Ni, B.; Tan, X.; Su, Q.; Wang, J.; Wang, L.; Wang, J., Overexpression of MSK1 is associated with tumor aggressiveness and poor prognosis in colorectal cancer. *Dig. Liver Dis.* **2017,** 49, 683-691.

111. Sunshine, J. C.; Jahchan, N. S.; Sage, J.; Choi, J., Are there multiple cells of origin of Merkel cell carcinoma? *Oncogene.* **2018,** 37, 1409-1416.

112. Mehrmohamadi, M.; Liu, X.; Shestov, A. A.; Locasale, J. W., Characterization of the usage of the serine metabolic network in human cancer. *Cell Rep.* **2014,** 9, 1507-1519.

113. Zhu, Y.; Li, T.; Ramos da Silva, S.; Lee, J. J.; Lu, C.; Eoh, H.; Jung, J. U.; Gao, S. J., A Critical Role of Glutamine and Asparagine gamma-Nitrogen in Nucleotide Biosynthesis in Cancer Cells Hijacked by an Oncogenic Virus. *MBio* **2017,** 8, e01179-17.

114. van Beek, J., The dynamic side of the Warburg effect: glycolytic intermediate storage as buffer for fluctuating glucose and O 2 supply in tumor cells. *F1000Res.* **2018,** 7, 1177.

115. Zhu, S.; Dong, Z.; Ke, X.; Hou, J.; Zhao, E.; Zhang, K.; Wang, F.; Yang, L.; Xiang, Z.; Cui, H., The roles of sirtuins family in cell metabolism during tumor development. *Semin. Cancer Biol.* **2018**, S1044-579X(18)30107-X.

116. Marquez, J.; Kratchmarova, I.; Akimov, V.; Unda, F.; Ibarretxe, G.; Clerigue, A. S.; Osinalde, N.; Badiola, I., NADH dehydrogenase complex I is overexpressed in incipient metastatic murine colon cancer cells. *Oncol. Rep.* **2019,** 41, 742-752.

117. Murray Stewart, T.; Dunston, T. T.; Woster, P. M.; Casero, R. A., Jr., Polyamine catabolism and oxidative damage. *J. Biol. Chem.* **2018,** 293, 18736-18745.

118. Taniguchi, N.; Kizuka, Y., Glycans and cancer: role of N-glycans in cancer biomarker, progression and metastasis, and therapeutics. *Adv. Cancer Res.* **2015,** 126, 11-51.

119. Uchiyama, K.; Jokitalo, E.; Kano, F.; Murata, M.; Zhang, X.; Canas, B.; Newman, R.; Rabouille, C.; Pappin, D.; Freemont, P.; Kondo, H., VCIP135, a novel essential factor for p97/p47-mediated membrane fusion, is required for Golgi and ER assembly in vivo. *J. Cell Biol.* **2002,** 159, 855-866.

120. Ju, L. G.; Lin, X.; Yan, D.; Li, Q. L.; Wu, M.; Li, L. Y., Characterization of WDR20: A new regulator of the ERAD machinery. *Biochim. Biophys. Acta. Mol. Cell Res.* **2018,** 1865, 970-980.

121. Mishra, S. J.; Ghosh, S.; Stothert, A. R.; Dickey, C. A.; Blagg, B. S., Transformation of the Non-Selective Aminocyclohexanol-Based Hsp90 Inhibitor into a Grp94-Seletive Scaffold. *ACS Chem. Biol.* **2017,** 12, 244-253.

122. Li, T.; Zhu, Y.; Cheng, F.; Lu, C.; Jung, J. U.; Gao, S. J., Oncogenic Kaposi's Sarcoma-Associated Herpesvirus Upregulates Argininosuccinate Synthase 1, a Rate-Limiting Enzyme of the Citrulline-Nitric Oxide Cycle, To Activate the STAT3 Pathway and Promote Growth Transformation. *J. Virol.* **2019,** 93, e01599-18.

123. Silberman, A.; Goldman, O.; Boukobza Assayag, O.; Jacob, A.; Rabinovich, S.; Adler, L.; Lee, J. S.; Keshet, R.; Sarver, A.; Frug, J.; Stettner, N.; Galai, S.; Persi, E.; Halpern, K. B.; Zaltsman-Amir, Y.; Pode-Shakked, B.; Eilam, R.; Anikster, Y.; Nagamani, S. C. S.; Ulitsky, I.; Ruppin, E.; Erez, A., Acid-Induced Downregulation of ASS1 Contributes to the Maintenance of Intracellular pH in Cancer. *Cancer Res.* **2019,** 79, 518-533.

124. Takahashi, A.; Okada, R.; Nagao, K.; Kawamata, Y.; Hanyu, A.; Yoshimoto, S.; Takasugi, M.; Watanabe, S.; Kanemaki, M. T.; Obuse, C.; Hara, E., Exosomes maintain cellular homeostasis by excreting harmful DNA from cells. *Nat. Commun.* **2017,** 8, 15287.

125. Guastafierro, A.; Feng, H.; Thant, M.; Kirkwood, J. M.; Chang, Y.; Moore, P. S.; Shuda, M., Characterization of an early passage Merkel cell polyomavirus-positive Merkel cell carcinoma cell line, MS-1, and its growth in NOD scid gamma mice. *J. Virol. Methods.* **2013,** 187, 6-14.

126. Pasternak, S.; Carter, M. D.; Ly, T. Y.; Doucette, S.; Walsh, N. M., Immunohistochemical profiles of different subsets of Merkel cell carcinoma. *Hum. Pathol.* **2018,** 82, 232-238.

127. Rush, P. S.; Rosenbaum, J. N.; Roy, M.; Baus, R. M.; Bennett, D. D.; Lloyd, R. V., Insulinoma-associated 1: A novel nuclear marker in Merkel cell carcinoma (cutaneous neuroendocrine carcinoma). *J. Cutan. Pathol.* **2018,** 45, 129-135.

128. Iwasaki, T.; Matsushita, M.; Nonaka, D.; Nagata, K.; Kato, M.; Kuwamoto, S.; Murakami, I.; Hayashi, K., Lower expression of CADM1 and higher expression of MAL in Merkel cell carcinomas are associated with Merkel cell polyomavirus infection and better prognosis. *Hum. Pathol.* **2016,** 48, 1-8.

129. Liu, W.; MacDonald, M.; You, J., Merkel cell polyomavirus infection and Merkel cell carcinoma. *Curr. Opin. Virol.* **2016,** 20, 20-27.

130. Rasheed, K.; Abdulsalam, I.; Fismen, S.; Grimstad, O.; Sveinbjornsson, B.; Moens, U., CCL17/TARC and CCR4 expression in Merkel cell carcinoma. *Oncotarget.* **2018,** 9, 31432-31447.

131. Strug, I.; Utzat, C.; Cappione, A., 3rd; Gutierrez, S.; Amara, R.; Lento, J.; Capito, F.; Skudas, R.; Chernokalskaya, E.; Nadler, T., Development of a univariate membrane-based mid-infrared method for protein quantitation and total lipid content analysis of biological samples. *J. Anal. Methods Chem.* **2014,** 2014, 657079.

132. Shevchenko, A.; Wilm, M.; Vorm, O.; Mann, M., Mass spectrometric sequencing of proteins silver-stained polyacrylamide gels. *Anal. Chem.* **1996,** 68, 850-858.

133. Tyanova, S.; Temu, T.; Sinitcyn, P.; Carlson, A.; Hein, M. Y.; Geiger, T.; Mann, M.; Cox, J., The Perseus computational platform for comprehensive analysis of (prote)omics data. *Nat. Methods.* **2016,** 13, 731-740.

134. Perez-Riverol, Y.; Csordas, A.; Bai, J.; Bernal-Llinares, M.; Hewapathirana, S.; Kundu, D. J.; Inuganti, A.; Griss, J.; Mayer, G.; Eisenacher, M.; Perez, E.; Uszkoreit, J.; Pfeuffer, J.; Sachsenberg, T.; Yilmaz, S.; Tiwary, S.; Cox, J.; Audain, E.; Walzer, M.; Jarnuczak, A. F.; Ternent, T.; Brazma, A.; Vizcaino, J. A., The PRIDE database and related tools and resources in 2019: improving support for quantification data. *Nucleic Acids Res.* **2019,** 47, D442-D450.